Research on Compound Kushen Injection (CKI):

Anti-cancer Mechanism Pathway/Network structure

By

JIAN CUI

THE UNIVERSITY of ADELAIDE

Department of Genetics and Evolution

School of Biological Sciences

A thesis presented for the degree of DOCTOR OF PHILOSOPHY

OCTOBER 2018

Foreword

"I have often been asked, which was the more important to the world, pure or applied science. To have the applications of a science, the science itself must exist. Should we stop its progress, and attend only to its applications, we should soon degenerate into a people like the Chinese, who have made no progress for generations, because they have been satisfied with the applications of science, and have never. sought for reasons in what they have done. The reasons constitute pure science. They have known the application of gunpowder for centuries; and yet the reasons for its peculiar action, if sought in the proper manner, would have developed the science of chemistry, and even of physics, with all their numerous applications. By contenting themselves with the fact that gunpowder will explode, and seeking no farther, they have fallen behind in the progress of the world; and we now regard this oldest and most numerous of nations as only barbarians."

— Rowland, Henry Augustus.
"*A plea for pure science.*"
Science 2.29 (1883): 242-250.

Abstract

Traditional Chinese medicine (TCM) is built on a foundation of more than 2,500 years of Chinese medical practice with most therapies relying on herbal formulae. In China and the surrounding countries, TCM has been the standard system of medicine. In the west medical system, it is gradually being accepted as alternative medicine, especially for some systems and chronic diseases. Although the efficacy of TCM is accepted by many, the lack of Western-style evidence-based medicine and scientific basis for diagnosis and treatment is a barrier to acceptance and wider adoption.

Compound Kushen injection (CKI) is a TCM anticancer agent commoditized for more than 20 years in China. It is primarily used in combination with chemotherapeutic agents in clinics to relieve cancer pain, cancer metastasis and to enhance immunity. Growing evidence indicates that several compounds isolated from CKI demonstrate significant anticancer activity, although questions still remain concerning its underlying mechanisms.

In this thesis, I used a systems-based approach to analyze transcriptomic data from different cancer cell lines in order to identify candidate molecular anticancer mechanisms of CKI. Previous research on this topic is incomplete because it was based on the collection and integration of data from the literature, and there was a lack of data from genome-scale experiments. I have addressed these limitations by generating transcriptome data from cancer cells treated with CKI, and have comprehensively analyzed data sets from different cancer cell types. I was able to identify a number of novel potential mechanisms of action and some previously overlooked anticancer effects of CKI. It was clear from the comparison of gene expression patterns of the cells treated with chemotherapy drugs that CKI acts through different mechanisms.

By integrating the analysis across different cancer cell types, core features of CKI dependent gene regulation were identified. CKI is able to regulate the expression of many genes, with the majority of those down-regulated. Functions associated with down-regulated genes include energy metabolism, cell cycle, cell migration, some cancer-relevant pathways and immune response. The genetic networks associated with these processes or pathways cover almost the entire physiological progression of cancer as well as the body's response to the illness. CKI, therefore, appears to act on cancer cells in a comprehensive fashion.

A preconceived notion of CKI mechanism only considers its effects to result from the additive combination of its components. My work has demonstrated this is not necessarily the case. I compared the effects of oxymatrine, the most abundant compound present in CKI to those of CKI. An equivalent amount of oxymatrine has some similar effects compared to CKI, but some of the effects are weaker, or even opposite to CKI.

Altogether, this thesis presents a systems-based approach for identifying the mechanism of action of CKI. By characterizing and validating the transcriptome data from three cancer cell lines, we provide candidate pathways for CKI as an anticancer agent.

Keywords: *systems biology approach, TCM, CKI, multi-target medicine, anticancer, pathway/ network research, MCF-7, MDA-MB-231, Hep G2, cell cycle, cancer metabolism, DSBs*

Dedication and Acknowledgements

From a small town in China, I traveled to the University of Adelaide. I have developed into a Ph.D. student. I would not have been able to achieve this without the support and guidance from some excellent people. I would like to express my special appreciation and thanks to all of them, particularly the following.

First of all. I would like to thank my supervisors David Adelson and Dan Kortschak. Together your supervision has taught me how to be an academic researcher with your rigorous academic excellence. Dave, though your schedule is filled up with everything, you can always remember every detail of my progress. And patiently answering our emails and working on the manuscripts no matter how late it is. I would like to thank you for encouraging my research and for allowing me to grow gradually. Your advice on both research as well as on my career have been invaluable. Dan, your wisdom and advice always provide new perspectives to my research. I am extremely appreciative of all your efforts.

To the wonderful people in the Adelson lab, you have been accompanying me at uni every day. For special mention, I would like to acknowledge Zhipeng and Yuka. You have always been considerate to offer me thoughtful suggestions and encouragement when I need it most. As for my lab mates in the Zhendong Center, Thazin, Hanyuan and Joy, I am sure you are beyond colleagues to me. We share ideas and have fun with each other. Your presence made my candidature a fun and enjoyable experience.

Also, I will seize the opportunity to thank my friends outside the lab. Chao, Yan and Pengfei, we have known each other for almost twenty years now. You guys are always thoughtful and helpful during my absence at home.

A special thanks to my family. Words cannot express how grateful I am to my mother and father for all of the sacrifices that you have made on my behalf. Your support for me was what sustained me thus far.

Finally, to Min, thank you for being there through the bad days and enjoying with me on the good days. Especially I cannot thank you enough for encouraging me throughout this experience.

Declaration

I certify that this work contains no material which has been accepted for the award of any other degree or diploma in my name in any university or other tertiary institution and, to the best of my knowledge and belief, contains no material previously published or written by another person, except where due reference has been made in the text. In addition, I certify that no part of this work will, in the future, be used in a submission in my name for any other degree or diploma in any university or other tertiary institution without the prior approval of the University of Adelaide and where applicable, any partner institution responsible for the joint award of this degree.

I give consent to this copy of my thesis when deposited in the University Library, being made available for loan and photocopying, subject to the provisions of the Copyright Act 1968.

The author acknowledges that copyright of published works contained within this thesis resides with the copyright holder(s) of those works.

I also give permission for the digital version of my thesis to be made available on the web, via the University's digital research repository, the Library Search and also through web search engines, unless permission has been granted by the University to restrict access for a period of time.

SIGNED: .... DATE: ..26../10../2018.....

Table of Contents

		Page
1	Introduction	1
2	Identification of Candidate Anti-cancer Molecular Mechanisms of Compound Kushen Injection Using Functional Genomics	34
3	The Effect of Compound Kushen Injection on Cancer Cells: Integrated Identification of Candidate Molecular Mechanisms.	54
4	Cell Cycle, Glycolysis and DNA Repair Pathways in Cancer Cells are Suppressed by Compound Kushen Injection	87
5	Traditional Chinese Herbal Formula YQCT Reduces Gefitinib-induced Drug Resistance in Non-Small Cell Lung Cancer by Targeting Apoptosis and Autophagy Pathways	111
6	Conclusions and Future Directions	140
A	Supplementary Tables	142
B	Supplementary for Chapter 2	144
C	Supplementary for Chapter 3	154
D	Supplementary for Chapter 4	159
E	Abbreviations	162

Chapter 1

Introduction

In this chapter, we provide an overview of TCM extracts and review the literature on their effects. I discuss how these ideas can be applied to research on CKI to understand its effects on biological networks and underlying mechanisms. Although TCM formulations are not widely accepted in Western countries, some pure compounds derived from TCM extracts have been widely clinically adopted including as cancer therapies. This chapter reviews some popular herbal extracts and their compounds. We also introduce CKI, the primary extract investigated in this thesis, and summarise research methods applied to TCM formulations. We conclude by reviewing the effects of CKI, and the drawbacks of most current studies. We then describe our research questions and specific research methods to address those questions. We intend to identify the mechanisms underlying the modes of action of CKI, which we hope will contribute to the scientific understanding of TCM.

Statement of Authorship

Title of Paper	The anticancer agents from traditional Chinese medicine and compound kushen injection: a review
Publication Status	☐ Published ☐ Accepted for Publication ☐ Submitted for Publication ☑ Unpublished and Unsubmitted w ork w ritten in manuscript style
Publication Details	

Co-Author

Name of Principal Author (Candidate)	Jian Cui
Contribution to the Paper	Analysed literature, prepare figures and wrote manuscript
Overall percentage (%)	70%
Certification:	This paper reports on original research I conducted during the period of my Higher Degree by Research candidature and is not subject to any obligations or contractual agreements with a third party that would constrain its inclusion in this thesis. I am the second author of this paper.
Signature	Date 18/6/18

Co-Author Contributions

By signing the Statement of Authorship, each author certifies that:

i. the candidate's stated contribution to the publication is accurate (as detailed above);

ii. permission is granted for the candidate in include the publication in the thesis; and

iii. the sum of all co-author contributions is equal to 100% less the candidate's stated contribution.

Name of Co-Author	David L. Adelson
Contribution to the Paper	Supervised the development of work and assisted in writing the manuscript
Signature	Date 18/6/2018

The anticancer candidates from traditional Chinese medicine (TCM) and Compound Kushen Injection (CKI): a review

1. PROJECT SUMMARY

This study will identify TCM anti-cancer mechanism pathway networks through bioinformatic methods. This paper compares the theoretical principles, clinical characteristics, and mechanisms of modern medicine and TCM, with the view that current research on TCM does not adequately address TCM theoretical features and clinical characteristics. Based on this point of view, a system based analytical methodology has been designed to study the anti-cancer effects of CKI, and to achieve the following aims:

1) To assess the effects of TCM on cancer cell phenotypes: specifically, the differences between the effects of single bio-active extracts and complex mixtures, and the characteristics of TCM that are distinct from single-agent chemotherapeutic agents.

2) To illustrate TCM anti-cancer mechanisms: dissect the effects of a complex mixture with multiple targets on phenotype [1, 2], in order to identify candidate molecular mechanisms.

In order to achieve the above aims, I have chosen CKI as a representative TCM anticancer drug for systems biology-based dissection of the molecular effects of TCM on cancer cells.

2. PROJECT DETAILS

2.1 Introduction

Cancer is a genetically heterogeneous disease that involves multiple molecular pathways. Currently, cancer treatments focus mainly on applying agents to inhibit specific targets or pathways.

The most widely adopted treatments for clinically advanced-stage cancer are chemotherapy and radiotherapy [3]. At the initial stage, tumors have not yet spread in a patient's body, and symptoms are not severe, so removal of tumors via surgery or radiotherapy can be curative. However, when cancer metastasis occurs, treatment options narrow, and systemic treatments such as chemotherapy are the accepted standard of care. Because the prognosis for advanced metastatic cancer is poor, patients often seek to try other therapies, such as novel agents or drugs from other medical systems. Among these options, traditional Chinese medicine (TCM) is an attractive choice.

Under normal circumstances, TCM is used as a compounded formula made up of different functional components. Besides, modern medical system regard TCM as combinations of variable bio-active herbal extracts. In this sense, TCM prescriptions are multi-target medicines containing different components. Although these components are clinically useful, quality control and consistency are still issues.

Most current research on TCM is not comprehensive since it tends to focus on the effects of single compounds. Also, it is often focused only on a few typical pathways regulated by these single compounds, rather than on the overall effect of TCM, which is expected to affect multiple targets and alter pathway regulation.

I propose that, by using modern system based methods, it will be possible to identify cancer pathways regulated by TCM, and to summarize the anti-cancer features of TCM in a systematic fashion. By comparing the differences between TCM and chemotherapeutic agents or single compounds, it may be

possible to supplement the limitations of present research on TCM, and to provide new models and ideas for further research on TCM formulas.

2.2 Literature Review

This review will discuss some well-characterized pathways that are involved in the processes of cancer development, as well as pathways relevant to anticancer therapies, such as apoptosis pathways, that are targets of both modern medicine and TCM. In addition, a broad selection of TCM ingredients will be systematically reviewed as potential anti-cancer candidates. By reviewing studies on the anticancer effects of TCM, I will also highlight and discuss the drawbacks of current methods. This review will contribute to a comprehensive understanding of TCM anticancer mechanisms and propose more detailed, reliable, and productive methods of identifying TCM mechanisms.

2.2.1 Pathways involved in cancer progression

Cancer progression is a complicated process involving a number of physiological and regulatory pathways. These pathways can play vital roles during all stages of cancer development and ultimately, the regulation of these pathways is based on gene expression, including oncogenes and tumor suppressor genes. Mutations in these genes, as well as dysregulation of gene expression, results in oncogenic transformation. The following sections will review major pathways and their key genes.

2.2.1.1 Metastasis/migration pathways and cell differentiation

The differentiation, metastasis, and migration of cancer cells are closely intertwined. Two of the most well-researched pathways relevant to these biological processes are cancer cells' epithelial-mesenchymal transition (EMT), and non-directional differentiation [4-6].

EMT plays a crucial role during cancer metastasis and is the product of dysregulation of Transforming growth factor β 1 (TGF-β), the absence of Phosphatase and tensin homolog (PTEN) and RAS/MAPK, Zinc Finger E-Box Binding Homeobox 1 (ZEB1), and action of microRNA families, such as miR-200 [7-10]. All of these factors can induce or promote EMT processes in cancer. EMT is the underlying change that governs how cancer cells can migrate throughout the body via the circulatory system. The invasive and metastatic features of tumor cells and cancer stem-like cells (CSCs) are triggered by this process, resulting in poor clinical prognosis [10]. Moreover, some studies have found that, in association with other pathways, EMT is also able to induce drug resistance and cancer recurrence [11-13]. Because of its complex regulation, EMT is a difficult target for cancer treatment.

2.2.1.2 Cell metabolism pathways

Cancer cell/tumor metabolism is different to healthy tissues and cells. These pathways are co-regulated and interact with each other; for example, carbohydrate, glutamine and lipid metabolic pathways are controlled by central regulators such as the Myc family, in post-transcription level [14]. The oncogene *MYC* and its extended protein superfamilies, such as Mondo, Mlx, and Max, not only regulate translation but also the glycolytic enzymes in cancer cells to regulate the balance of glutaminolysis and lipogenesis required to maintain metabolism [14-17].

In addition, RAC-α serine/threonine-protein kinase (AKT) and Hypoxia-inducible factors (HIFs) are also able to alter metabolic regulation in cancer cells. The pathways regulated by these proteins can maintain metabolism under physiologically extreme circumstances, such as nutrient deficiency and hypoxia[18, 19]. When cancer cells are exposed to nutrient deficiency, AKT promotes the alternative use of acetyl coenzyme A (acetyl-CoA) as an acetyl donor to increase histone acetylation required to regulate cancer metabolic processes [20]. Under hypoxia, HIF family proteins are upregulated in order

to cope with low oxygen tension. HIF-1α is the primary regulator for most HIF target genes and can regulate glycolysis by altering the rates of glycolytic enzymes and glucose transport [21-23].

Several recent studies have shown that signaling pathways, such as the Wingless and INT-1 (WNT) and P53 pathways, can regulate metabolism. These pathways usually cooperate with other factors or signals to affect cancer cell metabolism. Specifically, WNT can up-regulate the AKT-mTOR pathway [24], and P53 can be inhibited by CD147, a transmembrane glycoprotein, to regulate glucose metabolism [25].

2.2.1.3 Cell proliferation pathways

In terms of tumor proliferation angiogenesis is significant because this process can promote metastasis and is required for the metabolism of cancer cells[26]. There are multiple molecular factors involved in the regulation of tumor angiogenesis, including vascular endothelial growth factor (VEGF), fibroblast growth factor (FGF), platelet-derived growth factor (PDGF), stromal cell-derived factor 1 (SDF-1a), Tumor necrosis factor (TNF-a), interleukin 1 β (IL-1β) and interleukin 6 (IL-6)[27]. The best example is VEGF because this factor is able to promote vasodilatation and vascular permeability and to suppress cancer cell apoptosis [28]. Additionally, the expression of VEGF can also affect the EMT process, to increase tumorigenicity via angiogenesis [29]. There are also additional signaling pathways relevant to angiogenesis.

These signaling pathways are active in both normal and cancer cells but are dysregulated in cancer. From this point of view, the c-Jun N-terminal kinases (JNKs) pathway is a good example in terms of the regulation of cell proliferation [30-33]. Previous studies have revealed that the JNK pathway regulates cell proliferation in different ways by associating with different factors. For instance, JNK could be inhibited to reduce the viability of normal cells, liver/ pancreatic cancer, and colon cancers [34-36]. Conversely, under nutrient-depletion stress, IL-4 can induce prostate cancer cell proliferation by

activating the JNK pathway [37].

In addition, the WNT signaling pathway regulates not only proliferation and metabolism, but also affects cell migration and self-renewal in cancer stem cells [38, 39]. As a pro-oncogenic gene, *WNT* mutants have a variety of complex effects through its downstream pathways, β-catenin pathway in different cancer types.

2.2.1.4 Cell death pathways

Programmed cell death, or apoptosis, has many causes, and is triggered by a number of genes and factors, including some tumor suppressor genes and enzymes. Therefore, many anti-cancer drugs have been developed against these targets in order to kill tumors [40]. Cancer cell apoptosis caused by therapeutic agents can be divided into the following stages. First, agents induce damage to DNA, RNA or microtubules; this causes cells to release apoptosis signals to activate the apoptosis process. Then, a variety of enzymes, including proteases, DNases and RNases, cooperate to induce cell death [41]. P53, Fas, Bcl-2, Apaf-1 and several other pathways mentioned above are involved in triggering apoptosis by activating Caspases [42-46].

In summary, carcinogenesis and cancer treatments are complex processes, within which there are not only single pathway effects, but also crosstalk between pathways [47]. Furthermore, the same pathways often work differently depending on specific physiological processes [48]. TCM potentially offers a novel framework for the development of multi-target drugs. For this reason, TCM is gradually being accepted by modern medicine system as an adjuvant therapy. In the following sections, we will discuss some modern anti-cancer strategies and uses of TCM.

2.2.2 The pathways involved in anti-cancer medical therapies

First line anti-cancer agents can be classified into the following categories based on mechanisms of action: 1. Directly acting on DNA to alter the original structure and cause DNA damage; 2. Interfering with DNA synthesis or antimetabolite agents; 3. Antimitotic.

Inducing DNA damage There are several agents that can lead to DNA damage, such as alkylating drugs. Alkylating agents usually to alkylate DNA bases leading to DNA damage which inhibits certain processes, such as DNA replication and/or transcription[49]. As a result of inhibiting these processes, DNA repair pathways are activated including components of homologous recombination and non-homologous end-joining [50]. There are a number of rapidly acting cancer cell DNA damage agents that have been developed, such as nitrogen mustard (Fig.1A), ethylene, nitrosourea, and methane sulfonic acid ester [51-54].

Inhibiting metabolite pathways These agents inhibit metabolic pathways that synthesize folic acid, purine, pyrimidine, and pyrimidine nucleosides, thereby inhibiting tumor cell survival and replication under stress conditions [55]. For example, 5- Fluorouracil (5-FU), in the treatment of intestinal cancer, can inhibit the APAF-1/Caspase-9 Apoptotic Pathway [56] and the JNK pathway [57], both of which are pathways that cells use to respond to their environment [58]. Drugs inhibiting the production of folic acid, pyrimidines and purines all have similar mechanisms (Fig.1B).

Additionally, anti-cancer antibiotics are also able to affect metabolic pathways. As with normal antibiotics, anti-cancer antibiotics inhibit enzymes and mitosis or alter cell membranes, to alter DNA or chromatin status [59, 60]. Marcellomycin, mitomycin, bleomycin and actinomycin are commonly used anti-cancer antibiotic drugs.

Inhibiting DNA replication pathways. These anti-cancer agents consist mostly of heavy metal preparations, and bioactive peptides, such as TAT-N24 regulating multiple targets [61] (Fig.1C). These

agents can bind with protein receptors [62] and block cancer cell proliferation in S or G1/S phase of the cell cycle [63]. Platinum complexes are typical drugs with these functions and target pathways such as STAT signaling and HMGB-1. In addition, these agents, supplemented by other drugs or methods, can have more pronounced anti-cancer effects. For example, combining with X-ray therapy with platinum complexes to treat melanoma, affects more pathways[64].

Targeting Multiple pathways (Hormone therapy) In contrast to the above-mentioned agents, drugs for hormone therapy affect multiple tumor cell pathways, by inhibiting the effects of hormones on cancer cells. This type of therapy is used on hormone-sensitive tumors of the breast, prostate, ovary, and womb.[65-67]. The most commonly used agents are aromatase inhibitors, luteinising hormone blockers and some hormone receptor modulators, such as tamoxifen [68-70]. Obacunone, an aromatase inhibitor, has been reported to block the p38 MAPK signaling pathway in human breast cancer MCF-7 cells *in vitro* [71]. Tamoxifen exhibits different effects on different cancers. In the treatment of breast cancer, the mutated PI3K/AKT pathway is inhibited by tamoxifen [72], and in stomach cancer, this pathway is inhibited to reduce multidrug resistance [73]. Although these kinds of agents are reported to be effective, they cause significant damage to normal tissues. For example, aromatase inhibitors lead to painful joint symptoms [74], and osteoporosis [75].

Chemotherapy agents are considered to be the most efficient antitumor drugs, and the benefits of these agents are manifold, but drawbacks of these agents cannot be ignored. Take DNA damaging drugs as an example, efficacy is always influenced by compensatory effects in patients, and this antagonistic process will dramatically affect the effective dose that can be used [76, 77]. In addition, after long-term medication, drug resistance is a concern, and frequent replacement of medications can also produce significant damage to normal tissues during combination therapy [78]. The significance of these problems to patient quality of life makes better combination therapy or the development of more

advanced drugs imperative.

2.2.3 Molecular pathways affected by traditional medicine extracts

Due to the side effects of chemotherapies and radiotherapies[79], improvements of current methods are necessary. Researchers have begun to explore some effective natural products from traditional medicine systems, such as Chinese and Indian medicines. Compared to modern medical concepts, the most prominent advantage of TCM is the collection of verified medicinal plants [80]. In some areas, TCM is used to supplement modern therapies in the treatment of cancer [81, 82].

TCM is often characterized by the use of mixtures of multiple compounds as active ingredients to enhance blood circulation, improve immunity and induce the removal of lesions [83]. These pharmacologic effects of TCM are reflected in how they are prescribed and combined. The compounds introduced here are known to be major bioactive ingredients in traditional medical formulas.

Although most of the *materia medica* of TCM is from herbs, animal drugs, and mineral drugs are not uncommon in TCM. There are different anti-cancer ingredients in each category. Some highly toxic plant-extracts have been applied in Western medicine, such as Taxol, Vincristine and Camptothecin (Fig.2). These agents originally were found in plant-based treatments and are now pre-compounds extracted from plants. Besides these highly effective but toxic plant extracts, TCM can potentially provide effective and less toxic formulas for clinical use and offers potential resources to be exploited.

2.2.3.1 Plant Extracts

2.2.3.1.1 Alkaloids (Fig 2)

Herbs commonly used in TCM to treat cancer are classified by different practitioners [84]. The

representative drugs and their main bioactive alkaloids are: matrine and oxymatrine (Fig.2) in Kushen (*Sophora flavescens var. flavescens*), paclitaxel (Taxol) in Hongdoushan (*Taxus chinensis*), camptothecin in Xishu (*Camptotheca acuminata*), triptolide and tripdiolide (Fig.2) in Leigongteng (*Tripterygium wilfordii Hook.f*), vinblastine and oxyvinblastione in Changchunhua (*Catharanthus roseus*), and berberine (Fig.2) in Huanglian (*Coptis chinensis Franch, Coptis deltoidea C. Y. Cheng et Hsiao, Coptis teeta Wall*) etc. The bioactive ingredients from these herbs are considered as alkaloids[84-86].

Alkaloids are regarded as the most bioactive ingredients in TCM material, with different kinds of sources. Within the herb category, alkaloids exist in forms of organic salts, glycosides, organic acid esters, and amides [87]. These high water-soluble forms provide favorable conditions for active ingredients isolation in TCM practice. In recent studies on these water-soluble components, researchers have started to pay more attention to understand molecular mechanisms and signal regulatory pathways and networks that relate to cancer cells apoptosis which will be discussed below.

Agents triggering the apoptosis pathways

Matrine and oxymatrine This group has been considered as promising anti-cancer agents, because of their pleiotropic effect and nontoxicity to normal cells [88]. Matrine can upregulate Fas and Bax, and downregulate Bcl-2 to trigger apoptosis pathways in cancer cells such as MCF-7 and A549 [89]. It has been revealed in one recent study that matrine induced the apoptosis of myeloid leukemia cells by reducing the expression of Bcl-xL, Cyclin D1, IL-6 and c-Myc, to affect the IL-6/JAK/STAT3 pathways [90]. Another experiment on mouse sarcoma showed that the TRPV 1 pathway can be inhibited by matrine or oxymatrine by decreasing the phosphorylation of ERK and AKT kinases and BAD to inhibit tumor growth [91]. Besides, Matrine can inhibit leukemia K562 cells differentiation [92, 93]. Oxymatrine can reverse the multidrug resistance of Hep G2/ ADM cells by uncharacterized pathways

[94].

Taxol and vinblastine Each of these agents are first-line clinical anti-cancer chemotherapeutic drugs, and they have similar anti-cancer mechanisms that affect the formation of microtubules in mitosis [95]. This achievement is often accompanied by the upregulation of PI3K/Akt and MAP kinase pathways [96]. According to clinical requirements for low toxicity and high efficiency, derivatives of both alkaloids with higher compatibility have also been developed. More influenced pathways are also getting revealed. For example, combined with curcumin, taxol induces the apoptosis of HPV-positive HeLa and CaSki cells by acting on the NF-κB-p53-caspase-3 pathway [97].

Camptothecin The anti-cancer mechanism of camptothecin stems from its ability to inhibit the activity of topoisomerase I leading to an irreversible break in DNA [98]. Thus the pathways it affects are related to DNA damages and hypoxia, such as ART, FA and BRCA pathways [99]. However, the dosage of camptothecin can also affect the apoptosis of cancer cells. A study has shown that low-dose camptothecin can induce autophagy and premature senescence respectively, via the AMPK-TSC2-mTOR pathway and ATM-Chk2-p53-p21 pathway [99].

Triptolide and tripdiolide Typically, anti-cancer research has focused more on triptolide than tripdiolide. The significant anti-tumor effects of both are on some well-known pathways, such as by inhibiting the Wnt/B-catenin pathway to induce the apoptosis of lung cancer cells, downregulating NF-κB to provide a potential opportunity for the treatment of Pancreatic ductal adenocarcinoma, and inducing apoptosis in endometrial cancer through a p53-independent mitochondrial pathway [100]. Additionally, the main active ingredients of the “blushwood” berry, which has been reported to kill cancer in 75% of animal transplanted tumor models tested [101, 102], has a similar chemical structure (Fig.2) with triptolide, and this might provide a new idea for cancer treatment using triptolide.

Berberine As a TCM herb used for 3000 years, Huanglian, whose main ingredient is berberine, is used as a drug for treating intestinal disease. The anti-cancer activity of berberine has been comprehensively studied. The alkaloid can promote AMPK and inhibit mTORC1, ERK to shorten the cell cycle of Human Pancreatic Cancer Cells *in vitro*, and *in vivo* [103], and downregulate EGFR-MEK-ERK to accelerate the apoptosis of human glioblastoma cells [104]. In terms of inducing apoptosis, berberine can enhance the content of reactive oxygen species to trigger the pro-apoptosis JNK signaling pathway in MCF-7 and MDA-MB-231 cells [105].

2.2.3.1.2 Flavonoids

Flavonoids are the most common compounds in nature, and have been established as possessing antioxidant, anti-angiogenic, anti-inflammatory and anti-cancer activities. There are approximately 10,000 different kinds of flavonoids found in plants, which are mainly contained in the flowers and leaves of Leguminosae sp., Ginkgoales Engler, Rutaceae, Compositae and Labiatae. In TCM herbs, the most commonly detected flavonoids are flavones, flavonols, anthocyanins, luteolin, quercetin, kaempferol, naringin, catechin, genistein etc. We will review the anti-cancer effect of different flavonoids in the next section.

Inhibiting the proliferation of cancer cells and inducing apoptosis

For inhibiting cancer cell proliferation or inducing apoptosis, flavonoids from vegetables and medicinal herbs have some common features, and TCM emphasizes the homology of medicine and food. Apigenin, from celery, can suppress the action of PI3K/Akt/FoxO pathways *in vivo* to improve the quality of life of mice with prostate cancer [106]. Silibinin, the extract of *Silybum marianum*, shows significant anti-cancer effects by decreasing the expression of Bcl-2 in the reactive oxygen species (ROS) pathway so as to induce cancer cell autophagy[107]. Recently, a newly isolated flavonoid from Streptomyces spp.

(ERINLG-4) has been reported that, with the assistance of Bcl-2 and caspase dependent pathway, induces apoptosis of cancer cells by suppressing p53 [108]. Isoliquiritigenin (ISL), a flavonoid extracted from licorice, shows promising cancer cell toxicity in different cancer cell lines, and can induce DNA damage in different ways. For example, by downregulating the β-catenin pathway, and promoting the expression of the WIF1 gene, ISL can reduce the viability of breast cancer stem cells [109] to inhibit the downstream signals of ataxia telangiectasia mutated (ATM) pathway leading to DNA damage in oral cancer cells [110]. In addition, ISL also has the ability to reduce PI3K/AKT to limit the proliferation of breast cancer cells [111]. Apigenin and luteolin can also inhibit cancer cell proliferation by limiting the angiogenesis process through the HIF-1a and Akt signaling pathways [112, 113]. Furthermore, in the treatment of prostate cancer, apigenin can reduce VEGF expression by acting on the Smad2/3 mechanism [114]. Another flavonoid, acacetin, shows inhibition of tumor angiogenesis via Akt and HIF-1a pathways as well [115].

Moreover, although various flavonoids have been reported with the ability to inhibit cancer cell growth, the pathways contributing to the anti-cancer effects have not been demonstrated clearly enough, because many of these agents are utilized in association to enhance chemotherapy drugs' efficacy. Some examples show luteolin increases interferon-induced JAK/STAT activation, in order to promote its antiproliferative effect [116], and by inhibiting nrf2[117] or promoting PPRγ/COTN2[118] to improve the efficacy of colorectal anti-cancer drugs. Other flavonoids, for instance, chrysin, from the seeds and bark of *Oroxylum indicum(L.)Vent*, have the ability to reverse drug resistance by inhibiting the PI3K/Akt/Nrf2 and ERK/Nrf2 pathways [119]. The compounds of chrysin, dimethoxyflavone (DMF) displayed the most effective toxicity leading to breast cancer stem cell death by damaging DNA[120]. DMF can also remarkably decrease the migration and invasion of glioma cells via p38 and ERK pathways[121]. Galangin, a flavonoid found in galangal, has the ability to change the migration

characteristics of Hep G2 cells by weakening the TPA induced signaling through PKC/ERK pathways [122].

Metabolic pathways

ISL can also limit arachidonic acid metabolic pathways in breast cancer cells *in vitro* [111]. In the treatment to non-small cell lung cancer cells, a dietary flavonoid, fisetin, has shown good efficacy in the inhibition of PI3K/Akt and mTOR signaling pathways to regulate cancer cell metabolism [123].

2.2.3.1.3 Polysaccharide

So far, there are approximately 300 species of polysaccharides that have been extracted from TCM materials, and many of these isolations have been applied in clinical practice in China, such as lentinan, Astragalus polysaccharide, Polyporus polysaccharide, *Achyranthes bidentata* polysaccharide and so on [124]. Most polysaccharides are mainly used as adjuvants to enhance the immune system and activate innate immune factors such as IL-1, IL-2, IL-6, TNF-α, and INF-γ [125].

Apoptosis pathways

Dioscorea polysaccharides can induce TNF-a through Toll-like receptor 4-mediated protein kinase signaling pathways [126]. Furthermore, it can also promote the anti-melanoma efficacy of DNA vaccine by inhibiting NF-κB signaling pathway [127]. After red mold fermentation, Dioscorea polysaccharide shows a stronger anti-leukemic effect, by the activation of IL-1β, TNF-α, IFN-γ in the leukemic cell THP-1 [128]. Another polysaccharide extracted from the fruit body of *Trametes robiniophila* induces apoptosis in osteosarcoma xenograft cancer cells by increasing Bax expression and decreasing Bcl-2 expression [129]. A study of RAW 264.7 murine leukemia virus-induced tumor cells revealed that the polysaccharides from *Taraxacum officinale* show an anti-inflammatory and anti-oxidant properties

through the PI3K-Akt signaling pathway [130, 131].

Metastasis pathways

Herbal medicines such as ginseng Panax that contain polysaccharides as their main bioactive, also have an effect on cancer. Polysaccharides can suppress cancer metastasis by reducing TWIST and AKR1C2 gene expression, and the EMT process [77]. The polysaccharides from *Astragalus membranaceus* and *Codonopsis pilosulae* can alter network regulation to reduce mammary tumor cell metastasis [110]. A pectic acid polysaccharide from corn also shows a novel anti-cancer effect against cancer cell metastasis, and the ability to regulate the VEGF pathway [132].

2.2.3.2 Mineral active ingredients

The minerals used in TCM anti-cancer are high toxicity agents, such as white arsenic (As_2O_3), realgar (As_2S_2), cinnabar (HgS) and other metals such as gold. Usually, these kinds of agents are used at a quite low dose to avoid patient poisoning. Modern medical research has shown that minerals do mainly induce cancer apoptosis either alone or by associating with other chemotherapeutic drugs [133, 134].

Apoptotic pathways

Arsenic (As) compounds can be used to treat leukemia and can affect a number of pathways [135, 136]. The main effects of these agents are to deregulate the pathways relating to cancer cell proliferation and apoptosis, for example, NF-κB, MAPK, mTOR, Hedgehog[135], and SLIT2–ROBO[137] pathways. Moreover, it can also suppress angiogenesis through ROS/miR-199a-5p/HIF-1a/COX-2 pathways [138].

Another TCM arsenide, realgar, has also been reported to have anti-cancer activity by inducing cancer cell apoptosis, particularly in the context of gastric cancer, liver cancer and leukemia [84]. In the

treatment of gastric cancer cells, realgar could up-regulate Bax pathways [139], and for leukemia, realgar could induce PI3-K/Akt pathways leading to cell death [140].

2.2.4 Previous research on Compound Kushen Injection (CKI)

In TCM, treatments are normally based on medical herb formulas, namely combinations of TCM containing a variety of ingredients from different herbs. Our research candidate, CKI, contains extracts from two herbs: kushen (*Radix Sophorae Flavescentis*) and baituling (*Rhizoma Smilacis Glabrae*).

Of these two herbs, kushen is believed to contain the major therapeutic activity [141]. The primary bioactive compounds from this plant are alkaloids and flavonoids. Although a lot of work on kushen has been done on the flavonoids, current studies focus more on the alkaloids [142]. Therefore, some alkaloids we have mentioned above, such as matrine and oxymatrine, have been comprehensively studied.

It is believed that the main effects of the alkaloids could reflect on inflammation and cancer and account for the main effects of CKI, which is used to treat inflammatory disease and cancer, In particular, cancer pain and bleeding. After 1995, when CKI was first commercialized, it has been widely used in combination with other therapies on a variety of different cancer types [141, 143, 144].

The main anticancer effects of CKI have been summarized as twofold: 1) direct activity against tumors by inhibiting cancer cell proliferation by increasing the proportion of cells in G1 phase and decreasing the proportion in S phase by arresting the progression of cancer cells into S phase and 2) enhance anti-tumor immune activity through B and T lymphocytes and macrophages [145]. However, as reviewed above, all these results came from focusing on one or several purified compounds, and involved limited characterization of effects on one or a few genes or pathways using qPCR or protein expression.

Because these studies did not use single compounds at the concentration/dose they are present at in CKI and because they did not consider interactions between multiple compounds, these studies do not reflect the activity of the overall formula. These limited results do not accurately identify the activity of CKI as a complex TCM formula.

With the development of systems biology, it is now possible to identify the underlying molecular mechanisms of TCM. Therefore, by profiling the system-wide effects of CKI on gene expression networks we can obtain a more accurate understanding of the overall mechanisms of CKI and demonstrate the application of these methods which we hope will be more broadly used within TCM.

2.2.5 Issues faced

Recent research on potential anti-cancer agent candidates has progressed significantly. However, because of the side effects of existing drugs, more novel and alternative or complementary drugs are still under development. Investigating clear anti-cancer pathways of these new multi-target drugs is difficult with current established study methodologies, because further steps are required to process large data sets, such as those from high-throughput assays that can investigate multiple targets and multiple pathways.

2.2.6 Systems biology and TCM research

Due to the complexing of TCM preparations and the interactions of their components, traditional molecular biology approaches face significant difficulties in explaining TCM's mechanisms of action. Therefore, the development of network-based systems biology and similar approaches have provided reasonable support for the revealing of mechanisms of TCM in the context of molecular networks.

Single TCM extracts have certain similarities to modern medicines [146]. Therefore, an approach to

researching TCM compounds at the molecular level would be to follow that taken with examining combination therapy of multi-component drugs [147].

The rapid development in 'omics' approaches and systems biology has promoted a systems-level understanding of biological processes including the interactions between genes, proteins and environmental factors. Therefore, systems biology provides new conceptions for uncovering the molecular mechanisms related to the therapeutic efficacy of TCM [148]. Systems biology enriched the complex interactions at different levels into different networks and illustrate the underlying mechanisms by analyzing these networks [149]. Applying network-based systems biology to learn effects of TCM may characterize specific targets of TCM components as well as interactions in the context at the molecular level.

2.3 Research significance

Currently, first line anti-cancer drugs are mostly chemotherapy agents. For breast cancer only, from 2012-2014 the top five drugs accounted for 62% of treatment costs. Their manufacturers monopolized nearly 75% of the market [150]. This indicates that there are relatively few TCM anti-cancer agents available clinically. Meanwhile, the cancer death rate is still increasing, as well as in some developed countries [151]. Hence, current anti-cancer treatments are necessary to be improved with complementary and alternative options. As a traditional medical approach, relying on its own unique treatment philosophy, TCM has served China and surrounding countries for centuries [152].

At the moment, there are obstructions for accepting the TCM validity outside of Asia. Since many anti-cancer TCM formulas for different purposes have been put on the market, with varying therapeutic efficacies, it is not easy to evaluate their efficacy. The complex-target feature of TCM agents lead to improper usage in the modern clinical system, resulting in many excellent anticancer agents being

misunderstood [153]. Consequently, because TCM theories are different, western consumers generally hold a cautious attitude to herbal medicines they do not understand.

Based on its theory, the TCM formulas are usually combining medical herbs to affect multiple targets. Most of the current studies attempt to isolate single components from certain formulas or herb extracts, to study the effects of major compounds. These methods are not able to determine the mode of action of TCM medicine; our preliminary experimental results show that the effects of major components are not equivalent to the effects of the complex mixture they are parts of. Based on this, our research on TCM formula should provide an integrated understanding of TCM, and better theoretical support on molecular anticancer mechanisms.

2.4 Research questions

In order to better understand TCM, and to provide clinical support, this project focuses on compound Kushen injection (CKI), which is an anti-cancer agent, as a candidate. By using a series of bioinformatics research methods, it should be possible to address the following questions:

- Is CKI, as a type of TCM, a potential anti-cancer agent? This will include studies using the formulation, the herbs used and some individual molecular components, to determine whether the single ingredients can represent overall efficacy.
- Can these research methods be used to investigate more anti-cancer pathways/ networks of TCM?
- Can this research method establish novel TCM QC & research systems via evaluating the molecular effects of agents?

2.5 Hypotheses and Specific Aims.

My central hypothesis is: *CKI contains multiple potential anti-cancer candidates, and it regulates multiple targets/pathways.* This gives rise to several sub-hypotheses.

- Sub-hypothesis 1: *the molecular mechanism* of *CKI is different from chemotherapy agents that affect specific targets.*
    - Aim 1: Determine time- and dose-dependent effects of CKI on perturbed gene expression networks/pathways in multiple cancer cell lines.
    - Aim 2: Compare the effects of CKI and 5-FU on the regulation of gene expression networks/pathways.
- Sub-hypothesis 2: *CKI is a complex mixture, and targets multiple pathways/networks.*
    - Aim 3: Identify candidate core pathways perturbed by CKI in multiple cancer cell lines.
    - Aim 4: Validate specific core CKI pathways perturbed by CKI in cancer cells and compare to the effects of major compounds on those pathways.

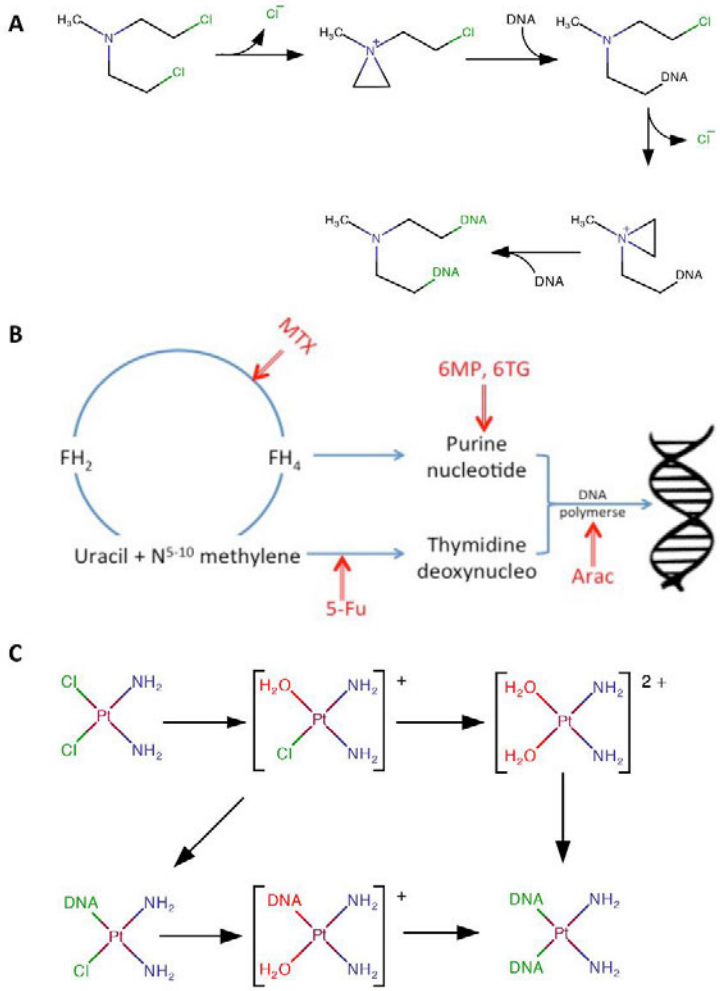

Figure 1. Simplified typical anticancer mechanisms. A. The mechanism by which nitrogen mustard induces DNA damage, in a low-halogen environment, nitrogen mustard loses chlorine, and then cross-links DNA, to damage DNA structure. B. The mechanism of anti-metabolite anti-cancer drugs, within the process of cell metastasis, Methotrexate (MXT), 5-Fluorouracil (5-Fu), 6-Mercaptopurine(6MP), 6-Thioguanine (6TG), Arabinosylcytosine (AraC) and similar drugs target different steps to affect the synthesis/replication of DNA. C. Platinum anti-cancer agents bind to DNA and form complexes, inhibiting DNA replication and transcription.

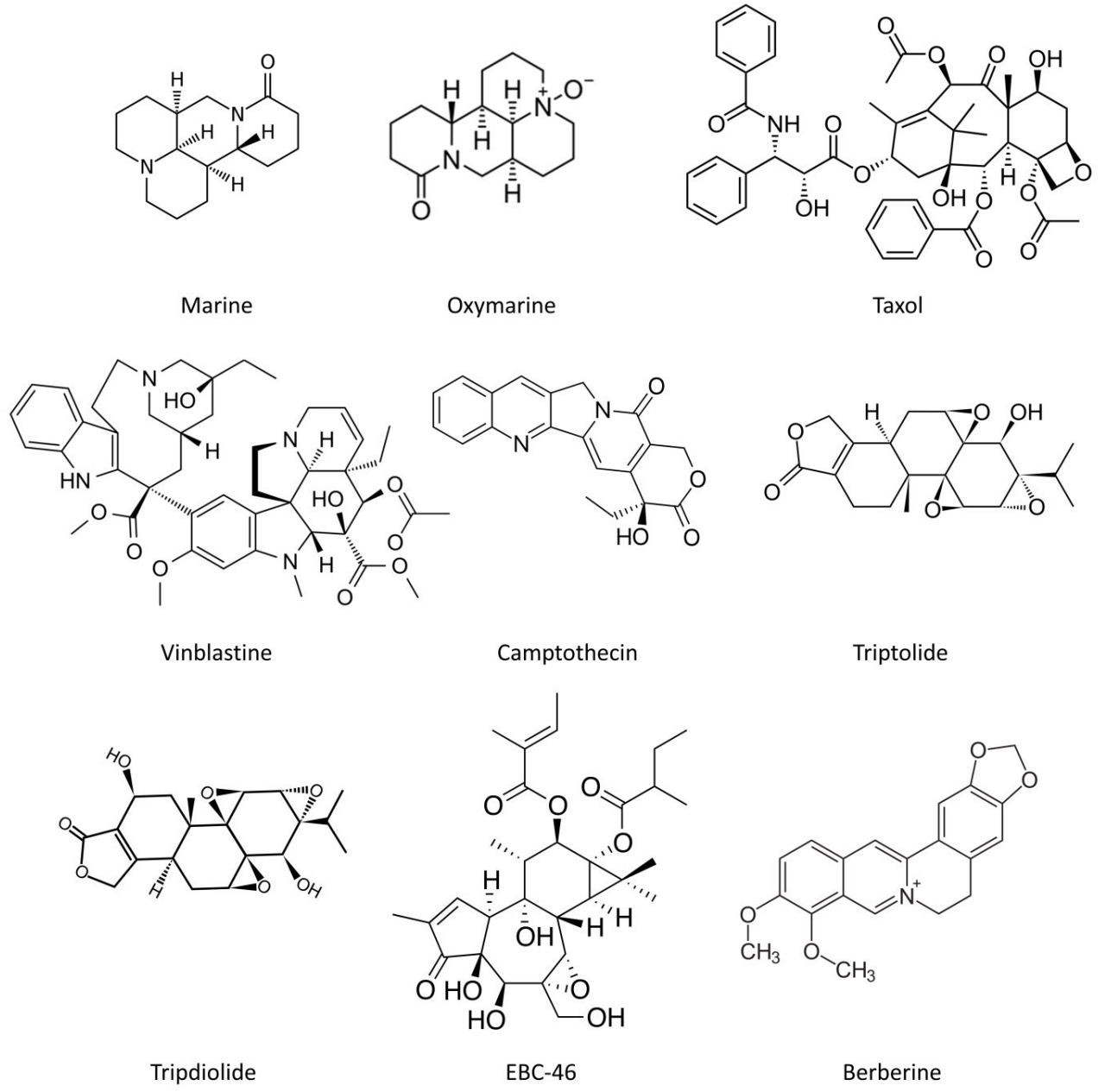

Figure 2. chemical structures of the alkaloids mentioned in the text. Among these extracts, EBC-46 is the active ingredient of Blushwood.

3. REFERENCES

1. Lao, L., L. Xu, and S. Xu, *Traditional chinese medicine*, in *Integrative Pediatric Oncology*. 2012, Springer. p. 125-135.
2. Hsiao, W. and L. Liu, *The role of traditional Chinese herbal medicines in cancer therapy–from TCM theory to mechanistic insights.* Planta medica, 2010. **76**(11): p. 1118.
3. Bartelink, H., et al., *Concomitant radiotherapy and chemotherapy is superior to radiotherapy alone in the treatment of locally advanced anal cancer: results of a phase III randomized trial of the European Organization for Research and Treatment of Cancer Radiotherapy and Gastrointestinal Cooperative Groups.* Journal of Clinical Oncology, 1997. **15**(5): p. 2040-2049.
4. De Craene, B. and G. Berx, *Regulatory networks defining EMT during cancer initiation and progression.* Nature Reviews Cancer, 2013. **13**(2): p. 97-110.
5. Thiery, J.-P., *[Epithelial-mesenchymal transitions in cancer onset and progression]*. Bulletin de l'Academie nationale de medecine, 2009. **193**(9): p. 1969-78; discussion 1978-9.
6. Ying, Q.-L., et al., *BMP induction of Id proteins suppresses differentiation and sustains embryonic stem cell self-renewal in collaboration with STAT3.* Cell, 2003. **115**(3): p. 281-292.
7. Mulholland, D.J., et al., *Pten loss and RAS/MAPK activation cooperate to promote EMT and metastasis initiated from prostate cancer stem/progenitor cells.* Cancer research, 2012. **72**(7): p. 1878-1889.
8. Genetta, T., et al., *THE TRANSCRIPTIONAL REPRESSOR ZINC‐FINGER E‐BOX BINDING PROTEIN TARGETED BY HYPOXIA‐INDUCIBLE FACTOR‐1a IN RESPONSE TO STROKE REPRESSES A NUMBER OF PROAPOPTOTIC GENES.: 116.* Journal of Investigative Medicine, 2006. **54**(1): p. S276.
9. Burk, U., et al., *A reciprocal repression between ZEB1 and members of the miR‐200 family promotes EMT and invasion in cancer cells.* EMBO reports, 2008. **9**(6): p. 582-589.
10. Singh, A. and J. Settleman, *EMT, cancer stem cells and drug resistance: an emerging axis of evil in the war on cancer.* Oncogene, 2010. **29**(34): p. 4741-4751.
11. Lee, H.-J., et al., *Drug resistance via feedback activation of Stat3 in oncogene-addicted cancer cells.* Cancer cell, 2014. **26**(2): p. 207-221.
12. Nurwidya, F., et al., *Epithelial mesenchymal transition in drug resistance and metastasis of lung cancer.* Cancer Research and Treatment, 2012. **44**(3): p. 151-156.
13. Xia, H., L.L.P. Ooi, and K.M. Hui, *MicroRNA‐216a/217‐induced epithelial‐mesenchymal transition targets PTEN and SMAD7 to promote drug resistance and recurrence of liver cancer.* Hepatology, 2013. **58**(2): p. 629-641.
14. Sloan, E.J. and D.E. Ayer, *Myc, mondo, and metabolism.* Genes & cancer, 2010. **1**(6): p. 587-596.
15. Dang, C.V., *Web of the Extended Myc Network Captures Metabolism for Tumorigenesis.* Cancer cell, 2015. **27**(2): p. 160-162.
16. Daye, D. and K.E. Wellen. *Metabolic reprogramming in cancer: unraveling the role of glutamine in tumorigenesis*. in *Seminars in cell & developmental biology*. 2012. Elsevier.
17. Stoltzman, C.A., et al., *MondoA Senses Non-glucose Sugars REGULATION OF THIOREDOXIN-INTERACTING PROTEIN (TXNIP) AND THE HEXOSE TRANSPORT CURB.* Journal of Biological Chemistry, 2011. **286**(44): p. 38027-38034.

18. Fleming, I.N., A. Andriu, and T.A. Smith, *Early changes in [18F] FDG incorporation by breast cancer cells treated with trastuzumab in normoxic conditions: role of the Akt-pathway, glucose transport and HIF-1α.* Breast cancer research and treatment, 2014. **144**(2): p. 241-248.
19. Bao, S., et al., *Periostin potently promotes metastatic growth of colon cancer by augmenting cell survival via the Akt/PKB pathway.* Cancer cell, 2004. **5**(4): p. 329-339.
20. Lee, J.V., et al., *Akt-dependent metabolic reprogramming regulates tumor cell histone acetylation.* Cell metabolism, 2014. **20**(2): p. 306-319.
21. Kumar, H. and D.-K. Choi, *Hypoxia Inducible Factor Pathway and Physiological Adaptation: A Cell Survival Pathway?* Mediators of Inflammation, 2015.
22. Cheng, S.-C., et al., *mTOR-and HIF-1α–mediated aerobic glycolysis as metabolic basis for trained immunity.* Science, 2014. **345**(6204): p. 1250684.
23. Ferrer, C.M., et al., *O-GlcNAcylation regulates cancer metabolism and survival stress signaling via regulation of the HIF-1 pathway.* Molecular cell, 2014. **54**(5): p. 820-831.
24. Sherwood, V., *WNT signaling: An emerging mediator of cancer cell metabolism?* Molecular and cellular biology, 2015. **35**(1): p. 2-10.
25. Huang, Q., et al., *CD147 promotes reprogramming of glucose metabolism and cell proliferation in HCC cells by inhibiting the p53-dependent signaling pathway.* Journal of hepatology, 2014. **61**(4): p. 859-866.
26. Weis, S.M. and D.A. Cheresh, *Tumor angiogenesis: molecular pathways and therapeutic targets.* Nature medicine, 2011. **17**(11): p. 1359-1370.
27. Otjacques, E., et al., *Biological aspects of angiogenesis in multiple myeloma.* International journal of hematology, 2011. **94**(6): p. 505-518.
28. Kapahi, R., et al., *Association of VEGF and VEGFR1 polymorphisms with breast cancer risk in North Indians.* Tumor Biology, 2015: p. 1-12.
29. Fantozzi, A., et al., *VEGF-mediated angiogenesis links EMT-induced cancer stemness to tumor initiation.* Cancer research, 2014. **74**(5): p. 1566-1575.
30. Zhan, Y., et al., *Role of JNK, p38, and ERK in platelet-derived growth factor–induced vascular proliferation, migration, and gene expression.* Arteriosclerosis, thrombosis, and vascular biology, 2003. **23**(5): p. 795-801.
31. Seki, E., D.A. Brenner, and M. Karin, *A liver full of JNK: signaling in regulation of cell function and disease pathogenesis, and clinical approaches.* Gastroenterology, 2012. **143**(2): p. 307-320.
32. Sabapathy, K., et al., *Distinct roles for JNK1 and JNK2 in regulating JNK activity and c-Jun-dependent cell proliferation.* Molecular cell, 2004. **15**(5): p. 713-725.
33. Timokhina, I., et al., *Kit signaling through PI 3 - kinase and Src kinase pathways: an essential role for Rac1 and JNK activation in mast cell proliferation.* The EMBO Journal, 1998. **17**(21): p. 6250-6262.
34. Yoshizuka, N., et al., *PRAK suppresses oncogenic ras-induced hematopoietic cancer development by antagonizing the JNK pathway.* Molecular Cancer Research, 2012. **10**(6): p. 810-820.
35. Gupta, J., et al., *Dual Function of p38α MAPK in Colon Cancer: Suppression of Colitis-Associated Tumor Initiation but Requirement for Cancer Cell Survival.* Cancer cell, 2014. **25**(4): p. 484-500.
36. Korc, M., *p38 MAPK in Pancreatic Cancer: Finding a Protective Needle in the Haystack.* Clinical Cancer Research, 2014. **20**(23): p. 5866-5868.

37. Roca, H., et al., *IL‐4 induces proliferation in prostate cancer PC3 cells under nutrient‐depletion stress through the activation of the JNK‐pathway and survivin up‐regulation.* Journal of cellular biochemistry, 2012. **113**(5): p. 1569-1580.
38. Anastas, J.N. and R.T. Moon, *WNT signalling pathways as therapeutic targets in cancer.* Nature Reviews Cancer, 2013. **13**(1): p. 11-26.
39. Holland, J.D., et al., *Wnt signaling in stem and cancer stem cells.* Current opinion in cell biology, 2013. **25**(2): p. 254-264.
40. Ashkenazi, A., *Targeting the extrinsic apoptotic pathway in cancer: lessons learned and future directions.* The Journal of clinical investigation, 2015. **125**(2): p. 487-489.
41. Sharma, S., et al., *Cell Cycle and Apoptosis Regulatory Protein (CARP)-1 is Expressed inOsteoblasts and Regulated by PTH.* Biochemical and biophysical research communications, 2013. **436**(4): p. 607-612.
42. Kaufmann, S.H. and W.C. Earnshaw, *Induction of apoptosis by cancer chemotherapy.* Experimental cell research, 2000. **256**(1): p. 42-49.
43. Sabirzhanov, B., et al., *Downregulation of miR-23a and miR-27a following experimental traumatic brain injury induces neuronal cell death through activation of proapoptotic Bcl-2 proteins.* The Journal of Neuroscience, 2014. **34**(30): p. 10055-10071.
44. Chaudhary, P. and J.K. Vishwanatha, *c-Jun NH 2-terminal kinase-induced proteasomal degradation of c-FLIP L/S and Bcl 2 sensitize prostate cancer cells to Fas-and mitochondria-mediated apoptosis by tetrandrine.* Biochemical pharmacology, 2014. **91**(4): p. 457-473.
45. Elkholi, R. and J.E. Chipuk, *How do I kill thee? Let me count the ways: p53 regulates PARP‐1 dependent necrosis.* Bioessays, 2014. **36**(1): p. 46-51.
46. Hough, K.P., et al., *Transformed cell-specific induction of apoptosis by porcine circovirus type 1 viral protein 3.* Journal of General Virology, 2015. **96**(Pt 2): p. 351-359.
47. Connolly, R.M., N.K. Nguyen, and S. Sukumar, *Molecular pathways: current role and future directions of the retinoic acid pathway in cancer prevention and treatment.* Clinical Cancer Research, 2013. **19**(7): p. 1651-1659.
48. Liu, L., et al., *Sorafenib blocks the RAF/MEK/ERK pathway, inhibits tumor angiogenesis, and induces tumor cell apoptosis in hepatocellular carcinoma model PLC/PRF/5.* Cancer research, 2006. **66**(24): p. 11851-11858.
49. Kuwahara, Y., et al., *Targeting of tumor endothelial cells combining 2 Gy/day of X‐ray with Everolimus is the effective modality for overcoming clinically relevant radioresistant tumors.* Cancer medicine, 2014. **3**(2): p. 310-321.
50. Takata, M., et al., *Homologous recombination and non‐homologous end‐joining pathways of DNA double‐strand break repair have overlapping roles in the maintenance of chromosomal integrity in vertebrate cells.* The EMBO journal, 1998. **17**(18): p. 5497-5508.
51. Ewig, R.A. and K.W. Kohn, *DNA damage and repair in mouse leukemia L1210 cells treated with nitrogen mustard, 1, 3-bis (2-chloroethyl)-1-nitrosourea, and other nitrosoureas.* Cancer research, 1977. **37**(7 Part 1): p. 2114-2122.
52. Ward, J.F., *DNA damage produced by ionizing radiation in mammalian cells: identities, mechanisms of formation, and reparability*, in *Progress in nucleic acid research and molecular biology*. 1988, Elsevier. p. 95-125.
53. Fatur, T., T.T. Lah, and M. Filipič, *Cadmium inhibits repair of UV-, methyl methanesulfonate- and N-methyl-N-nitrosourea-induced DNA damage in Chinese hamster ovary cells.* Mutation Research/Fundamental and Molecular Mechanisms of Mutagenesis, 2003. **529**(1): p. 109-116.

54. H Koch, W. and M.R. Chedekel, *Photoinitiated DNA damage by melanogenic intermediates in vitro.* Photochemistry and photobiology, 1986. **44**(6): p. 703-710.
55. DeBerardinis, R.J. and N.S. Chandel, *Fundamentals of cancer metabolism.* Science advances, 2016. **2**(5): p. e1600200.
56. Shang, J., et al., *MicroRNA‐23a Antisense Enhances 5‐Fluorouracil Chemosensitivity Through APAF‐1/Caspase‐9 Apoptotic Pathway in Colorectal Cancer Cells.* Journal of cellular biochemistry, 2014. **115**(4): p. 772-784.
57. Sui, X., et al., *JNK confers 5-fluorouracil resistance in p53-deficient and mutant p53-expressing colon cancer cells by inducing survival autophagy.* Scientific reports, 2014. **4**: p. 4694.
58. Tournier, C., et al., *Requirement of JNK for stress-induced activation of the cytochrome c-mediated death pathway.* Science, 2000. **288**(5467): p. 870-874.
59. Tan, C., et al., *Daunomycin, an antitumor antibiotic, in the treatment of neoplastic disease. Clinical evaluation with special reference to childhood leukemia.* Cancer, 1967. **20**(3): p. 333-353.
60. Nakajima, H., et al., *FR901228, a potent antitumor antibiotic, is a novel histone deacetylase inhibitor.* Experimental cell research, 1998. **241**(1): p. 126-133.
61. Wang, G., et al., *Blocking p55PIK signaling inhibits proliferation and induces differentiation of leukemia cells.* Cell death and differentiation, 2012. **19**(11): p. 1870.
62. Shao, R.G., et al., *Replication‐mediated DNA damage by camptothecin induces phosphorylation of RPA by DNA‐dependent protein kinase and dissociates RPA: DNA‐PK complexes.* The EMBO journal, 1999. **18**(5): p. 1397-1406.
63. Niculescu, A.B., et al., *Effects of p21Cip1/Waf1 at both the G1/S and the G2/M cell cycle transitions: pRb is a critical determinant in blocking DNA replication and in preventing endoreduplication.* Molecular and cellular biology, 1998. **18**(1): p. 629-643.
64. Hato, S.V., et al., *Molecular pathways: the immunogenic effects of platinum-based chemotherapeutics.* Clinical Cancer Research, 2014. **20**(11): p. 2831-2837.
65. Glass, A.G., et al., *Breast cancer incidence, 1980–2006: combined roles of menopausal hormone therapy, screening mammography, and estrogen receptor status.* Journal of the National Cancer Institute, 2007. **99**(15): p. 1152-1161.
66. Paridaens, R., et al., *Mature results of a randomized phase II multicenter study of exemestane versus tamoxifen as first-line hormone therapy for postmenopausal women with metastatic breast cancer.* Annals of oncology, 2003. **14**(9): p. 1391-1398.
67. Henderson, V.W., *Alzheimer's disease: Review of hormone therapy trials and implications for treatment and prevention after menopause.* The Journal of steroid biochemistry and molecular biology, 2014. **142**: p. 99-106.
68. Gomez-Coronado, D., et al., *Effect of tamoxifen, raloxifene and toremifene on ldl receptor activity in lymphocytes from normolipidemic and familial hypercholesterolemic subjects.* Atherosclerosis, 2014. **235**(2): p. e105-e106.
69. Goss, P.E., et al., *See also Breast Cancer; Breast Cancer Treatments; Gynecomastia; Hormones.* Cultural Encyclopedia of the Breast, 2014: p. 129.
70. Bao, T., et al., *Patient‐reported outcomes in women with breast cancer enrolled in a dual‐center, double‐blind, randomized controlled trial assessing the effect of acupuncture in reducing aromatase inhibitor‐induced musculoskeletal symptoms.* Cancer, 2014. **120**(3): p. 381-389.

71. Kim, J., G. Jayaprakasha, and B.S. Patil, *Obacunone exhibits anti-proliferative and anti-aromatase activity in vitro by inhibiting the p38 MAPK signaling pathway in MCF-7 human breast adenocarcinoma cells.* Biochimie, 2014. **105**: p. 36-44.
72. Sabine, V.S., et al., *Mutational analysis of PI3K/AKT signaling pathway in tamoxifen exemestane adjuvant multinational pathology study.* Journal of Clinical Oncology, 2014. **32**(27): p. 2951-2958.
73. Mao, Z., et al., *Tamoxifen reduces P-gp-mediated multidrug resistance via inhibiting the PI3K/Akt signaling pathway in ER-negative human gastric cancer cells.* Biomedicine & Pharmacotherapy, 2014. **68**(2): p. 179-183.
74. Orchard, T.S., et al., *Abstract P1-09-30: Relationship of dietary and red blood cell polyunsaturated fatty acids to inflammatory markers in breast cancer survivors taking aromatase inhibitors.* Cancer Research, 2015. **75**(9 Supplement): p. P1-09-30-P1-09-30.
75. Kwan, M.L., et al., *Prior bone health history in breast cancer patients on aromatase inhibitors.* Cancer Research, 2014. **74**(19 Supplement): p. 2162-2162.
76. Huang, X., et al., *Polysaccharides derived from Lycium barbarum suppress IGF-1-induced angiogenesis via PI3K/HIF-1α/VEGF signalling pathways in MCF-7 cells.* Food Chemistry, 2012. **131**(4): p. 1479-1484.
77. Cai, J.-P., et al., *Panax ginseng polysaccharide suppresses metastasis via modulating Twist expression in gastric cancer.* International journal of biological macromolecules, 2013. **57**: p. 22-25.
78. Boon, H.S., F. Olatunde, and S.M. Zick, *Trends in complementary/alternative medicine use by breast cancer survivors: comparing survey data from 1998 and 2005.* BMC women's health, 2007. **7**(1): p. 4.
79. Siegel, R., et al., *Cancer treatment and survivorship statistics, 2012.* CA: a cancer journal for clinicians, 2012. **62**(4): p. 220-241.
80. Wang, S., et al., *Traditional chinese medicine.* Complementary and alternative therapies for epilepsy, 2005: p. 177-182.
81. Efferth, T., et al., *From traditional Chinese medicine to rational cancer therapy.* Trends in molecular medicine, 2007. **13**(8): p. 353-361.
82. Qi, F., et al., *Chinese herbal medicines as adjuvant treatment during chemoor radio-therapy for cancer.* Bioscience trends, 2010. **4**(6).
83. Li, W., et al., *Natural medicines used in the traditional Chinese medical system for therapy of diabetes mellitus.* Journal of ethnopharmacology, 2004. **92**(1): p. 1-21.
84. Hsiao, W.W. and L. Liu, *The role of traditional Chinese herbal medicines in cancer therapy–from TCM theory to mechanistic insights.* Planta medica, 2010. **76**(11): p. 1118-1131.
85. Lu, J.-J., et al., *Alkaloids isolated from natural herbs as the anticancer agents.* Evidence-Based Complementary and Alternative Medicine, 2012. **2012**.
86. Cai, Y., et al., *Antioxidant activity and phenolic compounds of 112 traditional Chinese medicinal plants associated with anticancer.* Life sciences, 2004. **74**(17): p. 2157-2184.
87. Cragg, G.M. and D.J. Newman, *Plants as a source of anti-cancer agents.* Journal of ethnopharmacology, 2005. **100**(1-2): p. 72-79.
88. Liu, Y., et al., *Anti-tumor activities of matrine and oxymatrine: literature review.* Tumor Biology, 2014. **35**(6): p. 5111-5119.
89. Yong, J., X. Wu, and C. Lu, *Anticancer advances of matrine and its derivatives.* Current pharmaceutical design, 2015. **21**(25): p. 3673-3680.

90. Ma, L., et al., *Matrine suppresses cell growth of human chronic myeloid leukemia cells via its inhibition of the interleukin-6/Janus activated kinase/signal transducer and activator of transcription 3 signaling cohort.* Leukemia & lymphoma, 2015. **56**(10): p. 2923-2930.
91. Zhao, Z., et al., *Fufang Kushen injection inhibits sarcoma growth and tumor-induced hyperalgesia via TRPV1 signaling pathways.* Cancer letters, 2014. **355**(2): p. 232-241.
92. Jiang, H., et al., *Matrine upregulates the cell cycle protein E2F-1 and triggers apoptosis via the mitochondrial pathway in K562 cells.* European journal of pharmacology, 2007. **559**(2-3): p. 98-108.
93. Liu, X.-S. and J. Jiang, *Molecular mechanism of matrine-induced apoptosis in leukemia K562 cells.* The American journal of Chinese medicine, 2006. **34**(06): p. 1095-1103.
94. Wang, P., et al., *Overcome cancer cell drug resistance using natural products.* Evidence-Based Complementary and Alternative Medicine, 2015. **2015**.
95. Jordan, M., *Mechanism of action of antitumor drugs that interact with microtubules and tubulin.* Current Medicinal Chemistry-Anti-Cancer Agents, 2002. **2**(1): p. 1-17.
96. Liu, Z., et al., *The Upregulation of PI3K/Akt and MAP Kinase Pathways is Associated with Resistance of Microtubule‐Targeting Drugs in Prostate Cancer.* Journal of cellular biochemistry, 2015. **116**(7): p. 1341-1349.
97. Dang, Y.-P., et al., *Curcumin improves the paclitaxel-induced apoptosis of HPV-positive human cervical cancer cells via the NF-κB-p53-caspase-3 pathway.* Experimental and therapeutic medicine, 2015. **9**(4): p. 1470-1476.
98. Hsiang, Y.-H., M.G. Lihou, and L.F. Liu, *Arrest of replication forks by drug-stabilized topoisomerase I-DNA cleavable complexes as a mechanism of cell killing by camptothecin.* Cancer research, 1989. **49**(18): p. 5077-5082.
99. Dietlein, F., L. Thelen, and H.C. Reinhardt, *Cancer-specific defects in DNA repair pathways as targets for personalized therapeutic approaches.* Trends in genetics, 2014. **30**(8): p. 326-339.
100. Long, C., et al., *Triptolide inhibits transcription of hTERT through down-regulation of transcription factor specificity protein 1 in primary effusion lymphoma cells.* Biochemical and biophysical research communications, 2016. **469**(1): p. 87-93.
101. Simpson, B., et al., *Arid awakening: new opportunities for Australian plant natural product research.* The Rangeland Journal, 2016. **38**(5): p. 467-478.
102. Boyle, G.M., et al., *Intra-lesional injection of the novel PKC activator EBC-46 rapidly ablates tumors in mouse models.* PLoS One, 2014. **9**(10): p. e108887.
103. Ming, M., et al., *Dose-dependent AMPK-dependent and independent mechanisms of berberine and metformin inhibition of mTORC1, ERK, DNA synthesis and proliferation in pancreatic cancer cells.* PloS one, 2014. **9**(12): p. e114573.
104. Liu, Q., et al., *Berberine induces senescence of human glioblastoma cells by downregulating the EGFR–MEK–ERK signaling pathway.* Molecular cancer therapeutics, 2015. **14**(2): p. 355-363.
105. Kim, J., et al., *The alkaloid Berberine inhibits the growth of Anoikis-resistant MCF-7 and MDA-MB-231 breast cancer cell lines by inducing cell cycle arrest.* Phytomedicine, 2010. **17**(6): p. 436-440.
106. Shukla, S., et al., *Apigenin inhibits prostate cancer progression in TRAMP mice via targeting PI3K/Akt/FoxO pathway.* Carcinogenesis, 2013. **35**(2): p. 452-460.
107. Jiang, K., et al., *Silibinin, a natural flavonoid, induces autophagy via ROS-dependent mitochondrial dysfunction and loss of ATP involving BNIP3 in human MCF7 breast cancer cells.* Oncology reports, 2015.

108. Balachandran, C., et al., *A flavonoid isolated from Streptomyces sp.(ERINLG-4) induces apoptosis in human lung cancer A549 cells through p53 and cytochrome c release caspase dependant pathway.* Chemico-biological interactions, 2014. **224**: p. 24-35.
109. Wang, N., et al., *Dietary compound Isoliquiritigenin prevents mammary carcinogenesis by inhibiting breast cancer stem cells through WIF1 demethylation.* Oncotarget, 2015.
110. Chang, W.T., et al., *Specific Medicinal Plant Polysaccharides Effectively Enhance the Potency of a DC-Based Vaccine against Mouse Mammary Tumor Metastasis.* PloS one, 2015. **10**(3).
111. Safdari, Y., et al., *Natural inhibitors of PI3K/AKT signaling in breast cancer: Emphasis on newly-discovered molecular mechanisms of action.* Pharmacological Research, 2015. **93**: p. 1-10.
112. Fernando, W., H. Vasantha Rupasinghe, and D. W Hoskin, *Regulation of Hypoxia-inducible Factor-1α and Vascular Endothelial Growth Factor Signaling by Plant Flavonoids.* Mini reviews in medicinal chemistry, 2015. **15**(6): p. 479-489.
113. Park, S.T., et al., *Suppression of VEGF expression through interruption of the HIF-1α and Akt signaling cascade modulates the anti-angiogenic activity of DAPK in ovarian carcinoma cells.* Oncology reports, 2014. **31**(2): p. 1021-1029.
114. Mirzoeva, S., C.A. Franzen, and J.C. Pelling, *Apigenin inhibits TGF‐β‐induced VEGF expression in human prostate carcinoma cells via a Smad2/3‐and Src‐dependent mechanism.* Molecular carcinogenesis, 2014. **53**(8): p. 598-609.
115. Liu, L.-Z., et al., *Acacetin inhibits VEGF expression, tumor angiogenesis and growth through AKT/HIF-1α pathway.* Biochemical and biophysical research communications, 2011. **413**(2): p. 299-305.
116. Tai, Z., et al., *Luteolin sensitizes the antiproliferative effect of interferon α/β by activation of Janus kinase/signal transducer and activator of transcription pathway signaling through protein kinase A-mediated inhibition of protein tyrosine phosphatase SHP-2 in cancer cells.* Cellular signalling, 2014. **26**(3): p. 619-628.
117. Chian, S., et al., *Luteolin sensitizes two oxaliplatin-resistant colorectal cancer cell lines to chemotherapeutic drugs via inhibition of the nrf2 pathway.* Asian Pac J Cancer Prev, 2014. **15**(6): p. 2911-2916.
118. Qu, Q., et al., *Luteolin potentiates the sensitivity of colorectal cancer cell lines to oxaliplatin through the PPARγ/OCTN2 pathway.* Anti-cancer drugs, 2014. **25**(9): p. 1016-1027.
119. Gao, A.-M., et al., *Chrysin enhances sensitivity of BEL-7402/ADM cells to doxorubicin by suppressing PI3K/Akt/Nrf2 and ERK/Nrf2 pathway.* Chemico-biological interactions, 2013. **206**(1): p. 100-108.
120. Tran, T.A., et al., *Mechanism of 2′, 3′-dimethoxyflavanone-induced apoptosis in breast cancer stem cells: Role of ubiquitination of caspase-8 and LC3.* Archives of biochemistry and biophysics, 2014. **562**: p. 92-102.
121. Bae, I.H., et al., *3-Hydroxy-3′, 4′-dimethoxyflavone suppresses Bcl-w-induced invasive potentials and stemness in glioblastoma multiforme.* Biochemical and biophysical research communications, 2014. **450**(1): p. 704-710.
122. Chien, S.-T., et al., *Galangin, a novel dietary flavonoid, attenuates metastatic feature via PKC/ERK signaling pathway in TPA-treated liver cancer HepG2 cells.* Cancer cell international, 2015. **15**(1): p. 15.
123. Khan, N., et al., *Dual inhibition of phosphatidylinositol 3‐kinase/Akt and mammalian target of rapamycin signaling in human nonsmall cell lung cancer cells by a dietary flavonoid fisetin.* International Journal of Cancer, 2012. **130**(7): p. 1695-1705.

124. He, X., et al., *Immunomodulatory activities of five clinically used Chinese herbal polysaccharides.* Journal of Experimental and Integrative Medicine, 2012. **2**(1): p. 15-27.
125. Liu, X., et al., *Structure characterization and antitumor activity of a polysaccharide from the alkaline extract of king oyster mushroom.* Carbohydrate polymers, 2015. **118**: p. 101-106.
126. Liu, J.-Y., et al., *Polysaccharides from Dioscorea batatas induce tumor necrosis factor-α secretion via Toll-like receptor 4-mediated protein kinase signaling pathways.* Journal of agricultural and food chemistry, 2008. **56**(21): p. 9892-9898.
127. Wei, W.-C., et al., *Polysaccharides from Dioscorea (山藥 Shān Yào) and other phytochemicals enhance antitumor effects induced by DNA vaccine against melanoma.* Journal of traditional and complementary medicine, 2014. **4**(1): p. 42-48.
128. Lee, B.-H., et al., *Inhibition of leukemia proliferation by a novel polysaccharide identified from Monascus-fermented dioscorea via inducing differentiation.* Food & function, 2012. **3**(7): p. 758-764.
129. Zhao, X., et al., *A polysaccharide from Trametes robiniophila inhibits human osteosarcoma xenograft tumor growth in vivo.* Carbohydrate polymers, 2015. **124**: p. 157-163.
130. Kennedy, L.C., et al., *A new era for cancer treatment: gold‐nanoparticle‐mediated thermal therapies.* Small, 2011. **7**(2): p. 169-183.
131. Park, C.M., C.W. Cho, and Y.S. Song, *TOP 1 and 2, polysaccharides from Taraxacum officinale, inhibit NFκB-mediated inflammation and accelerate Nrf2-induced antioxidative potential through the modulation of PI3K-Akt signaling pathway in RAW 264.7 cells.* Food and Chemical Toxicology, 2014. **66**: p. 56-64.
132. Jayaram, S., S. Kapoor, and S.M. Dharmesh, *Pectic polysaccharide from corn (Zea mays L.) effectively inhibited multi-step mediated cancer cell growth and metastasis.* Chemico-biological interactions, 2015. **235**: p. 63-75.
133. Shen, Z.-X., et al., *Use of arsenic trioxide (As2O3) in the treatment of acute promyelocytic leukemia (APL): II. Clinical efficacy and pharmacokinetics in relapsed patients.* Blood, 1997. **89**(9): p. 3354-3360.
134. Antman, K.H., *Introduction: the history of arsenic trioxide in cancer therapy.* The oncologist, 2001. **6**(Supplement 2): p. 1-2.
135. Beauchamp, E.M., R. Serrano, and L.C. Platanias, *Regulatory effects of arsenic on cellular signaling pathways: biological effects and therapeutic implications*, in *Nuclear Signaling Pathways and Targeting Transcription in Cancer*. 2014, Springer. p. 107-119.
136. Zhu, C., et al. *Treatment of acute promyelocytic leukemia with arsenic compounds: in vitro and in vivo studies*. in *Seminars in hematology*. 2001. Elsevier.
137. Göhrig, A., et al., *Axon guidance factor SLIT2 inhibits neural invasion and metastasis in pancreatic cancer.* Cancer research, 2014. **74**(5): p. 1529-1540.
138. He, J., et al., *Chronic arsenic exposure and angiogenesis in human bronchial epithelial cells via the ROS/miR-199a-5p/HIF-1α/COX-2 pathway.* Environmental health perspectives, 2014. **122**(3): p. 255.
139. Chen, S., et al., *Realgar exerts cytotoxic killing of gastric cancer cells through Bax apoptotic pathway.* Cancer Research, 2013. **73**(8 Supplement): p. 2110-2110.
140. Liu, X., et al., *Realgar induces apoptosis in the chronic lymphocytic leukemia cell line MEC-1.* Molecular medicine reports, 2013. **8**(6): p. 1866-1870.
141. Wang, W., et al., *Anti-tumor activities of active ingredients in Compound Kushen Injection.* Acta Pharmacologica Sinica, 2015. **36**(6): p. 676.

142. Sun, M., et al., *Antitumor activities of kushen: literature review.* Evidence-Based Complementary and Alternative Medicine, 2012. **2012**.
143. Guo, Y.-m., et al., *Efficacy of compound kushen injection in relieving cancer-related pain: a systematic review and meta-analysis.* Evidence-Based Complementary and Alternative Medicine, 2015. **2015**.
144. Qu, Z., et al., *Identification of candidate anti-cancer molecular mechanisms of Compound Kushen Injection using functional genomics.* Oncotarget, 2016. **7**(40): p. 66003-66019.
145. Zhou, S.-K., et al., *Antioxidant and immunity activities of Fufang Kushen injection liquid.* Molecules, 2012. **17**(6): p. 6481-6490.
146. Kong, D.X., et al., *How many traditional Chinese medicine components have been recognized by modern Western medicine? A chemoinformatic analysis and implications for finding multicomponent drugs.* ChemMedChem: Chemistry Enabling Drug Discovery, 2008. **3**(2): p. 233-236.
147. Herrick, T.M. and R.P. Million, *Tapping the potential of fixed-dose combinations*. 2007, Nature Publishing Group.
148. Verpoorte, R., Y.H. Choi, and H.K. Kim, *Ethnopharmacology and systems biology: a perfect holistic match.* Journal of Ethnopharmacology, 2005. **100**(1-2): p. 53-56.
149. Barabasi, A.-L. and Z.N. Oltvai, *Network biology: understanding the cell's functional organization.* Nature reviews genetics, 2004. **5**(2): p. 101.
150. Syed, B.A., *The breast cancer market.* Nature Reviews Drug Discovery, 2015. **14**(4): p. 233-234.
151. Torre, L.A., et al., *Global cancer statistics, 2012.* CA: a cancer journal for clinicians, 2015. **65**(2): p. 87-108.
152. Kang, X.-H., et al., *Bufalin reverses HGF-induced resistance to EGFR-TKIs in EGFR mutant lung cancer cells via blockage of Met/PI3k/Akt pathway and induction of apoptosis.* Evidence-Based Complementary and Alternative Medicine, 2013. **2013**.
153. CAI, M.-m., et al., *Study on the TCM constitution distribution of drug addicts under compulsory and its influence factors.* China Journal of Traditional Chinese Medicine and Pharmacy, 2014. **8**: p. 024.

Chapter 2

Identification of Candidate Anti-cancer Molecular Mechanisms of Compound Kushen Injection Using Functional Genomics

CKI is used as an adjuvant to cancer chemo- and radiotherapy in the clinic. Several cancer cell lines, including MCF-7, have been reported to be sensitive to treatment with CKI. In this chapter, we introduce an approach for comparing the effects on MCF-7 cells of CKI and the chemotherapeutic agent 5-Fluorouracil (5-FU) at the phenotype and transcriptome level, in order to identify similarities and differences in their molecular responses. We determined that CKI primarily affects regulation of the cell cycle and associated biological processes and that CKI behaved differently to 5-FU. We also identify lncRNA regulated by CKI, including one known to be important in tumor phenotype. This chapter is in the format of the manuscript that was published in *Oncotarget*.

Statement of Authorship

Title of Paper	Identification of candidate anti-cancer molecular mechanisms of Compound Kushen Injection using functional genomics
Publication Status	☑ Published ☐ Accepted for Publication ☐ Submitted for Publication ☐ Unpublished and Unsubmitted work written in manuscript style
Publication Details	Qu, Zhipeng, Jian Cui, Yuka Harata-Lee, Thazin Nwe Aung, Qianjin Feng, Joy M. Raison, Robert Daniel Kortschak, and David L. Adelson. "Identification of candidate anti-cancer molecular mechanisms of Compound Kushen Injection using functional genomics." Oncotarget 7, no. 40 (2016): 66003-66019. DOI: https://doi.org/10.18632/oncotarget.11788

Co-Author

Name of Principal Author (Candidate)	Jian Cui		
Contribution to the Paper	Experimental design, assisted with experiments, assisted with data analysis		
Overall percentage (%)	30%		
Certification:	This paper reports on original research I conducted during the period of my Higher Degree by Research candidature and is not subject to any obligations or contractual agreements with a third party that would constrain its inclusion in this thesis. I am the second author of this paper.		
Signature		Date	18/6/18

Co-Author Contributions

By signing the Statement of Authorship, each author certifies that:

i. the candidate's stated contribution to the publication is accurate (as detailed above);

ii. permission is granted for the candidate in include the publication in the thesis; and

iii. the sum of all co-author contributions is equal to 100% less the candidate's stated contribution.

Name of Principal Author	Zhipeng Qu		
Contribution to the Paper	Experimental design, carried out experiments, analysed data, wrote paper		
Signature		Date	18/06/18

Name of Co-Author	Yuka Harata-Lee		
Contribution to the Paper	Experimental design, assisted with experiments, assisted with data analysis, wrote paper		
Signature		Date	14.6.18

Name of Co-Author	Thazin Nwe Aung		
Contribution to the Paper	Assisted with experiments		
Signature		Date	12/06/2018

Name of Co-Author	Qianjin Feng		
Contribution to the Paper	Assisted with experimental design, assisted with experiments		
Signature		Date	2018. 6. 19.

Name of Co-Author	Joy M. Raison		
Contribution to the Paper	Experimental design		
Signature		Date	19/6/2018

Name of Co-Author	Robert Daniel Kortschak,		
Contribution to the Paper	Experimental design		
Signature		Date	18/6/18

Name of Co-Author	David L. Adelson		
Contribution to the Paper	Supervised the research, acquired funding for the experiments, experimental design, wrote paper		
Signature		Date	18/6/2018

Research Paper

Identification of candidate anti-cancer molecular mechanisms of Compound Kushen Injection using functional genomics

Zhipeng Qu[1], Jian Cui[1,*], Yuka Harata-Lee[1,*], Thazin Nwe Aung[1], Qianjin Feng[2], Joy M. Raison[1], Robert Daniel Kortschak[1], David L. Adelson[1]

[1]Department of Genetics and Evolution, School of Biological Sciences, The University of Adelaide, Adelaide, South Australia 5005, Australia

[2]Shanxi Modern Chinese Medicine Engineering Laboratory, Shanxi University of Traditional Chinese Medicine, Shanxi 030619, China

[*]These authors contributed equally to this work

Correspondence to: *David L. Adelson,* ***email:*** *david.adelson@adelaide.edu.au*

Keywords: *systems biology, traditional Chinese medicine, lncRNA, transcriptome*

Received: *March 02, 2016* ***Accepted:*** *August 24, 2016* ***Published:*** *September 01, 2016*

ABSTRACT

Compound Kushen Injection (CKI) has been clinically used in China for over 15 years to treat various types of solid tumours. However, because such Traditional Chinese Medicine (TCM) preparations are complex mixtures of plant secondary metabolites, it is essential to explore their underlying molecular mechanisms in a systematic fashion. We have used the MCF-7 human breast cancer cell line as an initial *in vitro* model to identify CKI induced changes in gene expression. Cells were treated with CKI for 24 and 48 hours at two concentrations (1 and 2 mg/mL total alkaloids), and the effect of CKI on cell proliferation and apoptosis were measured using XTT and Annexin V/Propidium Iodide staining assays respectively. Transcriptome data of cells treated with CKI or 5-Fluorouracil (5-FU) for 24 and 48 hours were subsequently acquired using high-throughput Illumina RNA-seq technology. In this report we show that CKI inhibited MCF-7 cell proliferation and induced apoptosis in a dose-dependent fashion. We integrated and applied a series of transcriptome analysis methods, including gene differential expression analysis, pathway over-representation analysis, *de novo* identification of long non-coding RNAs (lncRNA) as well as co-expression network reconstruction, to identify candidate anti-cancer molecular mechanisms of CKI. Multiple pathways were perturbed and the cell cycle was identified as the potential primary target pathway of CKI in MCF-7 cells. CKI may also induce apoptosis in MCF-7 cells via a p53 independent mechanism. In addition, we identified novel lncRNAs and showed that many of them might be expressed as a response to CKI treatment.

INTRODUCTION

The complexity of carcinogenesis at the genetic level has been investigated more and more deeply by leveraging fast-developing omics-related techniques in the past decades [1–3]. Novel genetic mutations and molecular markers are now comprehensively identified in cancer genome sequencing projects. More importantly, whole transcriptome analyses are much more widely used to identify novel cancer-related transcripts or regulatory elements, such as long non-protein-coding RNAs (lncRNAs) and alternative splicing, and are also used to characterise the underlying molecular mechanisms based on global gene expression changes in different types of cancers *in vivo* or *in vitro* [4–6]. The current challenge is to integrate these new techniques to discover or evaluate novel cancer therapies [7].

Traditional Chinese Medicines (TCMs) are experience-based remedies derived from hundreds or thousands of years of clinical use in China. Most TCMs are extracted from one or more medicinal herbs. The existence of multiple bioactive ingredients makes many TCMs potential novel resources for the discovery of new cancer drugs, such as multi-targeted cancer drugs [8]. Compound Kushen Injection (CKI, also known as Yanshu injection) is a State Administration of Chinese Medicine-

approved TCM formula used in the clinical treatment of various types of cancers in China [9, 10]. It is extracted from the roots of two medicinal herbs, Kushen (*Radix Sophorae Flavescentis*) and Baituling (*Rhizoma smilacis Glabrae*), using modern standardised Good Manufacturing Processes (GMP) [11, 12]. The chemical fingerprint of CKI contains at least 8 different components, with primary compounds Matrine and Oxymatrine [12]. This indicates that multiple compounds in CKI may deliver an integrated anti-tumor effect through multiple targets and their associated molecular pathways.

By detecting the expression of key genes or proteins in single molecular pathways, the anti-tumor effects of Matrine or Oxymatrine, including the inhibition of cell proliferation and induction of apoptosis, have been demonstrated in various types of cancer [13–17]. The molecular mechanisms of CKI as a system have also been recently explored [11, 18]. Quantitative detection of expression changes of key regulators, including *beta-catenin*, *CyclinD1* and *c-Myc*, of the canonical Wnt/beta-catenin pathway, have shown that CKI can suppress the stem cells in MCF-7 cells by down-regulating this signalling pathway [11]. In addition, other studies suggest that CKI can inhibit mouse sarcoma growth and reduce tumor-induced hyperalgesia via the AKT and TRPV1 signalling pathways by reducing the phosphorylation of ERK and AKT kinases and BAD [18].

The main goal of modern pharmacology is to elucidate the molecular mechanisms that can be targeted by therapeutic compounds. Analyses using purified single components of TCM can be somewhat useful, but are limited when it comes to identifying integrated systemic effects resulting from a multi-compound formula. Furthermore, previous studies attempting to understand the mode of action of CKI have only focused on single or a few molecular pathways by assessing the expression of key regulators in these pathways. We have therefore, taken advantage of high throughput whole transcriptome analyses, and applied these to explore the system wide molecular mechanisms targeted by TCM. We have identified a comprehensive list of expressed genes perturbed by CKI, and used gene expression data to characterise molecular pathways potentially targeted by CKI in MCF-7 human breast cancer cells. Our results show that CKI can alter the expression of many cancer relevant genes and lncRNAs, correlated with the inhibition of cell proliferation through cell cycle arrest and the induction of apoptosis via p53 independent pathways.

RESULTS

CKI inhibits MCF-7 cell proliferation and induces cell apoptosis

To characterise the effect of CKI on proliferation of MCF-7 breast cancer cells, we used the XTT assay to measure cell viability after treating with different doses of CKI. The proliferation of MCF-7 cells was dramatically inhibited when treated with a high dose of CKI (2 mg/mL, based on the total alkaloid concentration in CKI) and showed a dose-dependent effect (Figure 1A and Supplementary Figure 1A). An Annexin V/Propidium Iodide (PI) assay was used to quantify cell apoptosis when MCF-7 cells were treated with CKI. Percentage of apoptotic cells, particularly at the higher dose of CKI, was increased at both time points compared with untreated cells, indicating that apoptosis was induced in cells treated with CKI (Figure 1B and 1C). The caspase3/7 colorimetric assay also showed that there was increased caspase3/7 activity in cells treated with CKI (Supplementary Figure 1B). Altogether, these results showed that CKI could inhibit growth and induce apoptosis of MCF-7 cells *in vitro*.

Global gene expression changes in MCF-7 cells treated with CKI

To further investigate the underlying molecular mechanisms of CKI on MCF-7 cells, we performed high-depth next generation sequencing using an Illumina HiSeq 2500. In total, more than 732 million stranded 100 basepairs (bp) paired-end reads were sequenced from 9 groups of MCF-7 cells treated with two doses of CKI or one dose of chemotherapy drug 5-Fluorouracil (5-FU) for 24 and 48 hours along with untreated cells (Supplementary Table 1) (GSE78512). The global gene expression profiles of CKI treated cells, particularly in cells treated with high dose CKI (2 mg/mL), were clearly different from the profile of 5-FU treated cells compared with untreated cells (Supplementary Figure 2). We then used edgeR to identify the statistically significant differentially expressed (DE) genes for the pairwise comparisons between cells treated with 1 mg/mL CKI, 2 mg/mL CKI and 5-FU for 24 or 48 hours respectively (Figure 2 and Supplementary Table 2). Compared with untreated cells, fewer than 200 genes had significantly altered expression in cells treated with low dose CKI (1 mg/mL) for 24 or 48 hours (Figure 2A and 2B). However, many more DE genes (1,826 genes for 24 hours and 2,904 for 48 hours) were identified in cells treated with high dose CKI (2 mg/mL). Interestingly, when comparing the number of DE genes in cells treated with high dose CKI with low dose CKI, we observed almost twice as many genes down-regulated but only a small number of genes (828 to 791) up-regulated (Figure 2A and 2B). Furthermore, we compared DE genes in cells treated with high dose CKI and in cells treated with 5-FU (Supplementary Figure 3). For up-regulated genes in cells treated with high dose CKI for 24 hours, approximately half (396 out of 791) of these were also identified as DE genes, with most (384) being up-regulated in 5-FU treated cells as well. 459 down-regulated genes were also shown as DE genes with most of these (424 out of 459) also being down-regulated in cells treated with 5- FU for 24 hours (Supplementary Figure 3A). After cells were treated with CKI or 5-FU for 48 hours, the number

of DE genes decreased dramatically in 5-FU treated cells, but greatly increased in cells treated with 2 mg/mL CKI (Supplementary Figure 3B). The common DE genes altered by CKI or 5-FU showed consistent expression changes at 48 hours (Supplementary Figure 3B).

To validate the gene expression changes from transcriptome analysis, we performed quantitative PCR (qPCR) for 6 genes and acquired overall consistent results (Figure 2C, Supplementary Figure 4 and Supplementary Table 2).

Annotation of the molecular pathways altered by CKI in MCF-7 cells

Since CKI likely contains multiple bioactive ingredients, we used a number of systems biology methods to explore the molecular mechanisms of CKI.

The over-represented Gene Ontology (GO) terms for all DE genes identified in cells treated with high dose CKI (2 mg/mL) for 24 hour and 48 hours are shown in Figure 3A and 3B. Based on their functional similarity, these GO terms were clustered into several primary categories, including "Regulation of biological process, cellular process and metabolic process", "Cell differentiation, development", "Transport, localisation", "Chromatin organisation, organelle organisation", "Cell motility and migration" and "Secondary metabolic processes and reactive oxygen species metabolic". Interestingly, we found that the majority of cell growth or proliferation related GO terms included more down-regulated genes, while GO terms associated with "Secondary metabolic processes and reactive oxygen species metabolic" showed enrichment of more up-regulated genes (Figure 3A). In MCF-7 cells treated with CKI for 48 hours, similar categories of over-represented GO terms seen at 24 hours were also observed, such as "Metabolic process", "Regulation of metabolic process" and "Localization". In addition, cell proliferation related terms, including "Cell cycle", "Cell growth" and "Cell death" were also over-represented in DE genes from cells treated with CKI for 48 hours (Figure 3B). Furthermore, we compared the over-representation of GO terms of the 200 most significantly

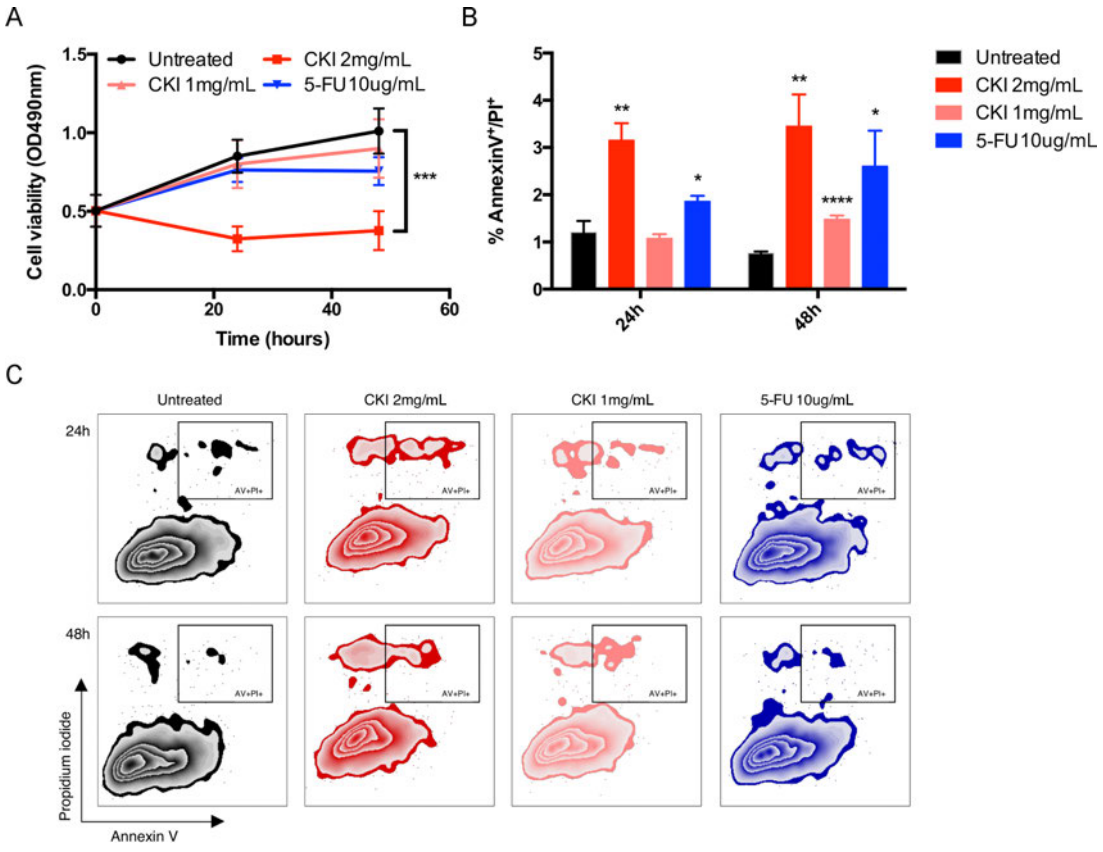

Figure 1: CKI inhibits proliferation and induces apoptosis of MCF-7 cells. A. Inhibition of MCF-7 cell proliferation with CKI treatment. The level of viability of cells under different treatments was measured using XTT:PMS. Data are represented as mean ±SEM (n=6). **B.** and **C.** Induction of apoptosis in MCF-7 cells with CKI treatment. The level of apoptosis was determined by measuring the levels of Annexin V and PI staining: B) Percentages of Annexin V^+/PI^+ cells, and C) representative plots of Annexin V and PI staining. Data are represented as mean ±SEM (n=6). Statistical analyses were performed using A) two-way ANOVA or B) t-test comparing with "untreated" (*p<0.05, **p<0.01, ****p<0.0001).

DE genes in cells treated with CKI or 5-FU for 24 hours or 48 hours (Figure 3C and 3D). In cells treated with CKI or 5-FU for 24 hours, over-represented GO terms were generally divided into two clusters with respect to the different expression status of the genes that contributed to each term. Terms such as "Cellular hormone metabolic process" and "Pigment metabolic process" were dominated by up-regulated genes, which were mainly DE genes from CKI treated cells only. On the other hand, terms represented by "Chromosome segregation", "Cell cycle",

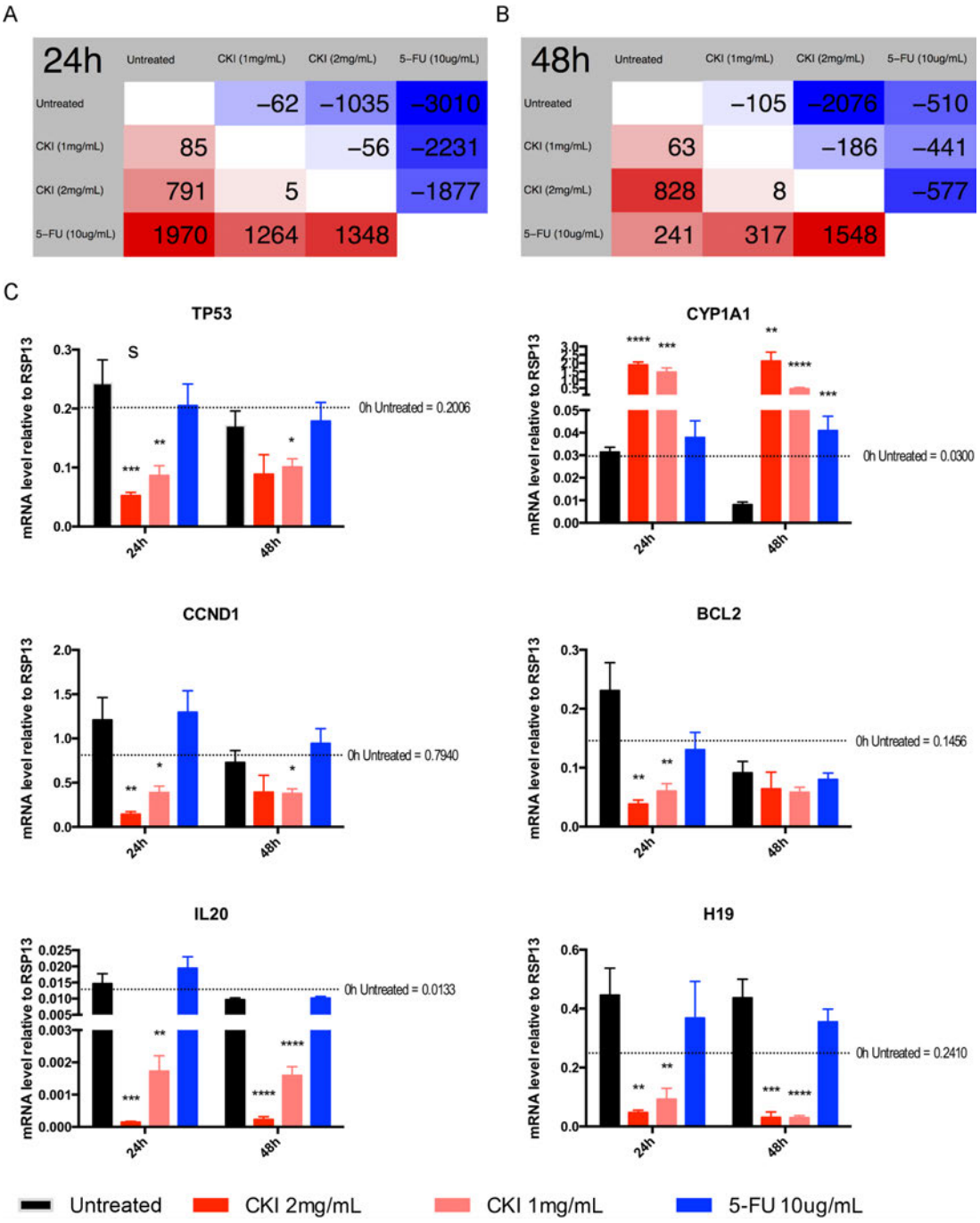

Figure 2: Differential gene expression in MCF-7 cells treated with CKI or 5-FU for 24 and 48 hours. Numbers of DE genes (FDR < 0.05 according to edgeR) between different groups at **A.** 24 hours or **B.** 48 hours time. Comparison is based on row against column. Therefore, cells with a red background show numbers of up-regulated genes and cells with a blue background show numbers of down-regulated genes. **C.** Validation of transcriptome sequencing. Total of 6 DE genes (*TP53*, *CCND1*, *CYP1A1*, *BCL2*, *IL-20* and *H19*) identified by transcriptome sequencing were selected and were subjected to validation analysis by qPCR. Data are represented as mean ±SEM (n=9). Statistical analyses were performed using t-test comparing with "untreated" (*p<0.05, **p<0.01, ***p<0.001, ****p<0.0001).

"Meiotic nuclear division" and "Somatic diversification of immune receptors", were mainly contributed by down-regulated genes, particularly DE genes from 5-FU treated cells. After 48 hours, the same over-represented GO terms in cells treated with CKI or 5-FU for 24 hours were found, but the proportions of DE genes from cells treated with CKI were increased for most of these terms, particularly for "Chromosome segregation" related terms. In addition, more significantly over-represented GO terms were found in cells treated with CKI or 5-FU for 48 hours compared to those in 24 hours, such as "Regulation of viral process" and "Negative regulation of intracellular transport", and the majority of DE genes that contributed to these terms were down-regulated in cells treated with CKI.

In order to further characterise the potential functional pathways altered by CKI, we performed over-representation analysis of Kyoto Encyclopedia of Genes and Genomes (KEGG) pathways for all DE genes in cells treated with high dose CKI. Metabolic pathways represented by "Steroid hormone biosynthesis", and including "Pentose and glucuronate interconversions" and "Drug metabolism" and so on, were over-represented based on DE genes in cells treated with CKI for 24 hours (Figure 4A). The majority of DE genes that contributed to these terms were up-regulated (Figure 4A). Over-represented cell growth related pathways, such as "Cell cycle" and "DNA replication", were also observed (Figure 4A). In addition, cancer-related pathways, such as "Prostate cancer", "Bladder cancer" and "MicroRNA in cancer", were also shown as over-represented pathways. It is also interesting to note that DE genes that contributed to cell growth and cancer related pathways were generally

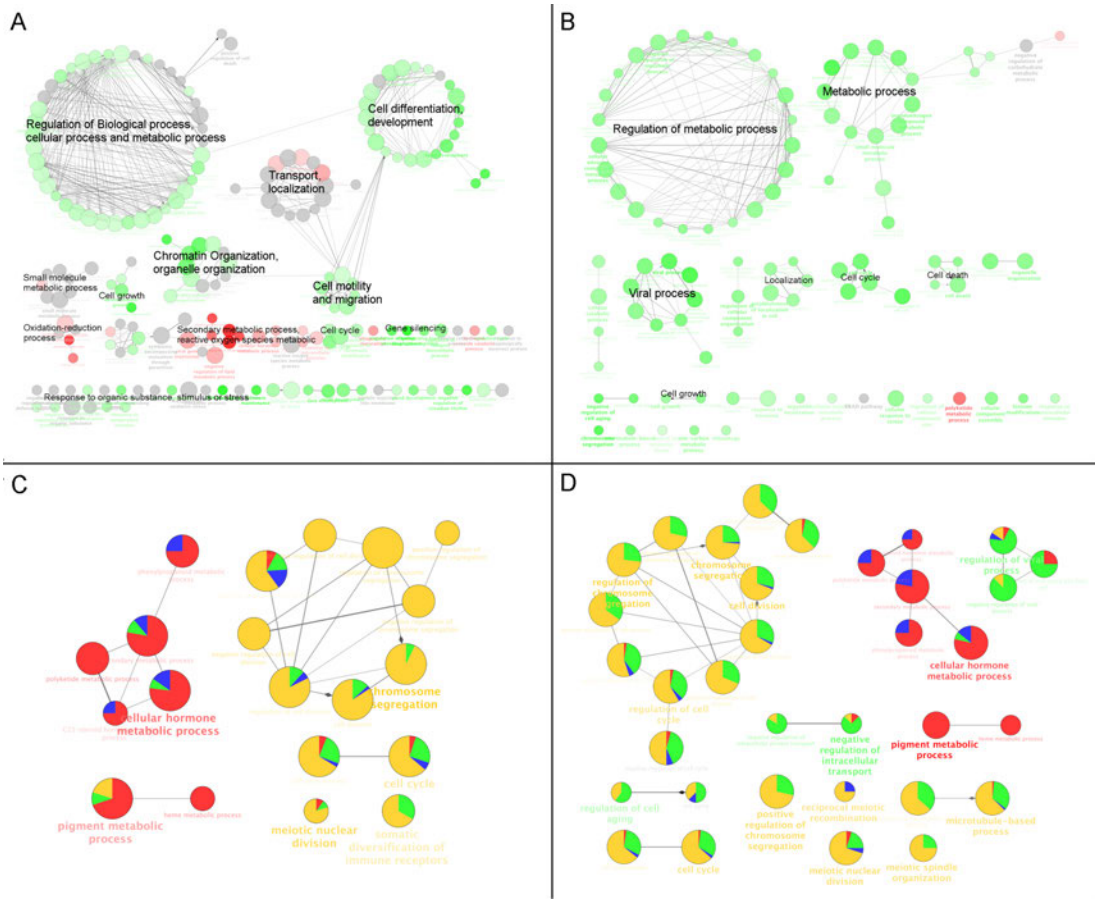

Figure 3: GO functional annotation of DE genes in CKI treated cells. *Over-represented GO terms (Biological Process at 3rd level) for DE genes identified from comparison of CKI treated cells against untreated cells for* **A.** *24 hours or* **B.** *48 hours.* Red coloured nodes mean more than 60% of DE genes that contributed to a term were up-regulated and green coloured nodes mean more than 60% of DE genes that contributed to a term were down-regulated. The colour gradient represents the proportion of up- or down- regulated genes between these cut offs, and the node size is proportional to the significance of over-representation. Terms with similar functional classifications are connected with edges and the most significant term in each cluster is shown in bold. *Comparison of over-represented GO terms for the top 200 significant DE genes in cells treated with 2 mg/mL CKI or 5-FU for* **C.** *24 hours or* **D.** *48 hours.* Four different colours were used to represent the proportion of DE genes from up- or down- regulated genes. For CKI (red = up-regulated and green = down-regulated) or 5-FU (blue = up-regulated and yellow = down-regulated). Node size is proportional to the significance of over-representation and terms with similar functional classifications are connected with edges and the most significant term in each cluster is shown in bold.

down-regulated in cells treated with CKI (Figure 4A). After cells were treated with CKI for 48 hours, most of the over-represented pathways found at 24 hours were still shown as significantly over-represented. However, some over-represented metabolic pathways and disease-related pathways at 48 hours were not shown as significantly over-represented pathways in cells treated with CKI for 24 hours. These pathways included "Arginine and proline metabolism", "Pyrimidine metabolism", "Fructose and mannose metabolism", "Parkinson's disease" and "Alzheimer's disease". In contrast to over-represented metabolic or disease related pathways in cells treated with CKI for 24 hours, these 48-hours-only significant over-represented metabolic or disease pathways were mostly a function of down-regulated DE genes (Figure 4B). Next, we compared the over-represented KEGG pathways based on the top 200 significantly DE genes in cells treated with CKI or 5-FU. Consistent with the results in Figure 4A and 4B, metabolic related pathways were primarily contributed by CKI up-regulated genes. Cell growth and cancer related pathways were also over-represented, and were mostly contributed by down-regulated genes in cells treated with CKI or 5-FU (Figure 4C and 4D). More significantly over-represented cancer-related pathways were found in cells treated with CKI or 5-FU after 48 hours, and DE genes in these pathways were mainly down-regulated (Figure 4D).

Many pathways perturbed by CKI in MCF-7 cells were inhibited

From the above gene set enrichment analysis, we observed that many over-represented GO terms or KEGG

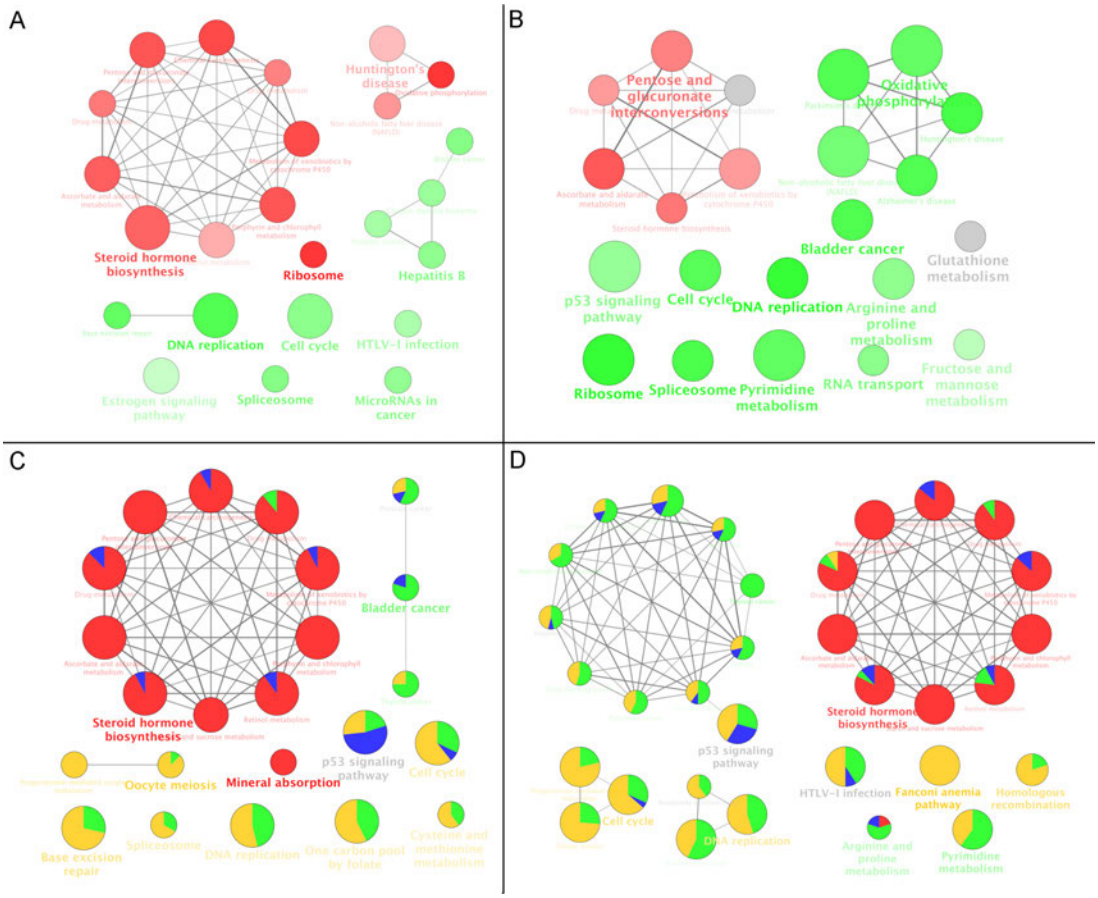

Figure 4: KEGG functional annotation of DE genes in cells treated with CKI. *Over-represented KEGG pathways for all DE genes identified from comparison of CKI treated cells with untreated cells for* **A.** *24 hours or* **B.** *48 hours.* Red coloured nodes mean that more than 60% of DE genes that contributed to this pathway were up-regulated and green coloured nodes mean that more than 60% of DE genes that contributed to this pathway were down-regulated. The colour gradient represents the proportion of up- or down- regulated genes between these two cut offs, and node size is proportional to the significance of over-representation. Pathways with similar functional classifications are connected with edges and the most significant term in each cluster is shown in bold. *Comparison of over-represented KEGG pathways for the top 200 significant DE genes in cells treated with 2 mg/mL CKI or 5-FU for* **C.** *24 hours or* **D.** *48 hours.* Four different colours were used to represent the proportion of DE genes from up- or down- regulated genes. For CKI (red = up-regulated and green = down-regulated) or 5-FU (blue = up-regulated and yellow = down-regulated). Node size represents the significance of over-representation and terms with similar functional classifications are connected with edges and the most significant term in each cluster is shown in bold.

pathways were enriched in down-regulated genes from cells treated with CKI. We used Signalling Pathway Impact Analysis (SPIA) to identify significantly perturbed functional pathways when integrating gene expression information with signalling pathway topology [19]. 21 KEGG pathways were identified as significantly perturbed in cells treated with high dose CKI (2 mg/mL) after 24 hours, and the majority of these pathways (16 out of 21) were shown as inhibited (Supplementary Table 3). In cells treated with 5-FU for 24 hours, more KEGG pathways (75) were identified as significantly perturbed, but only 22 of these were shown as inhibited (Supplementary Table 3). We then compared these significantly perturbed pathways in cells treated with CKI or 5-FU. Interestingly, all significantly altered pathways in cells treated with CKI were also shown as significantly perturbed in cells treated with 5-FU (Figure 5A). This suggests that at 24 hours, CKI and 5-FU perturbed some of the same pathways. However, the perturbation status of these common altered pathways in cells treated with CKI or 5-FU was quite different. The majority of inhibited pathways in cells treated with CKI were shown as activated in cells treated with 5-FU (Figure 5A). Although the perturbation status indicated by SPIA is just suggestive, it still provides some clues that CKI might target different genes even though it might perturb the same pathway as 5-FU. After cells were treated with CKI or 5-FU for 48 hours, 11 significantly perturbed pathways were identified in each of treatment group, but only 3 of these were shown as significantly perturbed pathways in both cells treated with CKI or 5-FU (Figure 5B).

In order to examine the perturbation of CKI on KEGG pathways at the individual gene level, we mapped the expression status of DE genes in cells treated with CKI or 5-FU on the cell growth and death related pathway "Cell cycle" as an example (Figure 6). Consistent with what we observed in the above KEGG over-representation analyses, the majority of DE genes in the "Cell cycle" pathway were down-regulated both in cells treated with CKI or 5-FU. Many essential regulators, such as *Cyclin-dependent kinase 2* (*CDK2*), *Transcription Factor Dp-1* (*DP-1*), *Origin recognition complex* (*ORC*) and *Minichromosome maintenance protein complex* (*MCM*) families, which are important in regulation of the G1/S transition [20, 21], were significantly down-regulated both in cells treated with CKI or 5-FU. However, some key regulators in this "Cell cycle" pathway had different expression status in cells treated with CKI or 5-FU. For example, *CCND1*, which encodes Cyclin-D1 (a member of the CycD protein family), was significantly down-regulated in cells treated with CKI compared with untreated cells. In contrast, *CCND3*, encoding Cyclin-D3 which also belongs to the CycD protein family, was significantly up-regulated in cells treated with 5-FU. Interestingly, as an important pro-apoptosis modulator, the expression of *p53* was opposite in cells treated with CKI (down-regulated) or 5-FU (up-regulated) compared to untreated cells. In addition, the protein levels of p53 were significantly decreased in cells treated with CKI for 24 hours and showed no significant change at 48 hours. In contrast p53 increased in cells treated with 5-FU for both 24 and 48 hours (Figure 6C). Taken together the results of down-regulated p53 mRNA and protein levels (Figure 2C and 6C) but elevated apoptosis activity (Figure 1B) in MCF-7 cells treated with CKI, suggest that CKI may induce cell apoptosis in a p53 independent fashion. In cells treated with CKI or 5-FU for 48 hours, essential genes for G1/S transition (as discussed above) were still shown as significantly down-regulated. In addition, more genes, such as *Cyclin A1* (*CCNA1*, encoding CycA), *Cyclin B1 and B2* (*CCNB1* and *CCNB2*, encoding CycB), *Mitotic Arrest Deficient 1* (*MAD1*, encoding mad1) and *Mitotic Arrest Deficient 2* (*MAD2*, encoding mad2), which are important regulators of G2 or M phase, were shown as significantly down-regulated in cells treated with CKI for 48 hours.

The cell cycle assay using flow cytometry indicated that proportions of cells in G1 and S phases were significantly lower in MCF-7 cells treated with high dose CKI (2 mg/mL), while significantly higher in G2/M phase, indicating a cell cycle arrest at G2/M phase by CKI in MCF-7 cells (Supplementary Figure 5). In summary, possible p53 independent apoptosis together with perturbation of other cancer cell growth associated pathways, such as "Cell cycle", probably contribute the anti-cancer effect of CKI.

The expression of many clinically relevant cancer genes was altered in MCF-7 cells treated with CKI

To investigate the potential molecular targets of CKI in MCF-7 cells, we examined the changes in expression of 135 genes in a curated database of Tumour Alterations Relevant for Genomics-driven Therapy (TARGET) from The Broad Institute (https://www.broadinstitute.org/cancer/cga/target). These genes are directly linked to a clinical outcome when somatically altered in cancer. Many genes showed similar expression changes in cells treated with CKI or 5-FU, and this confirmed what we observed in the pathway analysis (see above) (Figure 7A). However, the expression of some genes was either of a higher degree or in a different direction in cells treated with CKI compared with cells treated with 5-FU. For example, *ETS translocation variant 4* (*ETV4*), whose overexpression is oncogenic in prostate cells [22], was greatly down-regulated in cells treated with CKI compared with cells treated with 5-FU. On the other hand, *Cyclin-Dependent Kinase Inhibitor 1A* (*CDKN1A*, also named as *p21*) was highly up-regulated in 5-FU treated cells but not in CKI treated cells. We then examined how many significantly DE genes in cells treated with CKI or 5-FU were also in this TARGET gene list. In total, 27 DE genes in cells treated with CKI for 24 hours were in the TARGET gene

list, and more up-regulated genes (18 compared to 2) in cells treated with 5-FU for 24 hours were in the TARGET gene list (Figure 7B). In cells treated with CKI or 5-FU for 48 hours, 28 DE genes were in the TARGET list from cells treated with CKI, while only 6 of the DE genes from cells treated with 5-FU for 48 hours were in this list (Figure 7C).

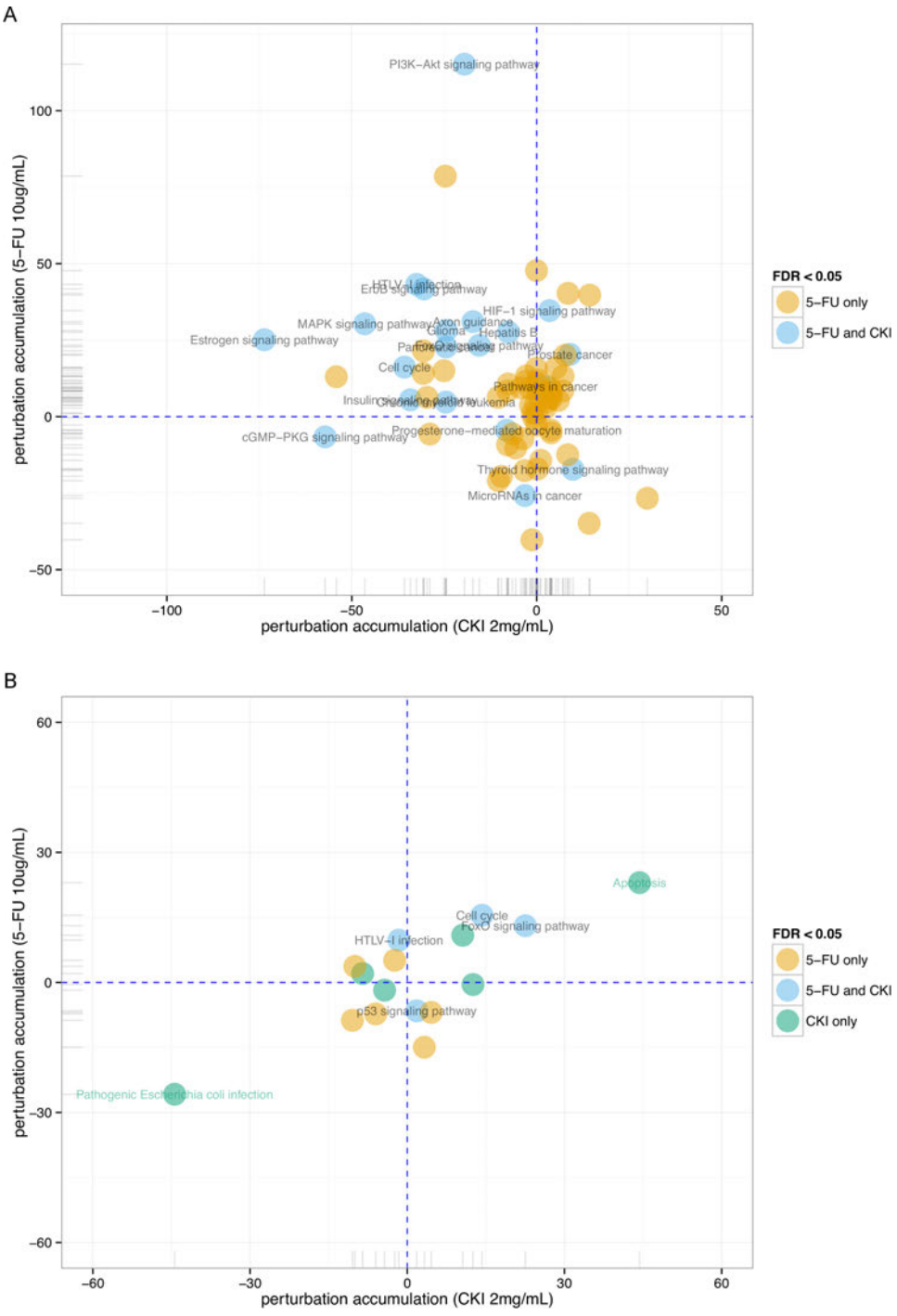

Figure 5: Perturbation of KEGG pathways in cells treated with CKI or 5-FU for A. 24 hours or **B.** 48 hours inferred with SPIA. Perturbation accumulation and significance of perturbation for each KEGG pathway were calculated based on the fold changes of expression of DE genes compared to untreated cells, integrated with the topology information in this pathway. Positive perturbation accumulation values mean this pathway is activated and *vice versa*. "5-FU only" or "CKI only" represent pathways that are only significantly perturbed in one condition not in the other.

Reconstruction of non-coding and protein-coding RNA co-expression networks altered by CKI

The differential expression analysis of refGenes showed that lncRNA, *H19*, was significantly down-regulated after cells were treated with CKI (Figure 2C and Supplementary Table 2). In order to better understand the potential expression change of lncRNAs in response to CKI in MCF-7 cancer cells, we carried out *de novo* identification of lncRNAs from this transcriptome dataset. In total, 2,576 lncRNA transcripts, which are from 2,287 unique genomic loci, were identified (Supplementary Figure 6). We also found that the majority of these lncRNAs were novel by comparing the genomic coordinates of these lncRNAs with two well-annotated human lncRNA datasets (Figure 8A) [23, 24]. The expression of many lncRNAs was changed in cells treated with CKI or 5-FU (Figure 8B). The expression of lncRNAs in cells treated with CKI for 24 hours was quite different compared with cells treated with 5-FU for 24 hours. While at 48 hours, we observed more similar lncRNA expression in cells treated with CKI or 5-FU (Figure 8B). These results indicate that some of these lncRNAs may play specific regulatory roles responding to different reagent treatments.

In order to identify potential lncRNA candidates that were highly relevant to CKI treatment in MCF-7 cells, we reconstructed the co-expression networks for 15,115 detectable refGenes and 2,287 lncRNAs in 9 different samples. 53 co-expression modules were reconstructed based on the expression profiles of refGenes or lncRNAs across 9 samples (Supplementary Figure 7 and Supplementary Table 4). Upon examination of the eigengene expression patterns of these 53 modules, we found three modules with expression profiles that were consistent with CKI-specific modules (Figure 8C and Supplementary Figure 8). Centrality analysis of these

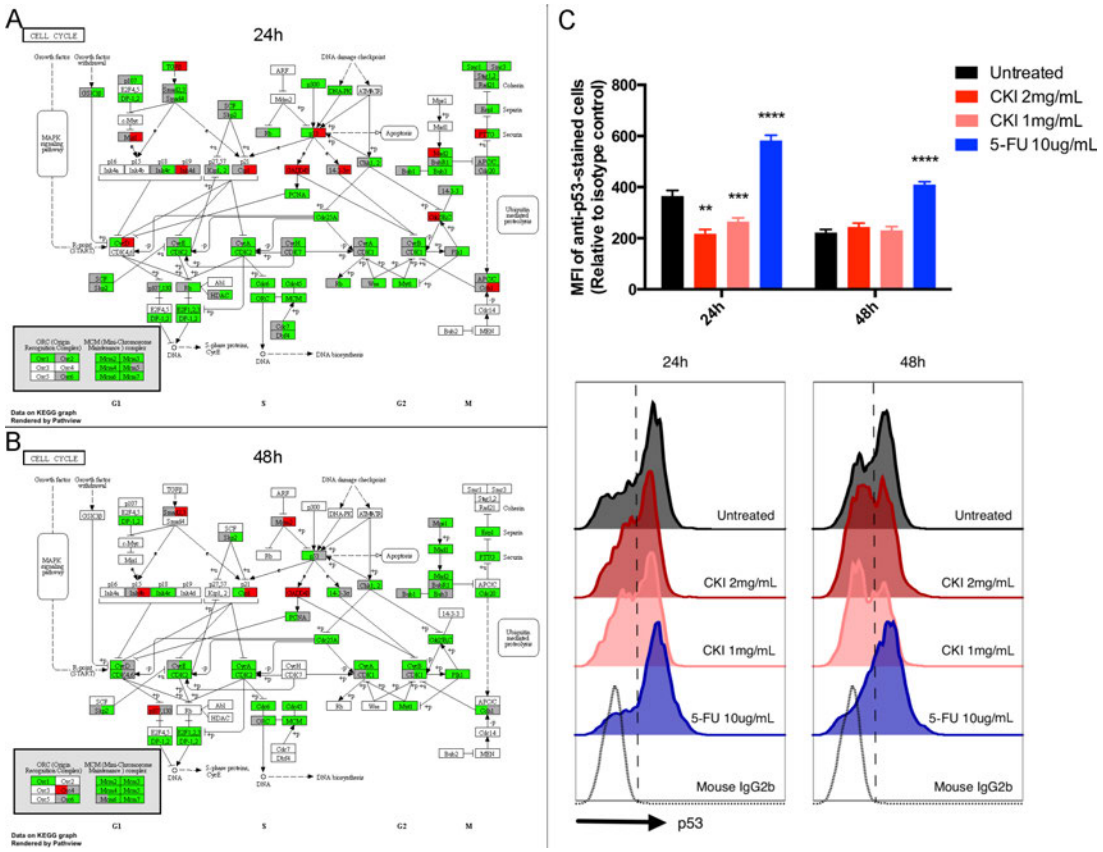

Figure 6: Comparison of individual gene expression change in MCF-7 cells treated with CKI (2 mg/mL) or 5-FU for A. 24 hours or **B.** 48 hours in the cell cycle pathway. Significant DE genes are coloured with red (up-regulated) or green (down-regulated). Each coloured box is separated into two parts, the left half represents the expression change status in cells treated with CKI and the right half represents the expression change status in cells treated with 5-FU. White or grey colours represent gene(s) that are not significantly differentially expressed. **C.** CKI caused down-regulation (24 hours) or no significant change (48 hours) of p53 protein level. The level of p53 protein present in cells treated with CKI was measured by flow cytometry. For the top panel, mean fluorescent intensity (MFI) of cells stained with anti-p53 where MFI of isotype control was subtracted. Data are represented as mean ±SEM (n=9). Statistical analyses were performed using t-test comparing with "untreated" (**p<0.01, ***p<0.001, ****p<0.0001). The bottom panel shows representative histograms of anti-p53 staining.

CKI-specific co-expression modules allowed us to identify "hub" nodes, many of which belonged to lncRNAs (Figure 8D and Supplementary Figure 8). These results showed that lncRNAs may be co-regulated or involved in the same regulatory pathways with protein-coding genes when MCF-7 cells are treated with CKI. We then performed GO and KEGG over-representation analysis for the protein-coding genes in these three CKI-specific modules, and "Cell proliferation" was identified as the most significantly over-represented functional term (Table 1). Interestingly, we also found genes in these CKI-specific co-expression modules are over-represented in functions involved in "intracellular signal cascade" and "second-messenger-mediated signaling" (Table 1), which might be triggered by the multiple molecular species present in CKI. In addition, we also identified three co-expression modules, which showed highly correlated co-expression profiles in both cells treated with CKI or 5-FU. We defined these as "CKI-5FU" modules (Supplementary Figure 9). These modules contained over-represented genes in "cell cycle", "DNA replication" and other cell growth related pathways (Supplementary Table 5). This result was consistent with what we observed in our DE analysis (see above).

DISCUSSION

Many TCMs or other herbal medicines, such as CKI used in this study, are extracted from multiple medicinal herbs. The fact that multiple potentially bioactive ingredients are present in these formulas suggests that they have multiple targets, and therefore perturb multiple biological pathways. Transcriptome analysis using high-throughput next generation sequencing technologies has been widely used in cancer biology for the identification of novel biomarkers, mutations and even novel transcripts, such as lncRNAs, in different cancer types [4, 5, 25, 26]. We have used whole transcriptome analysis to identify potential molecular mechanisms of CKI *in vitro*. We not only identified potential gene targets of CKI based

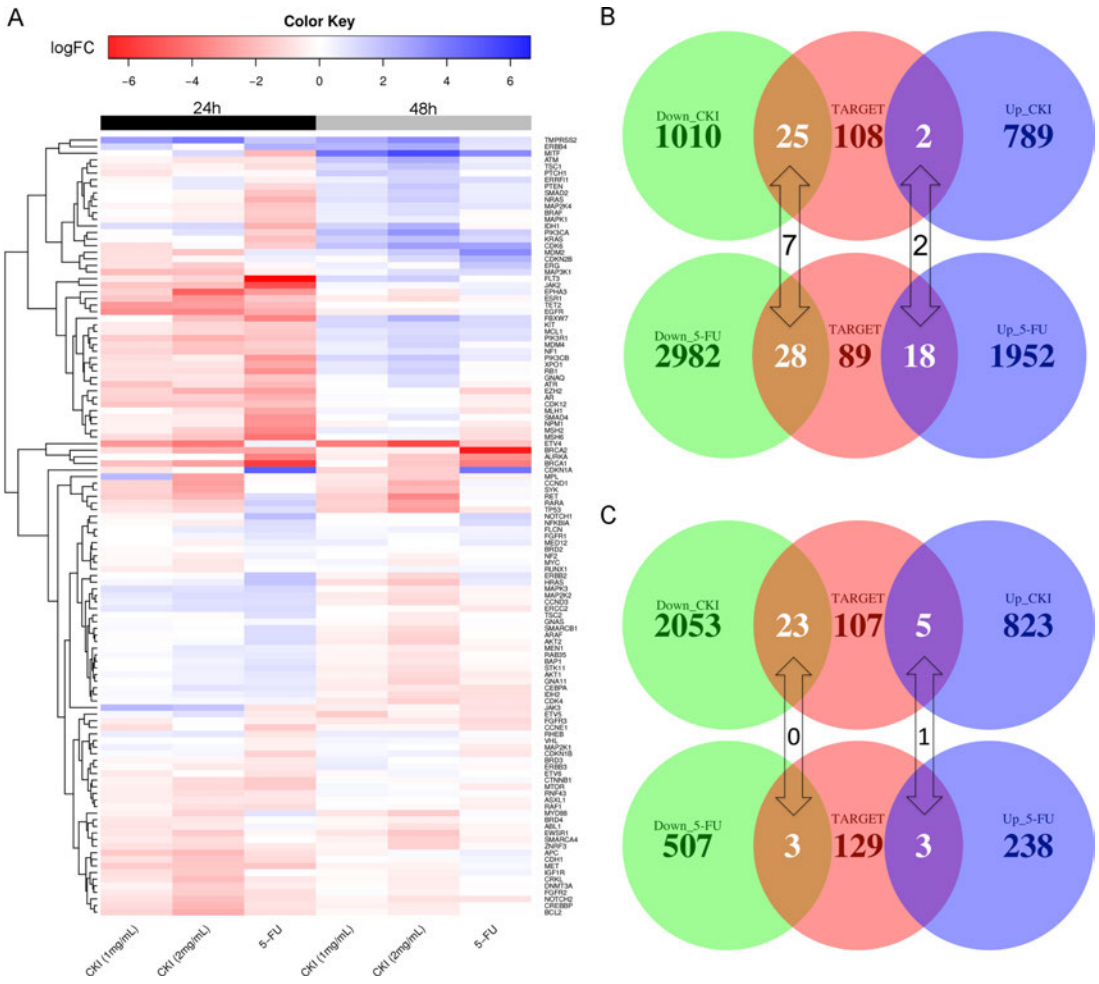

Figure 7: Expression change of clinically relevant cancer genes in cells treated with CKI or 5-FU. A. Heatmap showing the expression fold changes of cancer relevant genes from the TARGET database. Overlap of TARGET genes with DE genes in MCF-7 cells treated with 2 mg/mL CKI or 5-FU for **B.** 24 hours or **C.** 48 hours.

on differential gene expression, but also characterised potential biological pathways targeted by CKI. Although further experiments are required to validate these candidate targets, our results provide a very important starting point for subsequent experimental functional validation.

We have identified genes whose expression was significantly altered in MCF-7 cells treated with CKI. Consistent with the phenotypic analyses, the global gene expression changes in cells treated with CKI support a dose-dependent effect on MCF-7 cells, which had been

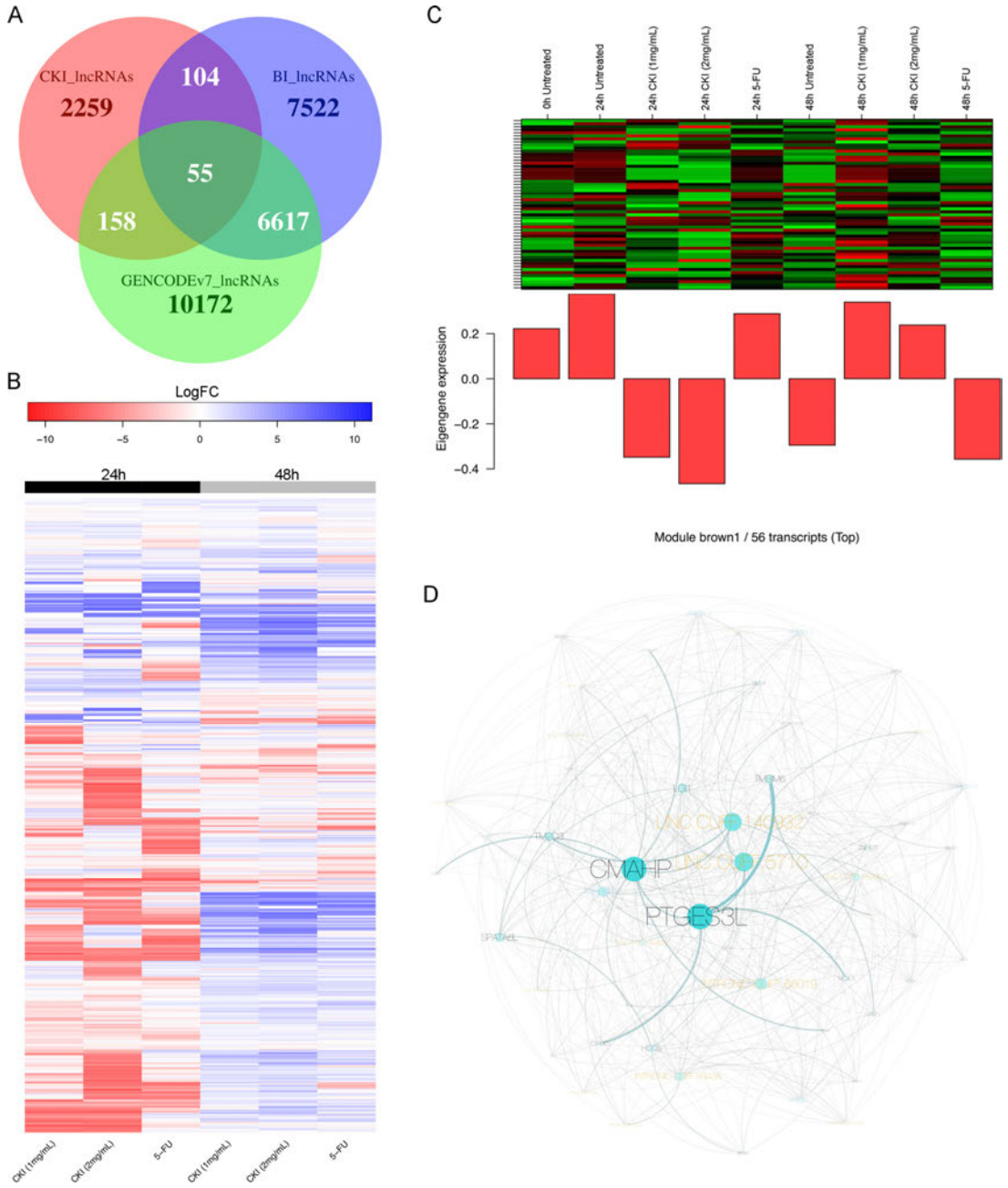

Figure 8: Expression change of *de novo* identified lncRNAs and an example of a CKI-specific co-expression module. **A.** Overlap of *de novo* identified lncRNAs (CKI_lncRNAs) with two annotated human lncRNA datasets: "BI_lncRNAs" as annotated lncRNAs from the Broad Institute and "GENCODEv7_lncRNAs" as lncRNAs from GENCODE version7. **B.** Heatmap showing expression fold change of 2,287 lncRNAs in 6 treated cell samples compared to corresponding untreated cells. **C.** Expression pattern of transcripts in CKI-specific module "brown1" is shown in top panel, and barplot in bottom panel shows the eigengene values in different samples. Green represents "under-expressed" and red represents "over-expressed" in the heatmap. The "eigengene value" is defined as the first principal component of this module, so it can be considered as a representative of the gene expression profiles in this module. **D.** Visualization of CKI-specific co-expression module "brown1". The black labels represent refGenes and gold labels represent lncRNAs. The size of the node/label and edge weight are proportional to between-ness betweeness centrality.

Table 1: Significantly over-represented GO and KEGG terms in protein-coding genes from three CKI-specific co-expression modules (count >4 and P-value < 0.05)

Category	Term	Count	Fold enrichment	P-value
GOTERM_BP_FAT	GO:0008283~cell proliferation	8	3.354	0.009
GOTERM_BP_FAT	GO:0010604~positive regulation of macromolecule metabolic process	11	2.346	0.016
GOTERM_BP_FAT	GO:0032989~cellular component morphogenesis	7	3.223	0.020
GOTERM_BP_FAT	GO:0048514~blood vessel morphogenesis	5	4.332	0.027
GOTERM_BP_FAT	GO:0035295~tube development	5	4.155	0.031
GOTERM_BP_FAT	GO:0007242~intracellular signaling cascade	13	1.892	0.036
GOTERM_BP_FAT	GO:0019932~second-messenger-mediated signaling	5	3.890	0.038
GOTERM_BP_FAT	GO:0000904~cell morphogenesis involved in differentiation	5	3.746	0.043
GOTERM_BP_FAT	GO:0000902~cell morphogenesis	6	3.081	0.043
GOTERM_BP_FAT	GO:0001568~blood vessel development	5	3.731	0.043
GOTERM_BP_FAT	GO:0001944~vasculature development	5	3.642	0.047
KEGG_PATHWAY	hsa05200:Pathways in cancer	7	3.391	0.013
KEGG_PATHWAY	hsa04020:Calcium signaling pathway	5	4.514	0.021

reported in MCF-7 stem cells and other types of cancer cells in previous studies [10, 11]. However, we have generated a far more comprehensive candidate gene list by considering CKI as a whole rather than looking at the effect of individual constituents. As expected, genes, including *Cytochrome P450 family 1* (*CYP1A1*), *Aldo-Keto Reductase Family 1*, *Member C2* (*AKR1C2*) and *Member C3* (*AKR1C3*), which are involved in xenobiotic compound metabolism, were significantly up-regulated when cells were treated with CKI [27, 28] but not with 5-FU. On the other hand, many genes involved in cell growth or used as biomarkers of carcinogenesis, such as *CCND1* [29], were significantly down-regulated. Interestingly, we observed one lncRNA *H19*, known to be over-expressed in several types of cancer [30, 31], was dramatically down-regulated in cells treated with CKI. Recently, many lncRNAs have been characterised as important gene regulators in various types or stages of carcinogenesis [32]. We hypothesise that lncRNAs may be also involved in the gene regulatory networks altered by CKI in MCF-7 cells. Whether lncRNAs are primary targets or secondary links to regulated pathway, still requires further study. Compared to traditional single-gene analyses used to understand the molecular mechanisms of TCM, transcriptome screening has significant advantages for identifying potential target genes.

Carcinogenesis is a complex cellular process involving multiple genetic alterations that perturb different biological processes or pathways [33]. By screening transcriptome-wide gene expression changes *in vitro*, one can do more than the mere identification of molecular markers for cancer diagnosis or therapy, one can also provide useful evidence to better characterise the underlying mechanisms of drug effects on cancer at pathway or network levels [34, 35]. Using whole transcriptome analysis, we identified multiple potential molecular pathways altered by CKI in MCF-7 cells. Cell growth related pathways, such as cell cycle, cell division, DNA replication and so on, were significantly altered in MCF-7 cells treated with CKI. By integrating the expression data and topologic information of genes involved in these pathways, it appears that cell cycle arrest might be one of the primary anti-tumour mechanisms of CKI in MCF-7 cells. As expected, 5-FU also significantly altered these cell growth related pathways, as reported in previous studies [36, 37]. However, when we consider the expression change of individual genes in these pathways, we found that many different genes were significantly altered by CKI or 5-FU, but the overall perturbation status of these pathways was consistent. We also noticed that CKI and 5-FU had opposite effects on some pathways, such as the p53 signalling pathway. Although the expression of the key *p53* gene in the p53 signalling pathway was significantly down-regulated in cells treated with CKI, we still observed changes in the expression of down-stream genes in the apoptosis pathway, such as *Bcl-2*. *Bcl-2* is an important anti-apoptotic gene [38], which was significantly down-regulated in CKI treated cells,

indicating that MCF-7 cells still underwent apoptosis when treated with CKI. The down-regulation of *Bcl-2* had been reported in other types of cancer cells treated with Matrine or Oxymatrine, two of the major components of CKI [16, 39–41]. Taking into account the results from the apoptosis assay, we propose that CKI may induce MCF-7 cell apoptosis via p53 independent pathways. As CKI is normally clinically used in combination with other cancer chemotherapies, our results also provide primary molecular evidence for this potential simultaneous effect in clinical usage [11].

Advances in omics technologies have allowed the development of new cancer therapies [42]. Improved gene therapies, such as targeted cancer therapies or precision medicine, are attracting more and more attention as a result of improved abilities to characterise cancer mechanisms in individual patients [42, 43]. On the other hand, therapies involving whole body system modulation, such as immunotherapy [44] and multiply-targeted therapies [45], are also proposed as potentially effective or complementary weapons for cancer treatment [46]. The nature of many TCMs or ancient medicines that include multiple bioactive ingredients, suggests that they can be a rich resource for identifying or developing multi-targeted cancer drugs [47]. However, most TCMs or ancient medicines are experience-based medicines developed from a long history of clinical use and little is known of their molecular modes of action. Classical pharmacology has used a reductionist strategy of purification and testing of single components from TCM, but this limits our understanding of the potential interaction or cumulative effects of multiple components on a functional system. The application of systems biology techniques, such as whole transcriptome analyses, is a good starting point to understand the functional system effects of TCMs, as a basis for further improvement and optimisation of existing TCMs in the context of evidence based medicine.

Studies have confirmed that many lncRNAs play important regulatory roles in cancer [32]. Our *de novo* identification of lncRNAs showed that some of these may contribute to regulatory networks, and even be specifically or differentially expressed in MCF-7 cancer cells treated by CKI. By integrating lncRNAs with protein-coding RNAs to reconstruct co-expression networks, we showed that this can be used as another powerful tool to understand global transcription changes potentially sensitive to TCM. We were able to confirm that "Cell cycle" and other cell growth related pathways might be the primary target pathways of CKI in MCF-7 cell line as shown in DE analysis, but were able to do this in a more general sense, because we included all expression detectable transcripts during the reconstruction of co-expression networks. In addition, we also showed co-expression networks may be useful in identifying potential co-expressed "hub" transcripts, including both protein-coding RNAs and lncRNAs, for further functional experiments [48]. In conclusion, we applied and integrated multiple transcriptome analysis tools to describe and analyse the complexity of molecular mechanisms altered by CKI in MCF-7 breast cancer cells, and we hope that this can be useful to harness the "magic power" of TCM.

MATERIALS AND METHODS

Cell culture and drugs

MCF-7 cells were purchased from ATCC (HTB-22™, VA, USA) and were cultured in DMEM medium (Thermo Fisher Scientific, MA, USA) supplemented with 10% fetal bovine serum (Thermo Fisher Scientific) and 0.01 mg/mL human recombinant insulin (Thermo Fisher Scientific) at 37°C with 5% CO_2. CKI (total alkaloids concentration of 20.8 mg/mL) was obtained from ZhenDong pharmaceutical Co.Ltd (Shanxi, China), and 5-FU was ordered from Sigma-Aldrich (MO, USA). For all *in vitro* experiments performed in this study, CKI was used at dilution of final concentration of either 1 mg/mL or 2 mg/mL of total alkaloids, and 5-FU was used at a final concentration of 10 ug/mL.

For cell culture in 6-well trays used for cell apoptosis assay, cell cycle assay, p53 protein staining assay and RNA extraction, each well was seeded with 5×10^5 cells in 2 mL of medium and cultured overnight. On the following day, 1 mL of either medium, CKI or 5-FU was added to the cells. After 24 and 48 hours of treatment, cells were harvested and used in the above assays.

Cell viability assay

The wells of 96-well trays were seeded with 1×10^4 cells in 50 µL of medium and cultured overnight. On the following day, 50 µL of either medium, CKI or 5-FU were added to the cells. Viability of the cells was measured at 0, 24 and 48 hours after the treatment by adding XTT:PMS (50:1; Sigma-Aldrich). After 4-hour incubation at 37°C optical density (OD) of each well was read at 490 nm. The background OD was also measured and the average was subtracted from the OD readings of appropriate wells.

Apoptosis assay by annexin V/PI staining

Cells were cultured in 6-well trays and treated with drugs as described above. After 24 and 48 hours of treatment, cells were harvested and the rate of apoptosis was measured using Annexin V-FITC detecton kit (Biotool, TX, USA) according to the manufacturer's instructions. The stained cells were sorted and data acquired on an LSRII (BD Biosciences, NJ, USA) and the data were analysed using FlowJo software (TreeStar Inc., OR, USA).

Caspase 3/7 colorimetric assay

Caspase 3/7 activity in cells was measured with a Caspase-3/7 Colorimetric Assay Kit (BioVision, CA, USA). Cells were cultured in 6-well trays and treated with drugs as described above. After 24 and 48 hours of treatment, cells were harvested and proteins from cells were extracted according to the manufacturer's instructions and concentrations were determined with a Nanodrop 2000 (Thermo Scientific). Caspase-3/7 activity was then measured according to the manufacturer's instructions.

Cell cycle assay

Cells were cultured in 6-well trays and treated with drugs as described above. After 24 and 48 hours of treatment, cells were harvested and subjected to cell cycle analysis by PI staining as described previously [49] and the stained cells were sorted and the data acquired on LSRII and the data were analysed using FlowJo software.

Intranuclear/intracellular staining for p53

Cells were cultured in 6-well trays and treated with drugs as described above. After 24 and 48 hours of treatment, cells were fixed and permeabilised using Nuclear Factor Fixation and Permeabilization Buffer Set (Biolegend, CA, USA) according to the manufacturer's instructions. 2×10^5 cells were labelled either with anti-p53-PE or mouse IgG2b-PE (1 μg/mL; Biolegend) and the cells were sorted and the data were acquired on an LSRII, and the data were analysed using FlowJo software.

RNA extraction and sequencing

Cells were cultured in 6-well plates with a seeding density of 5×10^5 cells/well and treated with CKI or 5-FU for 24 and 48 hours as above. Total RNA was isolated with the mirVana PARIS Kit (Thermo Fisher Scientific) according to the manufacturer's protocol. RNA samples were sent to the Cancer Genome Facility of the Australian Cancer Research Foundation (SA, Australia) for sequencing. The quality of the total RNA was verified on a Bioanalyzer ensuring all samples had RINs >7.0. Starting with 1 ug of total RNA, the polyA fraction was enriched using a NEBNext(r) Poly(A) mRNA Magnetic Isolation Module. Stranded mRNA libraries for Illumina sequencing were prepared using the NEBNext(r) Ultra Directional RNA kits from New England Biolabs, Inc. according to the manufacturer's protocol (Version 2.0 July 2013). Actinomycin D was added during cDNA synthesis to ensure high levels of strand specificity. All libraries were run on a Bionanalyzer to confirm library size and yield. Barcoded libraries were normalized and pooled based on concentrations determined by qPCR with Library Quantification kits from KAPA Biosystems. Libraries were sequenced using an Illumina HiSeq 2500 across 5 lanes with stranded paired-end 100 base pair reads. Raw and processed data were deposited at the Gene Expression Omnibus (GEO) data repository (GSE78512).

Data processing and functional annotation

Low quality and adaptor sequences in raw reads were trimmed using Trim_galore (v0.3.7, Babraham Bioinformatics) with the following parameters: --stringency 6 --paired. Then cleaned reads were aligned to the reference genome (hg19, UCSC) using STAR_2.4.0j with the following parameters: --outSAMstrandField intronMotif --outSAMattributes All --outFilterMismatchNmax 10 --seedSearchStartLmax 30 [50]. Differential expression analysis was performed with edgeR and DE genes were selected with a False Discovery Rate (FDR) < 0.05 [51].

GO and KEGG over-representation analyses were performed using ClueGO with the following settings: biological process at 3rd level (for GO); right-sided hypergeometric test for enrichment analysis; p values were corrected for multiple testing according to the Benjamini-Hochberg method. Over-represented terms/pathways were visualised with Cytoscape v3.2.1 [52, 53]. Signalling Pathway Impact Analysis (SPIA) was performed with SPIA package in R [19]. Gene expression status mapping in KEGG pathways was visualised with the R Pathview package [54].

Transcriptome validation with qPCR

Cells were cultured in 6-well trays and treated with drugs as described above. Untreated cells as well as cells treated for 24 and 48 hours were harvested and the cell pellets were snap-frozen in liquid nitrogen. Total RNA was extracted using PureLink RNA Mini Kit (Thermo Fisher Scientific) and treated with TURBO DNA-Free (Thermo Fisher Scientific) according to the manufacturer's instructions. cDNA synthesis was performed using High Capacity cDNA Reverse Transcription Kit (Thermo Fisher Scientific) according to the manufacturer's instructions.

qPCR reactions were set up with PowerUp SYBR Green Master Mix where forward and reverse primers were added at a final concentration of 400 nM each. Reactions were run on the StepOne Plus Real-Time PCR system and the data were analysed using its software v2.3 (Thermo Fisher Scientific). Relative levels of target mRNAs were calculated as $1/2^{\Delta CT}$, where ΔCT=CT of target − CT of *RSP13*. The sequences of all primers used in this study are provided in Supplementary Table 6.

LncRNA identification

The flowchart for lncRNA identification is shown in Supplementary Figure 6. In summary, short reads were mapped against the genome and assembled into

longer transcripts, and then transcripts shorter than 200 nucleotides (nt) were removed. Genomic coordinates of long transcripts were checked against refGenes from UCSC and classified into "refGene transcripts", "intergenic transcripts", "intronic transcripts" and "antisense transcripts". The latter three classes of transcripts were selected to filter unannotated protein-coding potential transcripts by following two steps: 1) Sequence similarity search against the Swiss-Prot protein database; 2) Predict Open Reading Frame(s) (ORF). In order to get a more reliable lncRNA dataset, we selected transcripts with expression higher than 1 count per million (CPM, normalised using the TMM method in edgeR) in at least 2 of 27 individual samples.

Reconstruction of co-expression networks

RefGenes were pre-filtered by expression (> 1 CPM in at least 2 of 27 individuals). Expression matrices for all pre-filtered refGenes and lncRNAs were merged to reconstruct co-expression networks with WGCNA [55]. "16" was selected as the soft thresholding power according to the protocol of WGCNA. Co-expression modules were visualized with Cytoscape v3.2.1. Betweenness centrality was used to select "hub" nodes. GO and KEGG over-representation analyses were performed with DAVID (Database For Annotation, Visualization and Integrated Discovery) [56].

ACKNOWLEDGMENTS

The Authors would like to thank Adriana Caon for technical help in cell culture and Seyyed Hani Moussavi Nik for technical help in RNA isolation.

CONFLICTS OF INTEREST

The authors declare no conflicts of interest.

REFERENCES

1. Berger MF, Lawrence MS, Demichelis F, Drier Y, Cibulskis K, Sivachenko AY, Sboner A, Esgueva R, Pflueger D, Sougnez C, Onofrio R, Carter SL, Park K, et al. The genomic complexity of primary human prostate cancer. Nature. 2011; 470: 214-20. doi: 10.1038/nature09744.
2. Pleasance ED, Cheetham RK, Stephens PJ, McBride DJ, Humphray SJ, Greenman CD, Varela I, Lin ML, Ordonez GR, Bignell GR, Ye K, Alipaz J, Bauer MJ, et al. A comprehensive catalogue of somatic mutations from a human cancer genome. Nature. 2010; 463: 191-6. doi: 10.1038/nature08658.
3. Saadatpour A, Lai S, Guo G, Yuan GC. Single-Cell Analysis in Cancer Genomics. Trends Genet. 2015; 31: 576-86. doi: 10.1016/j.tig.2015.07.003.
4. Barrett CL, DeBoever C, Jepsen K, Saenz CC, Carson DA, Frazer KA. Systematic transcriptome analysis reveals tumor-specific isoforms for ovarian cancer diagnosis and therapy. Proc Natl Acad Sci U S A. 2015; 112: E3050-7. doi: 10.1073/pnas.1508057112.
5. White NM, Cabanski CR, Silva-Fisher JM, Dang HX, Govindan R, Maher CA. Transcriptome sequencing reveals altered long intergenic non-coding RNAs in lung cancer. Genome Biol. 2014; 15: 429. doi: 10.1186/s13059-014-0429-8.
6. Prensner JR, Iyer MK, Balbin OA, Dhanasekaran SM, Cao Q, Brenner JC, Laxman B, Asangani IA, Grasso CS, Kominsky HD, Cao X, Jing X, Wang X, et al. Transcriptome sequencing across a prostate cancer cohort identifies PCAT-1, an unannotated lincRNA implicated in disease progression. Nat Biotechnol. 2011; 29: 742-9. doi: 10.1038/nbt.1914.
7. Simon R, Roychowdhury S. Implementing personalized cancer genomics in clinical trials. Nat Rev Drug Discov. 2013; 12: 358-69. doi: 10.1038/nrd3979.
8. Hsiao WL, Liu L. The role of traditional Chinese herbal medicines in cancer therapy--from TCM theory to mechanistic insights. Planta Med. 2010; 76: 1118-31. doi: 10.1055/s-0030-1250186.
9. Sun M, Cao H, Sun L, Dong S, Bian Y, Han J, Zhang L, Ren S, Hu Y, Liu C, Xu L, Liu P. Antitumor activities of Kushen: literature review. Evid Based Complement Alternat Med. 2012; 2012: 373219. doi: 10.1155/2012/373219.
10. Zhao Z, Fan H, Higgins T, Qi J, Haines D, Trivett A, Oppenheim JJ, Wei H, Li J, Lin H, Howard OM. Fufang Kushen injection inhibits sarcoma growth and tumor-induced hyperalgesia via TRPV1 signaling pathways. Cancer Lett. 2014; 355: 232-41. doi: 10.1016/j.canlet.2014.08.037.
11. Xu W, Lin H, Zhang Y, Chen X, Hua B, Hou W, Qi X, Pei Y, Zhu X, Zhao Z, Yang L. Compound Kushen Injection suppresses human breast cancer stem-like cells by down-regulating the canonical Wnt/beta-catenin pathway. J Exp Clin Cancer Res. 2011; 30: 103. doi: 10.1186/1756-9966-30-103.
12. Ma Y, Gao HM, Liu J, Chen LM, Zhang QW, Wang ZM. Identification and Determination of the Chemical Constituents in a Herbal Preparation, Compound Kushen Injection, by Hplc and Lc-Dad-Ms/Ms. Journal of Liquid Chromatography & Related Technologies. 2014; 37: 207-20. doi: 10.1080/10826076.2012.738623.
13. Yu P, Liu Q, Liu K, Yagasaki K, Wu E, Zhang G. Matrine suppresses breast cancer cell proliferation and invasion via VEGF-Akt-NF-kappaB signaling. Cytotechnology. 2009; 59: 219-29. doi: 10.1007/s10616-009-9225-9.
14. Liu T, Song Y, Chen H, Pan S, Sun X. Matrine inhibits proliferation and induces apoptosis of pancreatic cancer cells *in vitro* and *in vivo*. Biol Pharm Bull. 2010; 33: 1740-5.

15. Chen H, Zhang J, Luo J, Lai F, Wang Z, Tong H, Lu D, Bu H, Zhang R, Lin S. Antiangiogenic effects of oxymatrine on pancreatic cancer by inhibition of the NF-kappaB-mediated VEGF signaling pathway. Oncol Rep. 2013; 30: 589-95. doi: 10.3892/or.2013.2529.

16. Ling Q, Xu X, Wei X, Wang W, Zhou B, Wang B, Zheng S. Oxymatrine induces human pancreatic cancer PANC-1 cells apoptosis via regulating expression of Bcl-2 and IAP families, and releasing of cytochrome c. J Exp Clin Cancer Res. 2011; 30: 66. doi: 10.1186/1756-9966-30-66.

17. Zhang Y, Piao B, Zhang Y, Hua B, Hou W, Xu W, Qi X, Zhu X, Pei Y, Lin H. Oxymatrine diminishes the side population and inhibits the expression of beta-catenin in MCF-7 breast cancer cells. Med Oncol. 2011; 28: S99-107. doi: 10.1007/s12032-010-9721-y.

18. Guo YM, Huang YX, Shen HH, Sang XX, Ma X, Zhao YL, Xiao XH. Efficacy of Compound Kushen Injection in Relieving Cancer-Related Pain: A Systematic Review and Meta-Analysis. Evid Based Complement Alternat Med. 2015; 2015: 840742. doi: 10.1155/2015/840742.

19. Tarca AL, Draghici S, Khatri P, Hassan SS, Mittal P, Kim JS, Kim CJ, Kusanovic JP, Romero R. A novel signaling pathway impact analysis. Bioinformatics. 2009; 25: 75-82. doi: 10.1093/bioinformatics/btn577.

20. Bertoli C, Skotheim JM, de Bruin RA. Control of cell cycle transcription during G1 and S phases. Nat Rev Mol Cell Biol. 2013; 14: 518-28. doi: 10.1038/nrm3629.

21. Schaarschmidt D, Ladenburger EM, Keller C, Knippers R. Human Mcm proteins at a replication origin during the G1 to S phase transition. Nucleic Acids Res. 2002; 30: 4176-85.

22. Pellecchia A, Pescucci C, De Lorenzo E, Luceri C, Passaro N, Sica M, Notaro R, De Angioletti M. Overexpression of ETV4 is oncogenic in prostate cells through promotion of both cell proliferation and epithelial to mesenchymal transition. Oncogenesis. 2012; 1: e20. doi: 10.1038/oncsis.2012.20.

23. Cabili MN, Trapnell C, Goff L, Koziol M, Tazon-Vega B, Regev A, Rinn JL. Integrative annotation of human large intergenic noncoding RNAs reveals global properties and specific subclasses. Genes Dev. 2011; 25: 1915-27. doi: 10.1101/gad.17446611.

24. Derrien T, Johnson R, Bussotti G, Tanzer A, Djebali S, Tilgner H, Guernec G, Martin D, Merkel A, Knowles DG, Lagarde J, Veeravalli L, Ruan X, et al. The GENCODE v7 catalog of human long noncoding RNAs: analysis of their gene structure, evolution, and expression. Genome Res. 2012; 22: 1775-89. doi: 10.1101/gr.132159.111.

25. Lin KT, Shann YJ, Chau GY, Hsu CN, Huang CY. Identification of latent biomarkers in hepatocellular carcinoma by ultra-deep whole-transcriptome sequencing. Oncogene. 2014; 33: 4786-94. doi: 10.1038/onc.2013.424.

26. Liu J, Lee W, Jiang Z, Chen Z, Jhunjhunwala S, Haverty PM, Gnad F, Guan Y, Gilbert HN, Stinson J, Klijn C, Guillory J, Bhatt D, et al. Genome and transcriptome sequencing of lung cancers reveal diverse mutational and splicing events. Genome Res. 2012; 22: 2315-27. doi: 10.1101/gr.140988.112.

27. Walsh AA, Szklarz GD, Scott EE. Human cytochrome P450 1A1 structure and utility in understanding drug and xenobiotic metabolism. J Biol Chem. 2013; 288: 12932-43. doi: 10.1074/jbc.M113.452953.

28. Jin Y, Penning TM. Aldo-keto reductases and bioactivation/detoxication. Annu Rev Pharmacol Toxicol. 2007; 47: 263-92. doi: 10.1146/annurev.pharmtox.47.120505.105337.

29. Baldin V, Lukas J, Marcote MJ, Pagano M, Draetta G. Cyclin D1 is a nuclear protein required for cell cycle progression in G1. Genes Dev. 1993; 7: 812-21.

30. Hibi K, Nakamura H, Hirai A, Fujikake Y, Kasai Y, Akiyama S, Ito K, Takagi H. Loss of H19 imprinting in esophageal cancer. Cancer Res. 1996; 56: 480-2.

31. Adriaenssens E, Dumont L, Lottin S, Bolle D, Lepretre A, Delobelle A, Bouali F, Dugimont T, Coll J, Curgy JJ. H19 overexpression in breast adenocarcinoma stromal cells is associated with tumor values and steroid receptor status but independent of p53 and Ki-67 expression. Am J Pathol. 1998; 153: 1597-607. doi: 10.1016/S0002-9440(10)65748-3.

32. Huarte M. The emerging role of lncRNAs in cancer. Nat Med. 2015; 21: 1253-61. doi: 10.1038/nm.3981.

33. Vogelstein B, Papadopoulos N, Velculescu VE, Zhou S, Diaz LA, Jr., Kinzler KW. Cancer genome landscapes. Science. 2013; 339: 1546-58. doi: 10.1126/science.1235122.

34. Klijn C, Durinck S, Stawiski EW, Haverty PM, Jiang Z, Liu H, Degenhardt J, Mayba O, Gnad F, Liu J, Pau G, Reeder J, Cao Y, et al. A comprehensive transcriptional portrait of human cancer cell lines. Nat Biotechnol. 2015; 33: 306-12. doi: 10.1038/nbt.3080.

35. Abaan OD, Polley EC, Davis SR, Zhu YJ, Bilke S, Walker RL, Pineda M, Gindin Y, Jiang Y, Reinhold WC, Holbeck SL, Simon RM, Doroshow JH, et al. The exomes of the NCI-60 panel: a genomic resource for cancer biology and systems pharmacology. Cancer Res. 2013; 73: 4372-82. doi: 10.1158/0008-5472.CAN-12-3342.

36. Yoshikawa R, Kusunoki M, Yanagi H, Noda M, Furuyama JI, Yamamura T, Hashimoto-Tamaoki T. Dual antitumor effects of 5-fluorouracil on the cell cycle in colorectal carcinoma cells: a novel target mechanism concept for pharmacokinetic modulating chemotherapy. Cancer Res. 2001; 61: 1029-37.

37. Hernandez-Vargas H, Ballestar E, Carmona-Saez P, von Kobbe C, Banon-Rodriguez I, Esteller M, Moreno-Bueno G, Palacios J. Transcriptional profiling of MCF7 breast cancer cells in response to 5-Fluorouracil: relationship with cell cycle changes and apoptosis, and identification of novel targets of p53. Int J Cancer. 2006; 119: 1164-75. doi: 10.1002/ijc.21938.

38. Czabotar PE, Lessene G, Strasser A, Adams JM. Control of apoptosis by the BCL-2 protein family: implications for

physiology and therapy. Nat Rev Mol Cell Biol. 2014; 15: 49-63. doi: 10.1038/nrm3722.

39. Chang C, Liu SP, Fang CH, He RS, Wang Z, Zhu YQ, Jiang SW. Effects of matrine on the proliferation of HT29 human colon cancer cells and its antitumor mechanism. Oncol Lett. 2013; 6: 699-704. doi: 10.3892/ol.2013.1449.
40. Zhang Y, Zhang H, Yu P, Liu Q, Liu K, Duan H, Luan G, Yagasaki K, Zhang G. Effects of matrine against the growth of human lung cancer and hepatoma cells as well as lung cancer cell migration. Cytotechnology. 2009; 59: 191-200. doi: 10.1007/s10616-009-9211-2.
41. Liu J, Yao Y, Ding H, Chen R. Oxymatrine triggers apoptosis by regulating Bcl-2 family proteins and activating caspase-3/caspase-9 pathway in human leukemia HL-60 cells. Tumour Biol. 2014; 35: 5409-15. doi: 10.1007/s13277-014-1705-7.
42. Al-Lazikani B, Banerji U, Workman P. Combinatorial drug therapy for cancer in the post-genomic era. Nat Biotechnol. 2012; 30: 679-92. doi: 10.1038/nbt.2284.
43. Garman KS, Nevins JR, Potti A. Genomic strategies for personalized cancer therapy. Hum Mol Genet. 2007; 16: R226-32. doi: 10.1093/hmg/ddm184.
44. Mahoney KM, Rennert PD, Freeman GJ. Combination cancer immunotherapy and new immunomodulatory targets. Nat Rev Drug Discov. 2015; 14: 561-84. doi: 10.1038/nrd4591.
45. Petrelli A, Giordano S. From single- to multi-target drugs in cancer therapy: when aspecificity becomes an advantage. Curr Med Chem. 2008; 15: 422-32.
46. Vanneman M, Dranoff G. Combining immunotherapy and targeted therapies in cancer treatment. Nat Rev Cancer. 2012; 12: 237-51. doi: 10.1038/nrc3237.
47. Wang Y, Fan X, Qu H, Gao X, Cheng Y. Strategies and techniques for multi-component drug design from medicinal herbs and traditional Chinese medicine. Curr Top Med Chem. 2012; 12: 1356-62.
48. Yang Y, Han L, Yuan Y, Li J, Hei N, Liang H. Gene co-expression network analysis reveals common system-level properties of prognostic genes across cancer types. Nat Commun. 2014; 5: 3231. doi: 10.1038/ncomms4231.
49. Riccardi C, Nicoletti I. Analysis of apoptosis by propidium iodide staining and flow cytometry. Nat Protoc. 2006; 1: 1458-61. doi: 10.1038/nprot.2006.238.
50. Dobin A, Davis CA, Schlesinger F, Drenkow J, Zaleski C, Jha S, Batut P, Chaisson M, Gingeras TR. STAR: ultrafast universal RNA-seq aligner. Bioinformatics. 2013; 29: 15-21. doi: 10.1093/bioinformatics/bts635.
51. Robinson MD, McCarthy DJ, Smyth GK. edgeR: a Bioconductor package for differential expression analysis of digital gene expression data. Bioinformatics. 2010; 26: 139-40. doi: 10.1093/bioinformatics/btp616.
52. Bindea G, Mlecnik B, Hackl H, Charoentong P, Tosolini M, Kirilovsky A, Fridman WH, Pages F, Trajanoski Z, Galon J. ClueGO: a Cytoscape plug-in to decipher functionally grouped gene ontology and pathway annotation networks. Bioinformatics. 2009; 25: 1091-3. doi: 10.1093/bioinformatics/btp101.
53. Shannon P, Markiel A, Ozier O, Baliga NS, Wang JT, Ramage D, Amin N, Schwikowski B, Ideker T. Cytoscape: a software environment for integrated models of biomolecular interaction networks. Genome Res. 2003; 13: 2498-504. doi: 10.1101/gr.1239303.
54. Luo W, Brouwer C. Pathview: an R/Bioconductor package for pathway-based data integration and visualization. Bioinformatics. 2013; 29: 1830-1. doi: 10.1093/bioinformatics/btt285.
55. Langfelder P, Horvath S. WGCNA: an R package for weighted correlation network analysis. BMC Bioinformatics. 2008; 9: 559. doi: 10.1186/1471-2105-9-559.
56. Huang da W, Sherman BT, Lempicki RA. Systematic and integrative analysis of large gene lists using DAVID bioinformatics resources. Nat Protoc. 2009; 4: 44-57. doi: 10.1038/nprot.2008.211.

Chapter 3

The Effect of Compound Kushen Injection on Cancer Cells: Integrated Identification of Candidate Molecular Mechanisms.

The effects of CKI on biological processes of MCF-7 cells were characterized in the previous chapter. In this chapter, we extend this analysis to two additional cell lines to identify a core set of molecular responses to CKI associated with CKI induced apoptosis. The two cell lines used in this study are, a breast cancer cell line, MDA-MB-231, and a liver cancer cell line, Hep G2. After analyzing the shared transcriptional responses of these two cell lines, we then integrated the analysis with the data set from MCF-7 in the previous chapter. The identification of genes sharing similar patterns of regulation across the three cell lines after treatment with CKI has highlighted some core gene regulatory networks and pathways that respond to CKI. Integration of these data with available online data for gene regulation responses to single compounds found in plant extracts suggests functional roles for specific compounds present in CKI. This chapter is in the format of a manuscript that has been submitted to *Phytomedicine*.

Statement of Authorship

Title of Paper	The Effect of Compound Kushen Injection on Cancer Cells: Integrated Identification of Candidate Molecular Mechanisms.
Publication Status	☐ Published ☐ Accepted for Publication ☑ Submitted for Publication ☐ Unpublished and Unsubmitted work written in manuscript style
Publication Details	

Principal Author

Name of Principal Author (Candidate)	Jian Cui
Contribution to the Paper	Experimental design, carried out experiments, analysed data, wrote paper
Overall percentage (%)	60%
Certification:	This paper reports on original research I conducted during the period of my Higher Degree by Research candidature and is not subject to any obligations or contractual agreements with a third party that would constrain its inclusion in this thesis. I am the primary author of this paper.
Signature	Date 18/6/18

Co-Author Contributions

By signing the Statement of Authorship, each author certifies that:

i. the candidate's stated contribution to the publication is accurate (as detailed above);

ii. permission is granted for the candidate in include the publication in the thesis; and

iii. the sum of all co-author contributions is equal to 100% less the candidate's stated contribution.

Name of Co-Author	Zhipeng Qu
Contribution to the Paper	Experimental design, assisted with experiments, assisted with data analysis, wrote paper
Signature	Date 18/06/18

Name of Co-Author	Yuka Harata-Lee
Contribution to the Paper	Experimental design, assisted with experiments, assisted with data analysis, wrote paper
Signature	Date 14.6.18

Name of Co-Author	Hanyuan Shen		
Contribution to the Paper	Assisted with experiments		
Signature		Date	18/6/2018

Name of Co-Author	Thazin Nwe Aung		
Contribution to the Paper	Assisted with experiments		
Signature		Date	17/06/2018

Name of Co-Author	Wei Wang		
Contribution to the Paper	Assisted with experimental design, assisted with experiments		
Signature		Date	06/15/2018

Name of Co-Author	Robert Daniel Kortschak,		
Contribution to the Paper	Experimental design		
Signature		Date	18/6/18

Name of Co-Author	David L. Adelson		
Contribution to the Paper	Supervised the research, acquired funding for the experiments, experimental design, wrote paper		
Signature		Date	18/6/2018

The Effect of Compound Kushen Injection on Cancer Cells: Integrated Identification of Candidate Molecular Mechanisms.

Authors and affiliation:

Jian Cui[1], Zhipeng Qu[1], Yuka Harata-Lee[1], Hanyuan Shen[1], Thazin Nwe Aung[1], Wei Wang[1,2], R. Daniel Kortschak[1], and David L. Adelson[1,*]

[1]School of Biological Sciences, The University of Adelaide, South Australia, Australia, 5005.
[2]Zhendong Research Institute, Shanxi-Zhendong Pharmaceutical Co Ltd, Beijing, China

*Corresponding author:

David L. Adelson,

Room 261, The Braggs Bldg, School of Biological Sciences, the University of Adelaide, South Australia, 5005, AUSTRALIA

Ph: +61 8 8303 7555

Fax: +61 8 8303 5338

e-mail: david.adelson@adelaide.edu.au

Abstract

Background: Because TCM preparations are often combinations of multiple herbs containing hundreds of compounds, they have been difficult to study. Compound Kushen Injection (CKI) is a complex mixture cancer treatment used in Chinese hospitals for over twenty years.

Purpose: To demonstrate that a systematic analysis of molecular changes resulting from complex mixtures of bioactives from Traditional Chinese Medicine can identify a core set of differentially expressed (DE) genes and a reproducible set of candidate pathways.

Study Design: We used a cancer cell culture model to measure the effect of CKI on cell cycle phases, apoptosis and correlate those phenotypes with CKI induced changes in gene expression.

Methods: We treated cancer cells with CKI in order to generate and analyse high-throughput transcriptome data from two cancer cell lines. We integrated these differential gene expression results with previously reported results.

Results: CKI induced cell-cycle arrest and apoptosis and altered the expression of 363 core candidate genes associated with cell cycle, apoptosis, DNA replication/repair and various cancer pathways. Of these, 7 are clinically relevant to cancer diagnosis or therapy and 14 are cell cycle regulators, and most of these 21 candidates are downregulated by CKI. Comparison of our core candidate genes to a database of plant medicinal compounds and their effects on gene expression identified one-to-one, one-to-many and many-to-many regulatory relationships between compounds in CKI and DE genes.

Conclusions: By identifying promising candidate pathways and genes associated with CKI based on our transcriptome-based analysis, we have shown this approach is useful for the systematic analysis of molecular changes resulting from complex mixtures of bioactives.

Keywords:
Compound Kushen Injection, cancer cell, transcriptome, multiple targets, cell cycle, apoptosis

Abbreviations:

TCM, traditional Chinese medicine; CKI, compound Kushen injection; GO, Gene Ontology; DO, Disease Ontology; KEGG, Kyoto Encyclopedia of Gene and Genomes; PI, propidium iodide.

Introduction

The treatments of choice for cancer are often radiotherapy and/or chemotherapy, and while these can be effectie, they can cause quite serious side-effects, including death. These side-effects have driven the search for adjuvant therapies to both mitigate side-effects and/or potentiate the effectiveness of existing therapies. Traditional Chinese Medicine (TCM) is one of the options for adjuvant therapies, particularly in China, but increasingly so in the West. While clinical trial data on the effectiveness of TCM is currently limited, it remains an attractive option because of its long history and because its potential effectiveness is believed to result from the cumulative effects of multiple compounds on multiple targets (Jiang, 2005). Because TCM often has not been subjected to rigorous evidence based assessment and because it is based on an alternative theoretical system compared to Western medicine, adoption of its plant derived therapeutics has been slow.

In this report, we continue to characterise the molecular effects of Compound Kushen Injection (CKI) on cancer cells. CKI has been approved by the State Food and Drug Administration (SFDA) of China for clinical use since 1995 (Shu et al., 2014) (State medical license no. Z14021231). CKI is an herbal extract from two TCM plants, Kushen (*Sophora flavescens*) and Baituling (*Smilax Glabra*) and contains more than 200 different chemical compounds. These compounds include alkaloids and flavonoids such as matrine, oxymatrine and kurarinol that have been reported to have anti-cancer activities (Shu et al., 2014; Wang et al., 2015; Zhang et al., 2013; Zhao et al., 2014). Some of these activities have been shown to influence the expression of TP*53, BAX, BCL2* and other key genes known to be important in cancer cell growth and survival (Liao et al., 2015; Ninomiya and Koketsu, 2013; Wu et al., 2015; Zhang et al., 2001).

We have previously characterised the effect of CKI on the transcriptome of MCF-7 breast carcinoma cells and in this report, we extend our previous results to two additional human

cancer cell lines (MDA-MB-231, breast carcinoma and HEPG2, hepatocellular carcinoma). Both cell lines have also been shown to undergo apoptosis in response to the ingredients of CKI (Wang et al., 2015; Wu et al., 2015; Zhang et al., 2010; Zhao et al., 2014). HEPG2 is one of the most sensitive cancer cell lines with respect to exposure to CKI (Yang et al., 2017) and CKI is often used in conjunction with Western chemotherapy drugs for the treatment of liver cancer patients in China. While the specific mechanism of action of CKI is unknown, several recent studies have reported that CKI or its primary compounds affect the regulation/expression of oncogene products including *β-catenin, TP53*, *STAT3* and *AKT* (Liu et al., 2014; Ma et al., 2016; Shu et al., 2014; Wang et al., 2015; Yu et al., 2009).

However, these and other reports did not evaluate the entire range of molecular changes from treatment with a multi-component mixture such as CKI (Gao et al., 2018; Hao and Xiao, 2014). Whilst several research databases and tools for TCM research have been developed (Cui et al., 2014; Song et al., 2013; Wang and Chen, 2013), they are limited by the fact that most of the studies that contribute to the *corpus* of these databases are from different experimental systems, use single compounds or measure effects based on one or a handful of genes/gene products.

In contrast to previous studies, our strategy was to carry out comprehensive transcriptome profiling and network reconstruction from cancer cells treated with CKI. Instead of focusing on specific genes or pathways in order to design experiments, we have linked phenotypic assessment and RNA-seq analysis to CKI treatment. This allows us to present an unbiased, comprehensive analysis of CKI specific responses of biological networks associated with cancer. Our results indicate that different cancer cell lines that undergo apoptosis in response to CKI treatment can exhibit different CKI induced gene expression profiles that nonetheless implicate similar core genes and pathways in multiple cell lines.

The current study presents the effects of CKI on gene expression in cancer cells with an aim to identify candidate pathways and regulatory networks that may be perturbed by CKI *in vivo*. To this end we primarily use concentrations of CKI higher than used *in vivo* in order to be able to detect effects in the short time frames available to tissue culture experiments. We also combine our current analysis with previously published data to focus on a shared, much smaller set of candidate genes and pathways.

Material and Methods

Cell culture and reagents

CKI (total alkaloids concentration of 25 mg/mL) in 5 ml ampoules was provided by Zhendong Pharmaceutical Co. Ltd. (Beijing, China). Chemotherapeutic agent, Fluorouracil (5-FU) was purchased from Sigma-Aldrich (MO, USA). A human breast adenocarcinoma cell line, MDA-MB-231 and a hepatocellular carcinoma cell line HEPG2 were purchased from American Type Culture Collection (ATCC, Manassas, VA). The cells were cultured in Dulbecco's Modified Eagle Medium (DMEM; Thermo Fisher Scientific, MA, USA) supplemented with 10% foetal bovine serum (Thermo Fisher Scientific). Both cell lines were cultured at 37℃ with 5% CO_2.

For all *in vitro* assays, $4x10^5$ cells were seeded in 6-well trays and cultured overnight before being treated with either CKI (at 1 mg/mL and 2 mg/mL of total alkaloids) or 5-FU (150 μg/ml for HEPG2 and 20 μg/ml for MDA-MB-231. As a negative control, cells were treated with medium only and labelled as “untreated”. After 24 and 48 hours of treatment, cells were harvested and subjected to the downstream experiments.

Cell cycle and apoptosis assay

The assay was performed as previously described (Qu et al., 2016). For each cell line, three operators replicated the assay twice in order to ensure reproducibility of the observations. The results were obtained by flow cytometry using either FACScanto or LSRII (BD Biosciences, NJ, US).

RNA isolation and sequencing

The treated cells were harvested and the cell pellets were snap frozen with liquid nitrogen and stored at −80 °C. Total RNA was isolated with PureLink™ RNA Mini Kit (Thermo Fisher Scientific) according to the manufacturer’s protocol. After quantified using a NanoDrop Spectrophotometer ND-1000 (Thermo Fisher Scientific), the quality of the total RNA was verified on a Bioanalyzer by Cancer Genome Facility (SA, Australia) ensuring all samples had RINs >7.0.

For both cell lines, the sequencing was performed in Ramaciotti Centre for Genomics (NSW, Australia). The sample preparation for each cell line was TruSeq Stranded mRNA-seq with dual indexed, on the NextSeq500 v2 platform. The parameter was 75bp paired-end High Output. The fastq files were generated and trimmed through Basespace with application "FASTQ Generation v1.0.0".

Bioinformatics analysis of RNA sequencing

The clean HEPG2 reads were aligned to reference genome (hg38) using STAR v2.5.1 with following parameters: --outFilterMultimapNmax 20 --outFilterMismatchNmax 10 --outSAMtype BAM SortedByCoordinate --outSAMstrandField intronMotif (Dobin et al., 2013). The clean MDA-MB-231 reads were aligned to reference genome (hg19) using TopHat2 v2.1.1 with following parameters: --read-gap-length 2 --read-edit-dist 2 (Kim et al., 2013). Differential expression analysis for reference genes was performed with edgeR and differentially expressed (DE) genes were selected with a False Discovery Rate (FDR) < 0.05 (Robinson et al., 2010).

The DE genes in common for both HEPG2 and MDA-MB-231 cell lines at 24 hours and 48 hours after CKI treatment were selected as "shared" genes. These shared genes were utilized to describe the major anti-cancer functions and principal mechanisms of CKI.

Gene Ontology (GO), and Kyoto Encyclopedia of Gene and Genomes (KEGG) over-representation analyses of both cell lines were carried out using the online database system ConsensusPathDB (Kamburov et al., 2008) with the following settings: "Biological process" (BP) at third level (for GO); q values (<0.01) were corrected for multiple testing with the system default settings. Disease ontology (DO) over-representation analyses of both cell lines were performed by using the Bioconductor R package clusterProfiler v3.5.1 (Yu et al., 2012). For the function analyses of shared/core genes, the method was as similar as our previous study (Qu et al., 2016) using ClueGO app 2.2.5 in Cytoscape v3.6.0. We enriched our GO terms in the biological process category level 3 and KEGG pathways, showing only terms/pathways with p values less than 0.01. Specific Over-represented terms/pathways and gene expression status mapping in KEGG pathways were visualised with the R package "Pathview" (Luo and Brouwer, 2013).

Gene expression-based investigation of bioactive components in CKI

To integrate with previous data from MCF-7 cells (Qu et al., 2016), all the shared DE genes regulated by CKI identified in all three cell lines using edgeR were mapped to the BATMAN-TCM database (Liu et al., 2016). The pharmacophore modelling method (Li et al., 2012) was used to generate the interaction network between the key genes and TCM components using R package igraph (Csardi and Nepusz, 2006).

Reverse transcription quantitative polymerase chain reaction (RT-qPCR)

RT-qPCR was performed as previously described (Qu et al., 2016). The list of target genes selected for this study and the sequences of all primers are shown in Additional file 1: Table S1.

Results

Effect of CKI on the cell cycle and apoptosis

In our previous study, CKI significantly perturbed/suppressed cancer cell target genes/networks. In the current study we present results that confirm and generalise our previous work. We observed in the MCF-7 study, low concentrations of CKI in our short-term cell assay showed no/little phenotypic effect within 48 hours, and very high doses resulted in excessive cell death at 48 hours precluding the isolation of sufficient RNA for transcriptome analysis (Qu et al., 2016). Therefore, in our current study with the two additional cell lines, to ensure consistency, we also selected 1 mg/ml and 2 mg/ml total alkaloid concentrations of CKI for our assays because they generated reproducible and significant phenotypic effects in our cell culture assay.

We used flow cytometric analysis of propidium iodide (PI) stained cells to assess both CKI induced alterations to the cell cycle and apoptosis. In HEPG2 cells, CKI treatment resulted in an overall increase in the proportion of cells in G1 phase and decrease in S phase (Fig. 1a and b). Similarly in MDA-MB-231 cells, although a consistent increase in G1 phase was not observed, CKI caused a decrease in S phase particularly at the 24-hour time point (Fig. 1a and b) indicating possible incidence of cell cycle arrest at G1 phase. Furthermore, at 2 mg/ml of total alkaloids, CKI consistently induced significantly higher level of apoptosis in both cell lines at both time points compared to untreated controls (Fig. 1c). These data together suggest that CKI has effects on the cell cycle by interfering with the transition

between G1 to S phase as well as by acting on the apoptosis pathway and promoting cell death.

CKI perturbation of gene expression

In order to elucidate the molecular mechanisms of action of CKI on these cancer cells, transcriptome analysis of CKI treated cells was performed. As mentioned above, RNA samples from two cell lines were sequenced with 2x75 bp paired-end reads. We had previously sequenced transcriptomes from CKI treated MCF-7 cells (Qu et al., 2016) and have included those results for comparison below. The samples from each cell line contained 7 groups at 3 time points (Fig. 2a), in triplicate for every group. In the multidimensional scaling (MDS) analysis, each cell line clustered independently and generally, within the cell line clusters, untreated cells clustered apart from treated cells (Additional file 2: Fig. S1).

With the mapping rate were around 90% (Additional file 3: Table S2), a P-value based ranked list of DE genes (compared to untreated from each time point) was generated for both cell lines (Additional file 4: Table S3, sheet 1-4). This list was used to select the shared DE genes. This analysis generated thousands of DE genes (Additional file 4: Table S3, sheet 5) across two cell lines.

Because for each cell line the respective treatment groups clustered together on the MDS plot, there were large numbers of shared genes between them. As a result, we identified a set of 6852 shared DE genes by identifying common DE genes from HEPG2 and MDA-MB-231 cell lines, at 24hours and 48 hours (Fig. 2b). These shared genes might predict a common molecular signature for CKI's activity. However, there were still a large number of DE genes that were not shared by both cell lines, as seen in the heatmap in Fig. 2c. The expression of the shared gene set in both HEPG2 and MDA-MB-231 is highly consistent. Interestingly, this consistency is with respect to treatment time, rather than with respect to cell line.

RT-qPCR validation and dose response of gene expression to CKI

Based on our previous results (Qu et al., 2016), and analysis below, we selected the 4 top ranked DE genes expressed in G1-S phase of the cell cycle (*TP53* and *CCND1* for expression level validation and *E2F2*and *PCNA* for low dose response), as well as the proliferation and differentiation relevant ras subfamily encoding gene (*RAP1GAP1*) for low dose response. We also selected a prominently expressed gene (*CYP1A1*) for validation because of its sensitivity to CKI treatment. *CYP1A1, TP53* and *CCND1* expression changes were validated with RT-qPCR with all three genes showing similar patterns of expression in the transcriptome data and RT-qPCR (Fig. 3a).

Because low dose treatment with CKI did not cause significant gross phenotypic effects in either cell line, we decided to use gene expression as a more sensitive measure of phenotype to look at the effect of lower doses of CKI. We used 0.125 mg/ml, 0.25 mg/ml, 0.5 mg/ml and 1mg/ml concentrations to look for dose dependency of gene expression. Our results showed an obvious dose-dependent expression trend (Fig. 3b) in both cell lines. Because the 0.125mg/ml concentration of CKI is equivalent to what cancer patients are treated with, our results are potentially clinically relevant.

Function enrichment analysis

To identify candidate mechanisms of action of CKI, we carried out functional enrichment analysis. We used ConsensusPathDB(Kamburov et al., 2008) and Clusterprofiler (Li et al., 2012) along with GO and KEGG pathways for over-representation analysis, along with disease ontology (DO) (Schriml et al., 2011) enrichment.

GO over-representation test was determined based on Biological Process level 3 and *q* value <0.01. The results for both cell lines at both time points were summarised and visualized based on semantic analysis of terms in Fig. 4a. From this result, it was obvious that there were a large proportion of enriched GO terms relating to cell cycle, such as “cell cycle checkpoint”, “negative/positive regulation of cell cycle process” and so on prominently featured for all data sets (Additional file 5: Fig. S2, Additional file 6: Table S4, sheet 1-4).

We then used KEGG pathways to determine the specific pathways altered by CKI in cancer. The most regulated over-representative KEGG pathways are summarized according to KEGG

252 Orthology (KO) (Fig. 4b). Cell cycle related pathways such as “cell cycle”, “DNA replication”,
253 and “apoptosis” were also consistently seen in the KEGG enrichment results (Additional file
254 6: Table S4, sheet5-8) at both 24 and 48 hours. Moreover, in addition to the cell cycle
255 relevant pathways, some cancer related pathways were also observed, such as “prostate
256 cancer” and “chronic myeloid leukaemia”, and a large number of DE genes (283) from the
257 two cell lines were relevant in “pathways in cancer”.

258 Because the KEGG enrichment revealed many pathways relating to diseases, most of which
259 were cancers, we decided to explore the enrichment of DE genes with respect to DO terms
260 (Fig. 4c). In the DO list (Additional file 6: Table S4, sheet 9-12), all top ranked terms listed are
261 cancers. Interestingly, most cancer types listed are from the lower abdomen, for example
262 “ovarian cancer”, “urinary bladder cancer “and “prostate cancer” etc. occurring in
263 genitourinary organs (Additional file 6: Table S4, sheet 9-12). For both KEGG pathway and
264 DO enrichment, the effects of CKI on both cell lines were similar.

265 In addition to cell line specific functional enrichment of DE genes, we also analysed the over-
266 represented GO terms for shared DE genes (Fig. 5a). The most significant clusters were
267 highly relevant to metabolic process, such as “cellular macromolecule metabolic process”,
268 as well as the corresponding positive/negative regulatory biological process (Additional file
269 6: Table S4, sheet 13). Moreover, various signalling pathways, though not forming a large
270 cluster, were also significant, for example, “regulation of signal transduction” and
271 “intracellular receptor signalling pathway”. Finally, some “cell cycle” related terms
272 constituted relatively large sub-clusters, including “cell division” and “mitotic cell cycle
273 process”. The enriched GO analysis was consistent with the cell line specific enriched
274 results, and with our previous analysis of MCF-7 cells (Qu et al., 2016). It is worth noting that
275 for “cell cycle” related terms, most of the participating genes were down-regulated by CKI.

276 Similar results were observed from KEGG analysis (Fig. 5b, and Additional file 6: Table S4,
277 sheet 14) of shared genes. Various pathways related to cancer, formed a large cluster.
278 Pathways such as “DNA replication”, “Ribosome” and “cell cycle” were mostly down-
279 regulated, while up-regulated pathways included “inositol phosphate metabolism” and
280 “protein processing in endoplasmic reticulum”.

We also carried out over-representation analysis of DO terms (Fig. 5c) for all shared DE genes. The analysis results were consistent with the single cell line DO term analysis with mostly cancer related terms; in particular genitourinary or breast cancer terms. While this was also partially similar to the KEGG results for shared DE genes, there were some differences in the KEGG results for disease pathways compared to the DO results, such as "bacterial invasion of epithelial cells", "Fanconi anemia pathway" and "AGE-RAGE pathway in diabetic complications".

Regulation of specific pathways related to cancer

Specific to the therapeutic potential of CKI for cancer treatment, we applied our data set mapping to KEGG cancer pathways: pathways in cancer- homo sapiens (Additional file 7: Fig. S3). The R package Pathview (Luo and Brouwer, 2013) was used to integrate log fold change values of all the genes expression patterns into these target pathways. Within the 21 pathways in cancer, the "cell cycle" still featured prominently (Fig. 6a). The expression of almost every gene in the cell cycle pathway was affected by CKI, with most of them suppressed. We did not observe this kind of overall pathway suppression in any of the other pathways. We have displayed the summaries for the remaining 20 pathways in the heatmap in Fig. 6b. Although all the pathways were all perturbed by CKI, they include both over and under expressed genes in roughly equal proportions.

Collectively, these results suggest a direct anticancer effect of CKI, and implicate specific candidate mechanisms of action based on the perturbed molecular networks. The most obvious example is the cell cycle, where G1-S phase is significantly altered, resulting in the induction of apoptosis. The downstream process triggered by CKI is the suppression of gene expression of cell cycle regulators, including *P53* and *CCND1*. The other perturbed cancer pathways provide additional candidate mechanisms of action for CKI. In the following section we integrate these results with previous results reported in the literature to refine the core set of genes and pathways perturbed by CKI.

Discussion

Although HEPG2 (liver cancer – mesodermal tissue origin) and MDA-MB-231 (mammary epithelial adenocarcinoma – ectodermal tissue origin) are different cancer types, they shared a large number of CKI DE genes with similar expression profiles, presumably these

311 shared genes include CKI response genes that are essential to the apoptotic response
312 triggered by CKI. However, the number of shared CKI DE genes is too high to allow straight
313 forward identification of genes critical to the CKI response. We therefore decided to
314 combine these data with previously reported CKI DE genes from MCF-7 cells (Qu et al.,
315 2016) in order to reduce the number of core CKI response genes. The intersection of MCF-7
316 CKI DE genes with the shared CKI DE genes yielded 363 core CKI DE genes (Additional file 8:
317 Fig. S4).

318 Among the 363 core CKI DE genes, cytochrome P450 family 1 subfamily A member 1
319 (*CYP1A1*) gene is the most over-expressed. This gene is consistently up-regulated by CKI in
320 all three cell lines, and showed significant dose response. In liver cancer cells, over-
321 expression of *CYP1A1* induced by plant natural products has been associated with Aryl-
322 hydrocarbon Receptor transformation (Anwar-Mohamed and El-Kadi, 2009; Zhou et al.,
323 2016). Furthermore, as a steroid-metabolizing enzyme, CYP1A1 is part of cancer metabolic
324 processes relevant to steroid hormone responsive tumours, such as breast cancer, ovarian
325 cancer and prostate cancer (Mitsui et al., 2016; Nandekar et al., 2016; Ou et al., 2016;
326 Piotrowska-Kempisty et al., 2017). Therefore, *CYP1A1* may be of particular interest for
327 understanding the mechanism of action of CKI on cancer cells.

328 Comparison of the 363 core genes to the 135 Tumour Alterations Relevant for Genomics-
329 driven Therapy (TARGET) genes (version 3) from The Broad Institute
330 (https://www.broadinstitute.org/ cancer/cga/target) identified 7 DE genes that were shared
331 across the three cell lines and two time points (Fig. 7a). Of these seven genes, six (*TP53*,
332 *CCND1*, *MYD88* (Myeloid differentiation primary response gene 88) , *EWSR1*, *TMPRSS2* and
333 *IDH1* (isocitrate dehydrogenase 1)) were similarly regulated (either always over-expressed
334 or under-expressed), while *CCND3* was over-expressed in all three cell lines at both time
335 points except at 48 hours in MCF-7 cells, where it was under-expressed.

336 The *TP53* gene encodes a tumor suppressor protein, that can induce apoptosis (Harris and
337 Levine, 2005). However, in all cell lines *TP53* was down-regulated, and all cell lines showed
338 increased apoptosis. This suggests that CKI induced apoptosis was not *TP53*-dependent.
339 Support for this comes from the fact that transcripts for *PCNA* (proliferating cell nuclear
340 antigen), and a group of transcription factors: *MCM* (mini-chromosome maintenance)

complex and the *E2F* family are down-regulated. The *E2F* transcription factors regulate the cell cycle and *TP53*-dependent and -independent apoptosis (Hollern et al., 2014; Sun et al., 2013; Woods et al., 2007; Zaldua et al., 2016). In addition, other core genes present in the TARGET database have also been shown to induce apoptosis. For example, inhibition of *MYD88* induces apoptosis in both triple negative breast cancer and bladder cancer (Christensen et al., 2017; Zhang et al., 2016). The increased expression of *IDH1* may be important, as IDH1 is frequently mutated in cancers (Li et al., 2012) and when mutated, it causes loss of α–ketoglutarate production and may be important for the Warburg effect. *TMPRSS2* (transmembrane protease, serine 2) has also been shown to regulate apoptosis in cancer (Afar et al., 2001). Therefore, CKI may induce apoptosis through a variety of means.

In the GO (Fig. 7b) and KEGG (Fig. 7c) over-representation analysis of the 363 core genes yielded enrichment for cell cycle and cancer pathways. In the GO enriched genes, cell cycle and related pathways accounted for the majority of functional sub-clusters. In the KEGG enriched pathways, cell cycle and cancer pathways predominated in a single cluster. Most of the core genes in GO and KEGG clusters were down-regulated by CKI.

In addition to the cell cycle, CKI treatment also caused enrichment for terms or pathways related to cancer progression, such as “focal adhesion” and “blood vessel development”. (Additional file 6: Table S4, sheet 5-8). These developmental processes contribute to tumorigenesis and metastasis(Luo and Guan, 2010; Warren et al., 1995). It is tempting to speculate that CKI may alter these functions *in vivo*, possibly altering angiogenesis which is critical for tumours (Hanahan and Folkman, 1996). In addition, there were metabolic pathways and terms that were also identified as perturbed by CKI. Effects on many targets/pathways is one of the expected features of TCM drugs which likely hit multiple targets (Efferth et al., 2007).

We have examined the effect of a complex mixture of plant natural products (CKI) on different cancer cell lines and have identified specific, consistent effects on gene expression resulting from this mixture. However, the complexity of CKI makes it difficult to determine the mechanism of action of individual components, and often testing of individual components has resulted in either no effect or contradictory results in the research literature. In spite of this complexity, it is possible to map our results on to a pre-existing

corpus of work that links individual natural compounds to changes in gene expression. We have used BATMAN (Liu et al., 2016), an online TCM database of curated links between compounds and gene expression. Based on this resource, we have identified 14 components of CKI that have been linked to the regulation of 52 of our core genes (Fig. 7d). We can see from the network diagram in Fig. 7d that one to one, one to many and many to many relationships exist between CKI components and genes which is consistent with previous studies (Liu et al., 2014; Wu et al., 2015; Zhang and Yu, 2016). As more information becomes available for individual components, we will be able to construct a more comprehensive model of CKI mechanism based on network analysis.

Conclusions

Our systematic analysis of gene expression changes in cancer cells caused by a complex herbal extract used in TCM has proven to be effective at identifying candidate molecular pathways. CKI has consistent and specific effects on gene expression across multiple cancer cell lines and it also consistently induces apoptosis in vitro. These effects show that CKI can suppress the expression of cell cycle regulatory genes and other well characterized cancer related genes and pathways. Validation of a subset of DE genes at lower doses of CKI has shown a dose-response relationship that suggests that CKI may have similar effects in vivo at clinically relevant concentrations. Our results provide a molecular basis for further investigation of the mechanism of action of CKI.

391

392 Literature Cited
393

394 Afar, D.E., Vivanco, I., Hubert, R.S., Kuo, J., Chen, E., Saffran, D.C., Raitano, A.B., Jakobovits,
395 A., 2001. Catalytic cleavage of the androgen-regulated TMPRSS2 protease results in its
396 secretion by prostate and prostate cancer epithelia. Cancer research 61, 1686-1692.
397 Anwar-Mohamed, A., El-Kadi, A.O., 2009. Sulforaphane induces CYP1A1 mRNA, protein, and
398 catalytic activity levels via an AhR-dependent pathway in murine hepatoma Hepa 1c1c7 and
399 human HepG2 cells. Cancer letters 275, 93-101.
400 Christensen, A.G., Ehmsen, S., Terp, M.G., Batra, R., Alcaraz, N., Baumbach, J., Noer, J.B.,
401 Moreira, J., Leth‐Larsen, R., Larsen, M.R., 2017. Elucidation of Altered Pathways in Tumor‐
402 Initiating Cells of Triple‐Negative Breast Cancer: A Useful Cell Model System for Drug
403 Screening. STEM CELLS.
404 Csardi, G., Nepusz, T., 2006. The igraph software package for complex network research.
405 InterJournal, Complex Systems 1695, 1-9.
406 Cui, M., Li, H., Hu, X., 2014. Similarities between “Big Data” and traditional Chinese medicine
407 information. Journal of Traditional Chinese Medicine 34, 518-522.
408 Dobin, A., Davis, C.A., Schlesinger, F., Drenkow, J., Zaleski, C., Jha, S., Batut, P., Chaisson, M.,
409 Gingeras, T.R., 2013. STAR: ultrafast universal RNA-seq aligner. Bioinformatics 29, 15-21.
410 Efferth, T., Li, P.C., Konkimalla, V.S.B., Kaina, B., 2007. From traditional Chinese medicine to
411 rational cancer therapy. Trends in molecular medicine 13, 353-361.
412 Gao, L., Wang, K.-x., Zhou, Y.-z., Fang, J.-s., Qin, X.-m., Du, G.-h., 2018. Uncovering the
413 anticancer mechanism of Compound Kushen Injection against HCC by integrating
414 quantitative analysis, network analysis and experimental validation. Scientific reports 8, 624.
415 Hanahan, D., Folkman, J., 1996. Patterns and emerging mechanisms of the angiogenic
416 switch during tumorigenesis. cell 86, 353-364.
417 Hao, D.C., Xiao, P.G., 2014. Network pharmacology: a Rosetta Stone for traditional Chinese
418 medicine. Drug development research 75, 299-312.
419 Harris, S.L., Levine, A.J., 2005. The p53 pathway: positive and negative feedback loops.
420 Oncogene 24, 2899.
421 Hollern, D.P., Honeysett, J., Cardiff, R.D., Andrechek, E.R., 2014. The E2F transcription
422 factors regulate tumor development and metastasis in a mouse model of metastatic breast
423 cancer. Molecular and cellular biology 34, 3229-3243.
424 Jiang, W.-Y., 2005. Therapeutic wisdom in traditional Chinese medicine: a perspective from
425 modern science. Trends in pharmacological sciences 26, 558-563.
426 Kamburov, A., Wierling, C., Lehrach, H., Herwig, R., 2008. ConsensusPathDB—a database for
427 integrating human functional interaction networks. Nucleic acids research 37, D623-D628.
428 Kim, D., Pertea, G., Trapnell, C., Pimentel, H., Kelley, R., Salzberg, S.L., 2013. TopHat2:
429 accurate alignment of transcriptomes in the presence of insertions, deletions and gene
430 fusions. Genome Biol 14, R36.
431 Li, X., Xu, X., Wang, J., Yu, H., Wang, X., Yang, H., Xu, H., Tang, S., Li, Y., Yang, L., 2012. A
432 system-level investigation into the mechanisms of Chinese Traditional Medicine: Compound
433 Danshen Formula for cardiovascular disease treatment. PloS one 7, e43918.
434 Liao, C.-Y., Lee, C.-C., Tsai, C.-c., Hsueh, C.-W., Wang, C.-C., Chen, I., Tsai, M.-K., Liu, M.-Y.,
435 Hsieh, A.-T., Su, K.-J., 2015. Novel investigations of flavonoids as chemopreventive agents
436 for hepatocellular carcinoma. BioMed research international 2015.

Liu, Y., Xu, Y., Ji, W., Li, X., Sun, B., Gao, Q., Su, C., 2014. Anti-tumor activities of matrine and oxymatrine: literature review. Tumor Biology 35, 5111-5119.
Liu, Z., Guo, F., Wang, Y., Li, C., Zhang, X., Li, H., Diao, L., Gu, J., Wang, W., Li, D., 2016. BATMAN-TCM: a Bioinformatics Analysis Tool for Molecular mechANism of Traditional Chinese Medicine. Scientific reports 6.
Luo, M., Guan, J.-L., 2010. Focal adhesion kinase: a prominent determinant in breast cancer initiation, progression and metastasis. Cancer letters 289, 127-139.
Luo, W., Brouwer, C., 2013. Pathview: an R/Bioconductor package for pathway-based data integration and visualization. Bioinformatics 29, 1830-1831.
Ma, X., Li, R.-S., Wang, J., Huang, Y.-Q., Li, P.-Y., Wang, J., Su, H.-B., Wang, R.-L., Zhang, Y.-M., Liu, H.-H., 2016. The therapeutic efficacy and safety of compound kushen injection combined with transarterial chemoembolization in unresectable hepatocellular carcinoma: an update systematic review and meta-analysis. Frontiers in pharmacology 7.
Mitsui, Y., Chang, I., Kato, T., Hashimoto, Y., Yamamura, S., Fukuhara, S., Wong, D.K., Shiina, M., Imai-Sumida, M., Majid, S., 2016. Functional role and tobacco smoking effects on methylation of CYP1A1 gene in prostate cancer. Oncotarget 7, 49107.
Nandekar, P.P., Khomane, K., Chaudhary, V., Rathod, V.P., Borkar, R.M., Bhandi, M.M., Srinivas, R., Sangamwar, A.T., Guchhait, S.K., Bansal, A.K., 2016. Identification of leads for antiproliferative activity on MDA-MB-435 human breast cancer cells through pharmacophore and CYP1A1-mediated metabolism. European journal of medicinal chemistry 115, 82-93.
Ninomiya, M., Koketsu, M., 2013. Minor flavonoids (chalcones, flavanones, dihydrochalcones, and aurones), Natural Products. Springer, pp. 1867-1900.
Ou, C., Zhao, Y., Liu, J.-H., Zhu, B., Li, P.-Z., Zhao, H.-L., 2016. Relationship Between Aldosterone Synthase CYP1A1 MspI Gene Polymorphism and Prostate Cancer Risk. Technology in cancer research & treatment, 1533034615625519.
Piotrowska-Kempisty, H., Klupczyńska, A., Trzybulska, D., Kulcenty, K., Sulej-Suchomska, A.M., Kucińska, M., Mikstacka, R., Wierzchowski, M., Murias, M., Baer-Dubowska, W., 2017. Role of CYP1A1 in the biological activity of methylated resveratrol analogue, 3, 4, 5, 4′-tetramethoxystilbene (DMU-212) in ovarian cancer A-2780 and non-cancerous HOSE cells. Toxicology letters 267, 59-66.
Qu, Z., Cui, J., Harata-Lee, Y., Aung, T.N., Feng, Q., Raison, J.M., Kortschak, R.D., Adelson, D.L., 2016. Identification of candidate anti-cancer molecular mechanisms of Compound Kushen Injection using functional genomics. Oncotarget 7, 66003-66019.
Robinson, M.D., McCarthy, D.J., Smyth, G.K., 2010. edgeR: a Bioconductor package for differential expression analysis of digital gene expression data. Bioinformatics 26, 139-140.
Schriml, L.M., Arze, C., Nadendla, S., Chang, Y.-W.W., Mazaitis, M., Felix, V., Feng, G., Kibbe, W.A., 2011. Disease Ontology: a backbone for disease semantic integration. Nucleic acids research 40, D940-D946.
Shu, G., Yang, J., Zhao, W., Xu, C., Hong, Z., Mei, Z., Yang, X., 2014. Kurarinol induces hepatocellular carcinoma cell apoptosis through suppressing cellular signal transducer and activator of transcription 3 signaling. Toxicology and applied pharmacology 281, 157-165.
Song, Y.-N., Zhang, G.-B., Zhang, Y.-Y., Su, S.-B., 2013. Clinical applications of omics technologies on ZHENG differentiation research in traditional Chinese medicine. Evidence-Based Complementary and Alternative Medicine 2013.
Sun, H.X., Xu, Y., Yang, X.R., Wang, W.M., Bai, H., Shi, R.Y., Nayar, S.K., Devbhandari, R.P., He, Y.z., Zhu, Q.F., 2013. Hypoxia inducible factor 2 alpha inhibits hepatocellular carcinoma

484 growth through the transcription factor dimerization partner 3/E2F transcription factor 1–
485 dependent apoptotic pathway. Hepatology 57, 1088-1097.
486 Wang, P., Chen, Z., 2013. Traditional Chinese medicine ZHENG and Omics convergence: A
487 systems approach to post-genomics medicine in a global world. Omics: a journal of
488 integrative biology 17, 451-459.
489 Wang, W., You, R.-l., Qin, W.-j., Hai, L.-n., Fang, M.-j., Huang, G.-h., Kang, R.-x., Li, M.-h.,
490 Qiao, Y.-f., Li, J.-w., 2015. Anti-tumor activities of active ingredients in Compound Kushen
491 Injection. Acta Pharmacologica Sinica 36, 676-679.
492 Warren, R.S., Yuan, H., Matli, M.R., Gillett, N.A., Ferrara, N., 1995. Regulation by vascular
493 endothelial growth factor of human colon cancer tumorigenesis in a mouse model of
494 experimental liver metastasis. The Journal of clinical investigation 95, 1789-1797.
495 Woods, K., Thomson, J.M., Hammond, S.M., 2007. Direct regulation of an oncogenic micro-
496 RNA cluster by E2F transcription factors. Journal of Biological Chemistry 282, 2130-2134.
497 Wu, C., Huang, W., Guo, Y., Xia, P., Sun, X., Pan, X., Hu, W., 2015. Oxymatrine inhibits the
498 proliferation of prostate cancer cells in vitro and in vivo. Molecular medicine reports 11,
499 4129-4134.
500 Yang, X., Huang, M., Cai, J., Lv, D., Lv, J., Zheng, S., Ma, X., Zhao, P., Wang, Q., 2017.
501 Chemical profiling of anti-hepatocellular carcinoma constituents from Caragana tangutica
502 Maxim. by off-line semi-preparative HPLC-NMR. Natural product research 31, 1150-1155.
503 Yu, G., Wang, L.-G., Han, Y., He, Q.-Y., 2012. clusterProfiler: an R Package for Comparing
504 Biological Themes Among Gene Clusters. OMICS : a Journal of Integrative Biology 16, 284-
505 287.
506 Yu, P., Liu, Q., Liu, K., Yagasaki, K., Wu, E., Zhang, G., 2009. Matrine suppresses breast cancer
507 cell proliferation and invasion via VEGF-Akt-NF-κB signaling. Cytotechnology 59, 219-229.
508 Zaldua, N., Llavero, F., Artaso, A., Gálvez, P., Lacerda, H.M., Parada, L.A., Zugaza, J.L., 2016.
509 Rac1/p21‐activated kinase pathway controls retinoblastoma protein phosphorylation and
510 E2F transcription factor activation in B lymphocytes. FEBS journal 283, 647-661.
511 Zhang, H., Ye, Y., Li, M., Ye, S., Huang, W., Cai, T., He, J., Peng, J., Duan, T., Cui, J., 2016.
512 CXCL2/MIF-CXCR2 signaling promotes the recruitment of myeloid-derived suppressor cells
513 and is correlated with prognosis in bladder cancer. Oncogene.
514 Zhang, J.-Q., Li, Y.-M., Liu, T., He, W.-T., Chen, Y.-T., Chen, X.-H., Li, X., Zhou, W.-C., Yi, J.-F.,
515 Ren, Z.-J., 2010. Antitumor effect of matrine in human hepatoma G2 cells by inducing
516 apoptosis and autophagy. World journal of gastroenterology: WJG 16, 4281.
517 Zhang, L.P., Jiang, J.K., Tam, J.W.O., Zhang, Y., Liu, X.S., Xu, X.R., Liu, B.Z., He, Y.J., 2001.
518 Effects of Matrine on proliferation and differentiation in K-562 cells. Leukemia Research 25,
519 793-800.
520 Zhang, X., Yu, H., 2016. Matrine inhibits diethylnitrosamine-induced HCC proliferation in rats
521 through inducing apoptosis via p53, Bax-dependent caspase-3 activation pathway and
522 down-regulating MLCK overexpression. Iranian Journal of Pharmaceutical Research: IJPR 15,
523 491.
524 Zhang, X.-L., Cao, M.-A., Pu, L.-P., Huang, S.-S., Gao, Q.-X., Yuan, C.-S., Wang, C.-M., 2013. A
525 novel flavonoid isolated from Sophora flavescens exhibited anti-angiogenesis activity,
526 decreased VEGF expression and caused G0/G1 cell cycle arrest in vitro. Die Pharmazie-An
527 International Journal of Pharmaceutical Sciences 68, 369-375.
528 Zhao, Z., Fan, H., Higgins, T., Qi, J., Haines, D., Trivett, A., Oppenheim, J.J., Wei, H., Li, J., Lin,
529 H., 2014. Fufang Kushen injection inhibits sarcoma growth and tumor-induced hyperalgesia
530 via TRPV1 signaling pathways. Cancer letters 355, 232-241.

Zhou, Y., Li, Y., Zhou, T., Zheng, J., Li, S., Li, H.-B., 2016. Dietary natural products for prevention and treatment of liver cancer. Nutrients 8, 156.

Author contributions statement:

JC experimental design, carried out experiments, analysed data, wrote paper, ZQ experimental design, assisted with experiments, assisted with data analysis, wrote paper, YHL experimental design, assisted with experiments, assisted with data analysis, wrote paper, HS assisted with experiments, TNA assisted with experiments, WW assisted with experimental design, assisted with experiments, RDK experimental design, and DLA supervised the research, acquired funding for the experiments, experimental design, wrote paper.

Competing interests

While a generous donation was used to set up the Zhendong Centre by Shanxi Zhendong Pharmaceutical Co Ltd, they did not determine the research direction for this work or influence the analysis of the data. JC: no competing interests, ZQ: no competing interests, YHL: no competing interests, HS: no competing interests, TNA: no competing interests, WW: is an employee of Zhendong Pharma seconded to Zhendong Centre to learn bioinformatics methods, RDK: no competing interests, DLA: Director of the Zhendong Centre which was set up with a generous donation from the Zhendong Pharmaceutical Co Ltd. Zhendong Pharmaceutical has had no control over these experiments, their design or analysis and have not exercised any editorial control over the manuscript.

Data Availability

All RNAseq data raw and processed data were deposited at the Gene Expression Omnibus (GEO) data repository (XXXXXXX).

558

559 **Figure legends**

560 Fig. 1

561 Effects of different treatment on cell cycle and apoptosis of HEPG2 and MDA-MB-231 cells.
562 **a** The apoptosis and cell cycle distribution of each cell line after 24- and 48-hour treatments
563 with CKI or 5-Fu assessed PI staining. **b** Percentages of cells in different phases of cell cycle
564 resulting from treatment. **c** Percentage of apoptotic cells after treatment. Results shown are
565 mean ±SEM (n=6). Statistically significant differences from untreated control were identified
566 using two-way ANOVA (*p<0.05, **p<0.01, ****p<0.0001).

567 Fig. 2

568 DE genes shared in both cell lines at both time points. **a.** Work flow diagram showing
569 experimental design and sample collection. **b** Venn diagram showing the number of shared
570 DE genes between HEPG2 and MDA-MB-231. **c** Heatmap presenting the overall gene
571 expression pattern in both cell lines treated with CKI. Heatmap is split into four parts based
572 on gene content and expression pattern: 5442 differentially regulated genes with
573 expression not shared between the two cell lines, 3157 upregulated genes shared between
574 both cell lines, 3522 down-regulated genes shared between both cell lines, and 173
575 discordantly regulated genes with differential expression shared between both cell lines.

576 Fig. 3

577 Validation of gene expression and effects of low dose CKI using RT-qPCR. **a** Comparison of
578 DE genes between RNA-seq results (left) and RT-qPCR validation (right) for each cell line at 2
579 time-points. Three DE genes (*CYP1A1, TP53* and *CCND1*) were chosen for validation. Gene

580 expression was generally consistent between transcriptome data and qPCR data. **b** Dose
581 response of CKI using a subset of genes with conserved expression in HEPG2 (left), and
582 MDA-MB-231 (right) from 0 mg/ml to 1 mg/ml of total alkaloids. Six genes (*CYP1A1, TP53,*
583 *CCND1, Rap2GAP1, E2F2* and *PCNA*) were selected based on their relevance to important
584 pathways perturbed by CKI. RT-qPCR results are presented as expression relative to RPS13.
585 Data are represented as mean ±SEM (n>3). A t-test was used to compare CKI doses with
586 "untreated" (*p<0.05, **p<0.01, ***p<0.001, ****p<0.0001).

587 Fig. 4

588 Functional annotation of DE genes for each cell line as a result of CKI treatment. Summary of
589 over-represented **a** GO terms for Biological Process, **b** KEGG pathways and **c** DO terms for
590 DE genes as a result of CKI treatment in each cell line at two time points. For GO semantic
591 and enrichment analysis, Lin's algorithm was applied to cluster and summarize similar
592 functions based on GO terms found in every treatment. Similarly, by back-tracing the
593 upstream categories in the KEGG Ontology, we were able to obtain a more generalized
594 summary of KEGG pathways for each treatment. The size of each bubble represents the
595 number of GO terms/pathways, and the colour shows the statistical significance of the
596 relevant function or pathways. The DO summary for each treatment was determined by
597 back-tracing to parent terms.

598 Fig. 5

599 Functional annotation of DE genes with shared expression in both cell lines as a result of CKI
600 treatment. Over-representation analysis was performed to determine **a** GO terms for
601 Biological Process, **b** KEGG pathways, and **c** DO terms for DE genes shared in both cell lines.
602 In nodes for both GO terms and KEGG pathways, node size is proportional to the statistical

603 significance of over-representation. For DO terms, all the enriched terms are statistically
604 significant ($p<1x10^{-5}$) in each category, and the bar length represents the number of
605 expressed genes that map to the term.

606 Fig. 6

607 Comparison of shared genes expression in specific pathways across two cell lines. **a** Cell
608 cycle pathways, where each coloured box is separated into 4 parts, from left to right
609 representing 24h CKI treated HEPG2, 48h CKI treated HEPG2, 24h CKI treated MDA-MB-231
610 as well as 48h CKI treated MDA-MB-231. **b** Heatmap of pathways in cancer. The top two
611 heatmaps summarise the effects of CKI on HEPG2 cells for two time-points, and the bottom
612 two heatmaps show the effects of CKI on MDA-MB-231 cells. In addition to the cell cycle
613 pathway, there were 21 associated pathways in cancer that were perturbed by CKI. The
614 effects of CKI on both cell lines were similar, with changes in TARGET database genes
615 indicated by arrows. Compared to other pathways in cancer, the effects of CKI on the cell
616 cycle pathway showed overall down-regulation.

617 Fig. 7.

618 Analysis of CKI regulated core genes from this report combined with previous available data.
619 **a** Fold changes of TARGET and cell cycle regulatory gene expression in MDA-MB-231, HEPG2
620 and MCF-7(Qu et al., 2016) cell lines 24 and 48 hours after CKI treatment. Only seven
621 TARGET genes are affected by CKI in all three cell lines. Most of the 14 cell cycle regulatory
622 genes differentially expressed in all three cell lines are down-regulated. **b** GO term
623 enrichment analysis of 363 core genes from MDA-MB-231, HEPG2 and MCF-7 cell lines. **c**
624 KEGG pathway enrichment of 363 core genes from MDA-MB-231, HEPG2 and MCF-7 cell
625 lines. **d** Some individual compounds present in CKI linked to genes they regulate that are

626 also found in this report and our previous study (add citation number Qu et al, 2016). Node
627 size is proportional to the number of related components/genes.

628

629

630 **Figures:**

631 Fig. 1

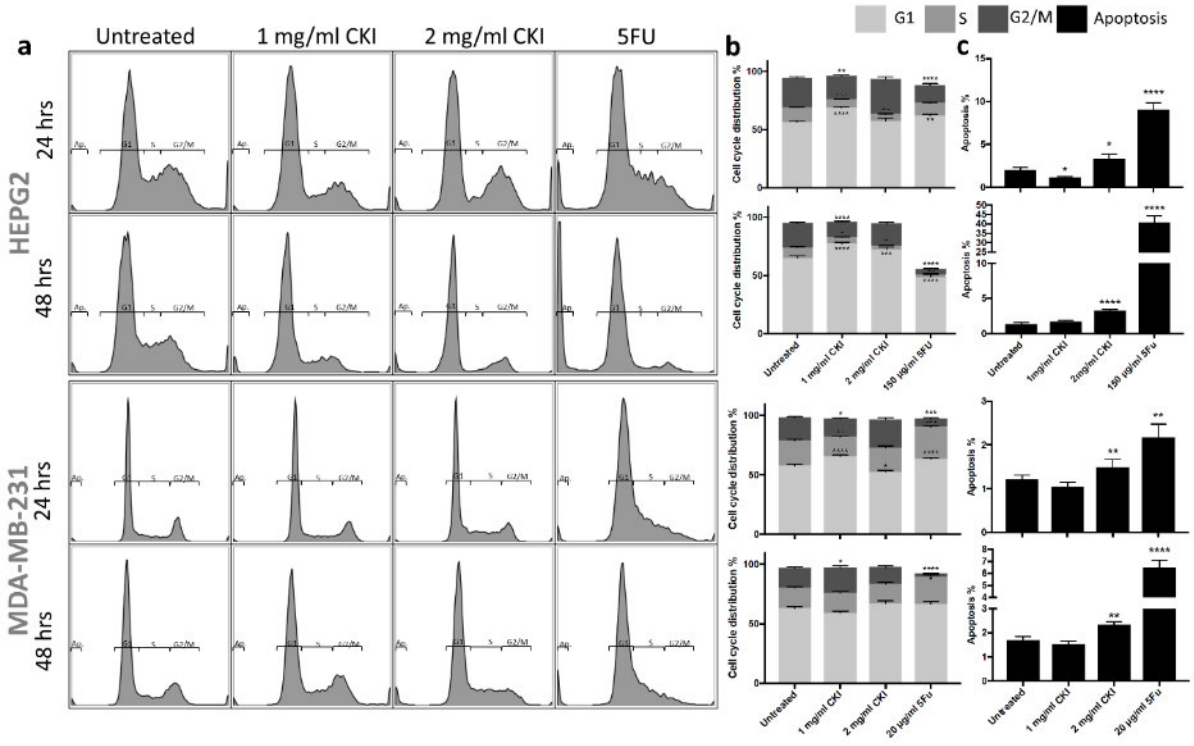

632

633

634 Fig. 2

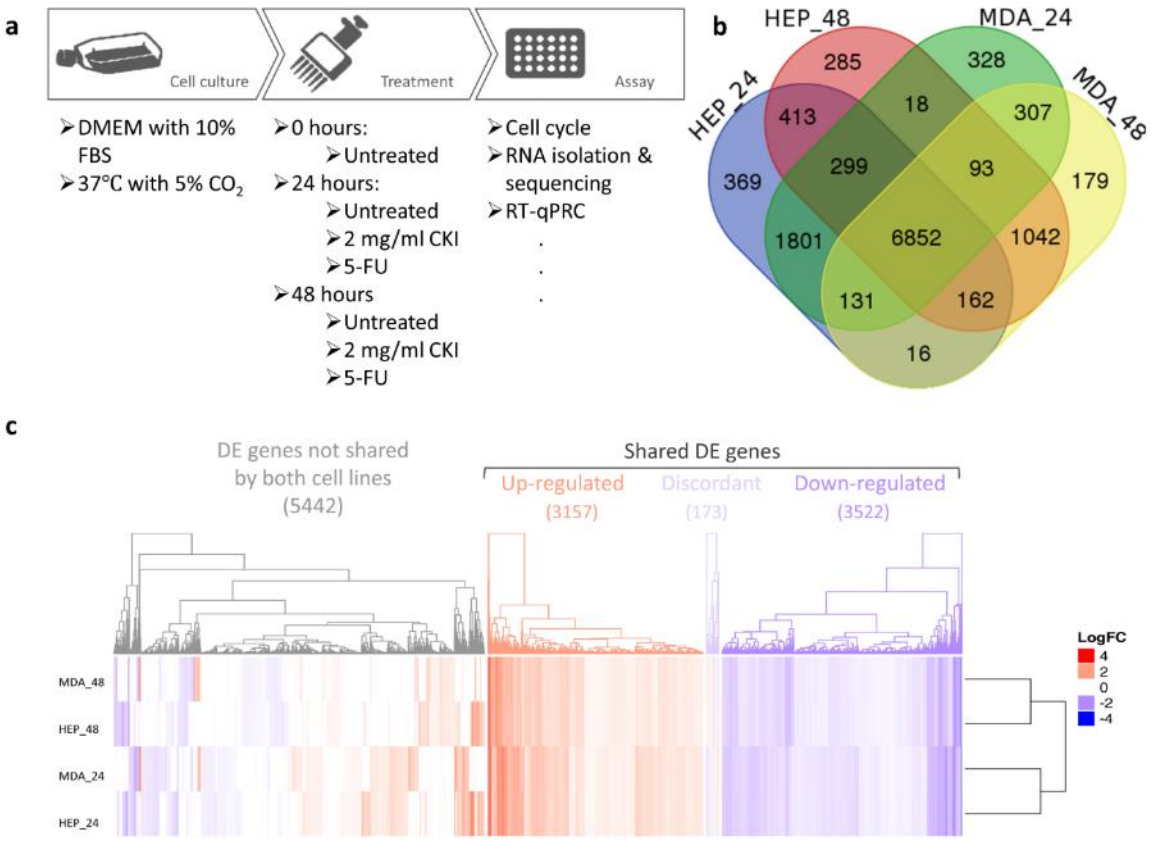

635

636

637 Fig. 3

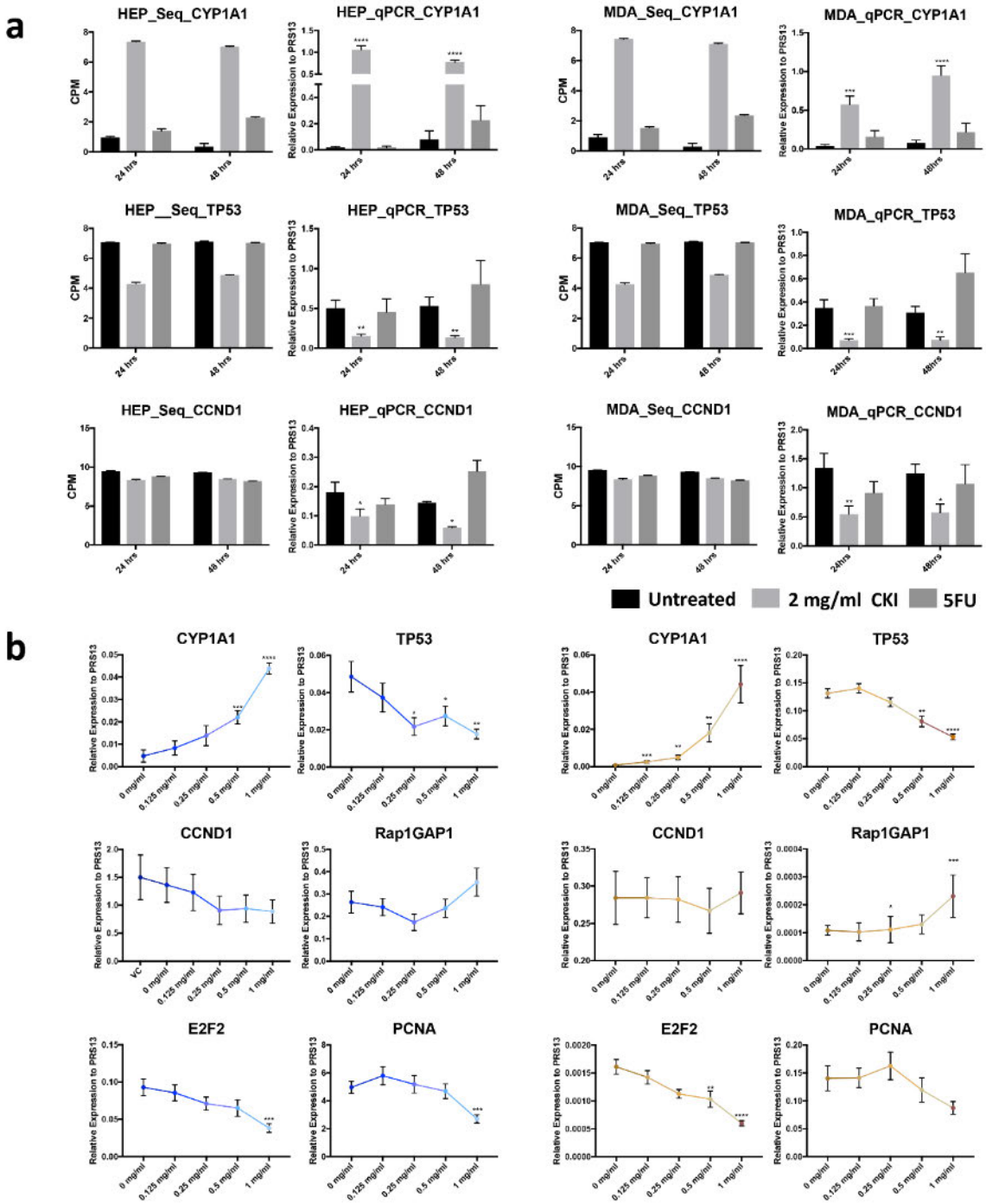

638

639

640 Fig. 4

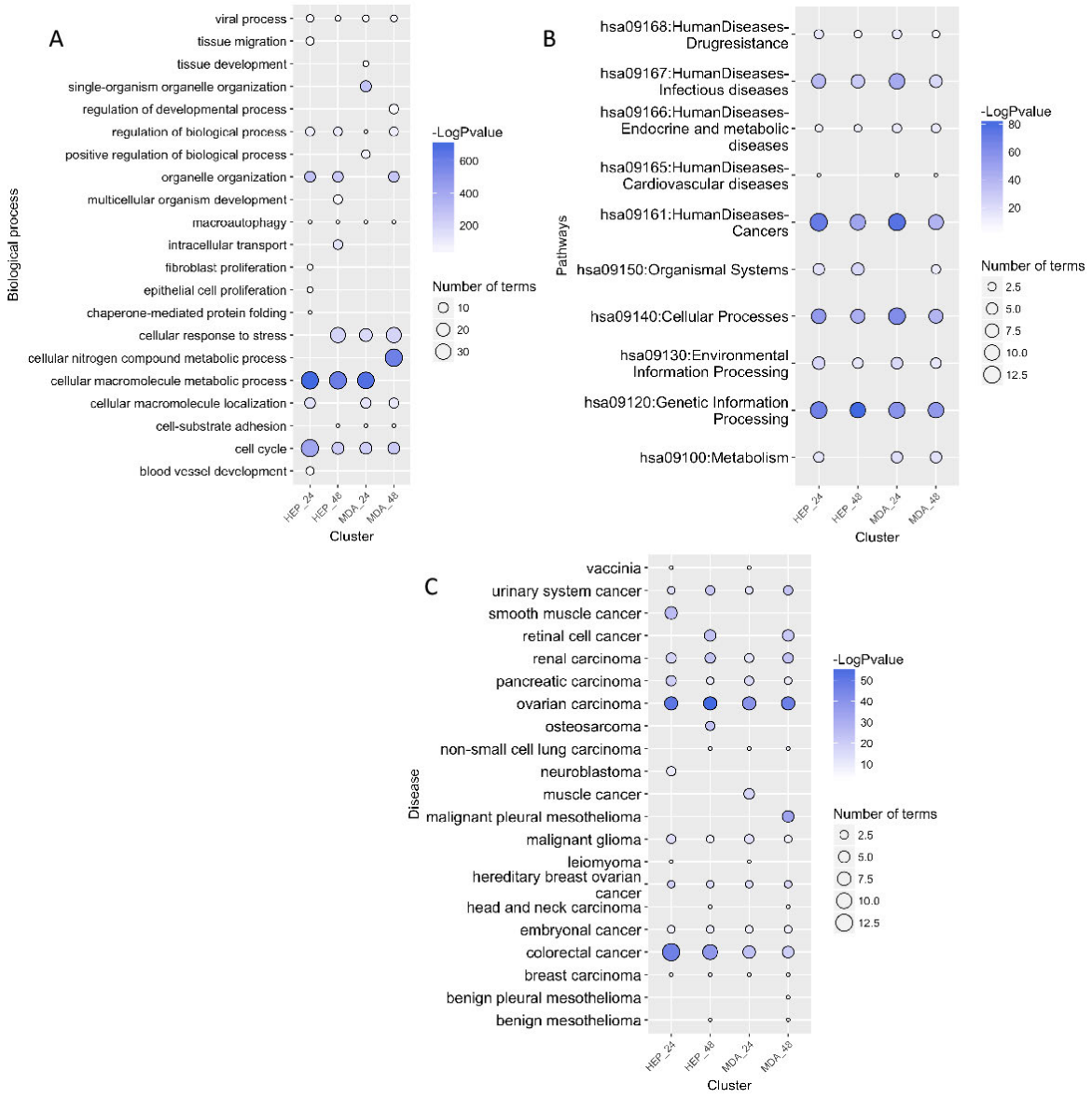

641

642

643 Fig. 5

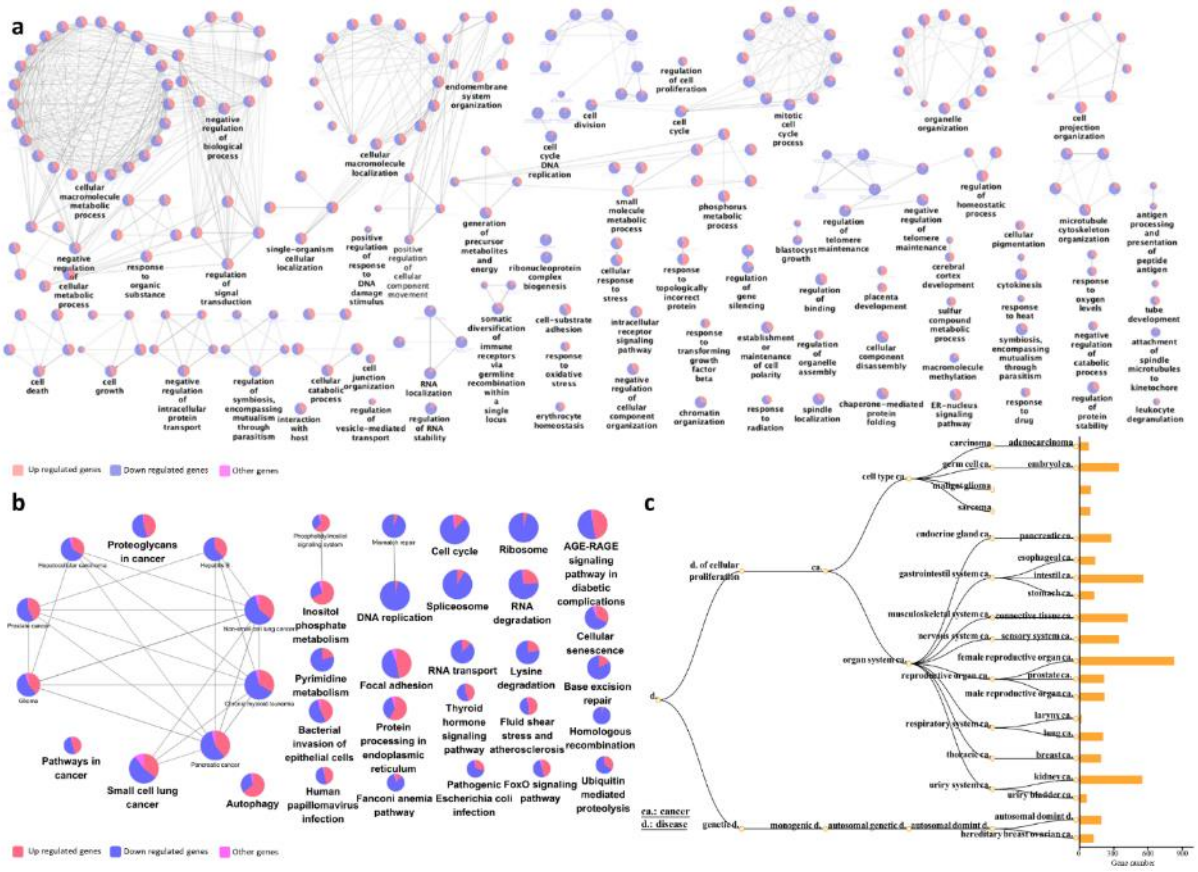

644

645

646 Fig. 6

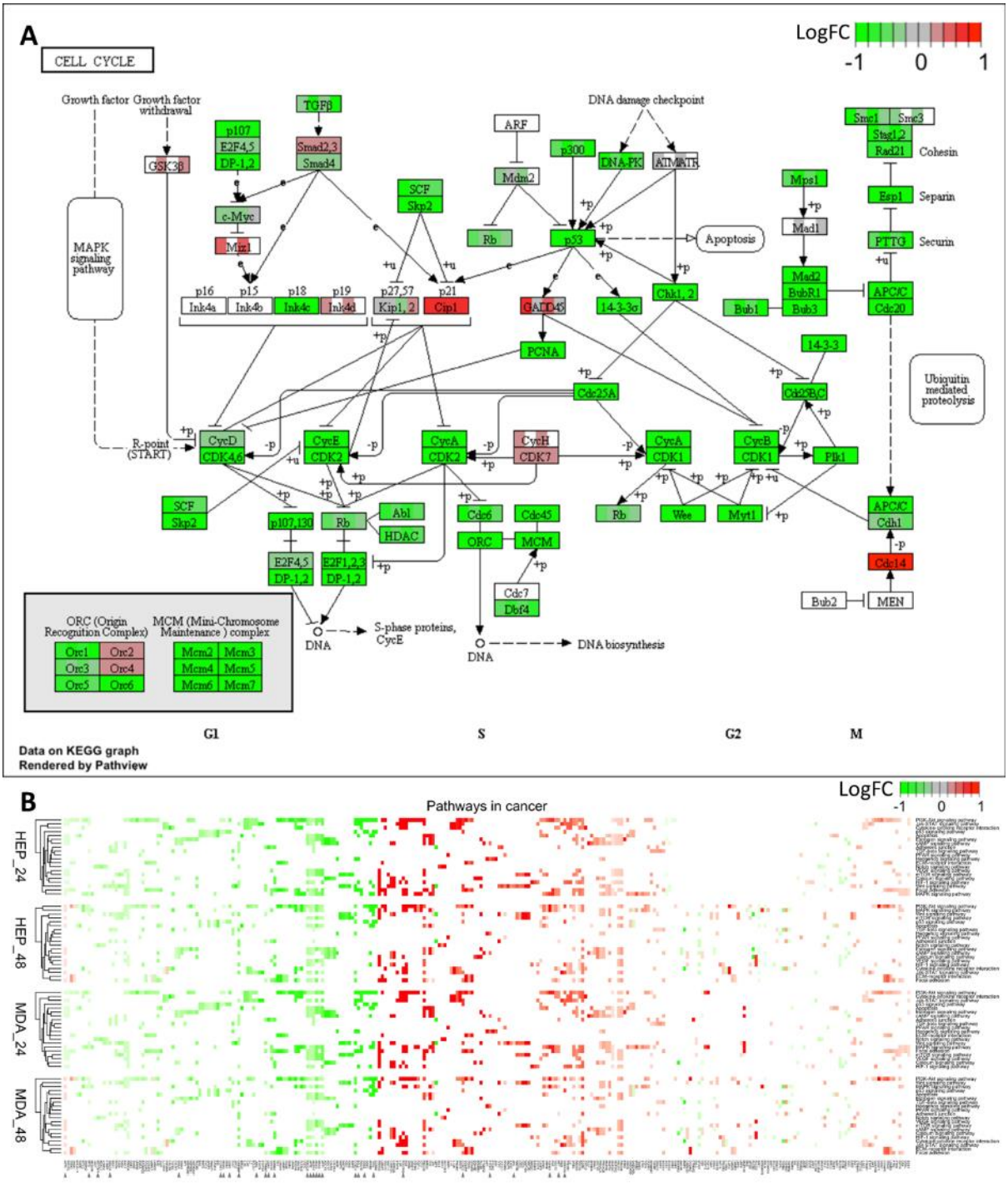

647

648

649 Fig. 7

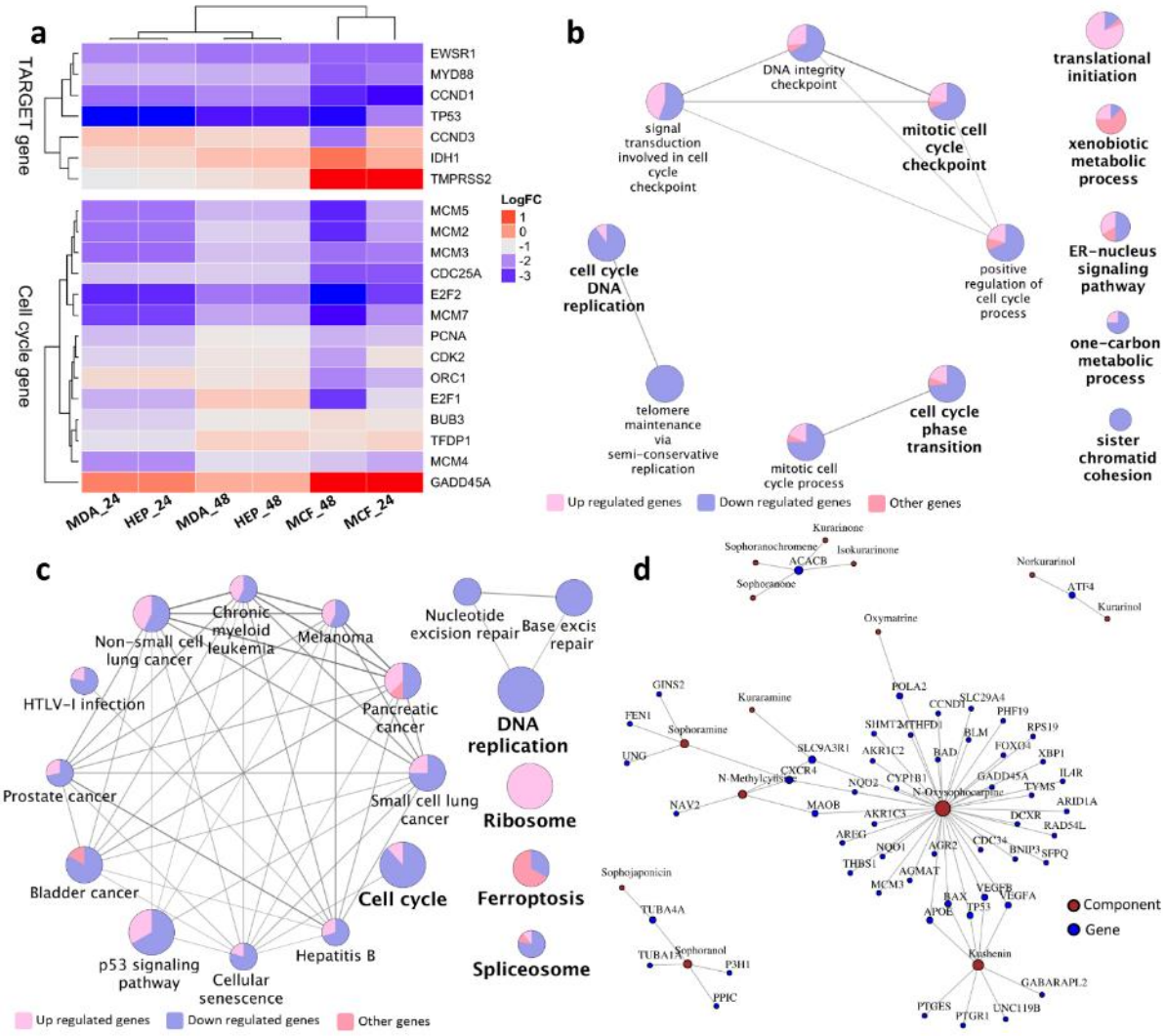

650

651

Chapter 4

Cell Cycle, Glycolysis and DNA Repair Pathways in Cancer Cells are Suppressed by Compound Kushen Injection

In the previous two chapters, I have focused on the analysis of transcriptome data from three cell lines treated with CKI. This integrated analysis identified specific biological processes and pathways perturbed by CKI. Specifically, three pathways; energy metabolism, DNA repair and cell cycle regulation were identified as promising candidates for validation at the protein level. In this chapter, I chose two cell lines with differing sensitivity to CKI: Hep G2 and MDA-MB-231, and validated expression levels of key proteins in these pathways in time series from untreated and CKI treated cells. I have also characterized the levels of key components in energy metabolism and the quantity and cellular distribution of DNA double strand breaks. This chapter largely validates the core pathways identified from our transcriptome analysis of CKI treated cells.

Statement of Authorship

Title of Paper	Cell Cycle, Glycolysis and DNA Repair Pathways in Cancer Cells are Suppressed by Compound Kushen Injection
Publication Status	☐ Published ☐ Accepted for Publication ☑ Submitted for Publication ☐ Unpublished and Unsubmitted work written in manuscript style
Publication Details	Cell Cycle, Energy Metabolism and DNA Repair Pathways in Cancer Cells are Suppressed by Compound Kushen Injection. Jian Cui, Zhipeng Qu, Yuka Harata-Lee, Thazin Nwe Aung, Hanyuan Shen, David Adelson DOI: https://doi.org/10.1101/348102

Principal Author

Name of Principal Author (Candidate)	Jian Cui
Contribution to the Paper	Experimental design, carried out experiments, analysed data, wrote paper
Overall percentage (%)	60%
Certification:	This paper reports on original research I conducted during the period of my Higher Degree by Research candidature and is not subject to any obligations or contractual agreements with a third party that would constrain its inclusion in this thesis. I am the primary author of this paper.
Signature	Date 18/6/18

Co-Author Contributions

By signing the Statement of Authorship, each author certifies that:

i. the candidate's stated contribution to the publication is accurate (as detailed above);

ii. permission is granted for the candidate in include the publication in the thesis; and

iii. the sum of all co-author contributions is equal to 100% less the candidate's stated contribution.

Name of Co-Author	Zhipeng Qu
Contribution to the Paper	Experimental design, assisted with experiments, assisted with data analysis, wrote paper
Signature	Date 18/06/18

Name of Co-Author	Yuka Harata-Lee
Contribution to the Paper	Experimental design, assisted with experiments, assisted with data analysis, wrote paper
Signature	Date 14.6.18

Name of Co-Author	Thazin Nwe Aung		
Contribution to the Paper	Assisted with experiments		
Signature		Date	12/06/2018

Name of Co-Author	Hanyuan Shen		
Contribution to the Paper	Assisted with experiments		
Signature		Date	18/6/2018

Name of Co-Author	David L. Adelson		
Contribution to the Paper	Supervised the research, acquired funding for the experiments, experimental design, wrote paper		
Signature		Date	18/6/2018

Cell Cycle, Energy Metabolism and DNA Repair Pathways in Cancer Cells are Suppressed by Compound Kushen Injection

Jian Cui[1,2], Zhipeng Qu[1,2], Yuka Harata-Lee[1,2], Thazin Nwe Aung[1,2] Hanyuan Shen[1,2] David L Adelson[1,2*],

1 Department of Molecular and Biomedical Science, The University of Adelaide, North Terrace, Adelaide, South Australia, Australia, 5005

2 Zhendong Australia - China Centre for Molecular Chinese Medicine, The University of Adelaide, North Terrace, Adelaide, South Australia, Australia, 5005

*Correspondence to: david.adelson@adelaide.edu.au

Abstract

In this report, we examine candidate pathways perturbed by Compound Kushen Injection (CKI) a Traditional Chinese Medicine (TCM) that we have previously shown to alter the gene expression patterns of multiple pathways and induce apoptosis in cancer cells. We have measured protein levels in Hep G2 and MDA-MB-231 cells for genes in the cell cycle pathway, DNA repair pathway and DNA double strand breaks (DSBs) previously shown to have altered expression by CKI. We have also examined energy metabolism by measuring [ADP]/[ATP] ratio (cell energy charge), lactate production and glucose consumption. Our results demonstrate that CKI can suppress protein levels for cell cycle regulatory proteins and DNA repair while increasing the level of DSBs. We also show that energy metabolism is reduced based on reduced glucose consumption and reduced cellular energy charge. Our results validate these pathways as important targets for CKI. We also examined the effect of the major alkaloid component of CKI, oxymatrine and determined that it had no effect on DSBs, a small effect on the cell cycle and increased the cell energy charge. Our results indicate that CKI likely acts through the effect of multiple compounds on multiple targets where the observed phenotype is the integration of these effects and synergistic interactions.

Keywords:
alkaloid, matrine, cyclin, Ku70, Ku80, cell-cycle

Abbreviations
DSBs, double strand breaks; Ku70/Ku80,the Ku heterodimer proteins

Introduction

Compound Kushen Injection (CKI) is a complex mixture of plant bioactives extracted from Kushen (*Sophora flavescens*) and Baituling (*Smilax Glabra*) that has been approved for use in China since 1995 by the State Food and Drug Administration (SFDA) of China (State medical license no. Z14021231). CKI is widely used in China as an adjunct for both radiotherapy and chemotherapy in cancer. While most of the data supporting its use have been anecdotal and there is little clinical trial data demonstrating its efficacy, it has been shown to be effective at reducing sarcoma growth and cancer pain in an animal model[1] and cancer pain in patients [2].

CKI contains over 200 chemical compounds including alkaloids and flavonoids such as matrine, oxymatrine and kurarinol, and has previously been shown to affect the cell cycle and induce apoptosis in cancer cells[1, 2, 3, 4, 5, 6, 7]. Furthermore, functional genomic characterization of the effect of CKI on cancer cells using transcriptome data indicated that multiple pathways were most likely affected by CKI [4]. These observations support a model wherein many/all of the individual compounds present in CKI can act on many single targets or on multiple targets to induce apoptosis.

Based on previously reported work [4] and our currently unpublished work (Cui *et al*)[8], specific pathways were selected for follow up experiments to validate their response to CKI in order to formulate more specific hypotheses regarding the mechanism of action of CKI on cancer cells. We had previously shown that CKI altered the cell cycle and induced apoptosis while altering the expression of many cell cycle genes in three cancer cell lines [4, 8]. We had also shown that DNA repair pathway genes were significantly down-regulated by CKI and that energy production related to NAD(P)H synthesis from glycolysis and oxidative phosphorylation was reduced by CKI. As a result, we focused on the following candidate pathways: cell cycle, DNA repair and glucose metabolism to validate their alteration by CKI. We used two cell lines for these validation experiments, one relatively insensitive to CKI (MDA-MB-231) and one sensitive to CKI (Hep G2). Furthermore, while the literature shows varying effects for major compounds present in CKI on cancer cells [9, 10], we also tested oxymatrine, the major alkaloid found in CKI and widely believed to be very important for the effects of CKI, on our selected pathways.

Materials and methods

Cell culture and chemicals

CKI with a total alkaloid concentration of 26.5 mg/ml in 5 ml ampoules was provided by Zhendong Pharmaceutical Co. Ltd. (Beijing, China). Cell culture methods have been previously described [4].

A human breast adenocarcinoma cell line, MDA-MB-231 and a hepatocellular carcinoma cell line Hep G2 were purchased from American Type Culture Collection (ATCC, Manassas, VA). The cells were cultured in Dulbecco's Modified Eagle Medium (DMEM; Thermo Fisher Scientific, MA, USA)

supplemented with 10% fetal bovine serum (Thermo Fisher Scientific). Both cell lines were cultured at 37 with 5% CO2. For all *in vitro* assays, cells were cultured overnight before being treated with either CKI (at 1 mg/ml and 2 mg/ml of total alkaloids). As a negative control, cells were treated with medium only and labeled as untreated. After 24 and 48 hours of treatment, cells were harvested and subjected to the downstream experiments.

All the *in vitro* assays employed either 6-well plates or 96-well plates. The seeding density for 6-well plates for both cell lines was 4×10^5 cells and treatment methods were as previously described [4]. The seeding density of Hep G2 cells for 96 well plates was 4×10^3 cells per well and for MDA-MB-231 cells was 8×10^4 cells per well, and used the same treatment method as above: after seeding and culturing overnight, cells were treated with 2 mg/ml CKI diluted with complete medium for the specified time.

Glucose consumption assay

Glucose consumption was determined by using a glucose oxidase test kit (GAGO-20, Sigma, St. Louis, MO). After culturing for different durations (3, 6, 12, 24 and 48 hours), 50 μl of culture medium was collected from untreated groups and treated groups. The cells were trypsinized for cell number determination using trypan blue exclusion assay and the number of bright, viable cells were counted using a hemocytometer. Collected suspension, blank medium and 2 mg/ml CKI, were all filtered and diluted 100 fold with MilliQ water. The absorbance at 560 nm was converted to glucose concentration using a 5μg/ml glucose standard from the kit as a single standard. Glucose consumption was calculated by subtracting the blank medium value from treated/collected medium values. Glucose consumption per cell was calculated from the number of cells determined above.

Measurement of [ADP]/[ATP] ratio

Cells were cultured in white 96-well plates with clear bottoms. The [ADP]/[ATP] ratio of both cell lines was determined immediately after the incubation period (24 and 48 hours) using an assay kit (MAK135; Sigma Aldrich, USA) according to the manufacturer's instructions. Levels of luminescence from the luciferase-mediated reaction were measured using a plate luminometer (PerkinElmer 2030

multilabel reader, USA for CKI experiments or Promega, USA for oxymatrine experiments). The [ADP]/[ATP] ratio was calculated from the luminescence values using a formula provided by the kit manufacturer.

Lactate content assay

The concentration of lactate, the end product of glycolysis, was determined using a lactate colorimetric assay kit (Abcam, Cambridge, MA, USA). Cells were cultured in 6-well plates, and then harvested and deproteinized according to the manufacturer's protocol. The optical density was measured at 450 nm and a standard curve plot (nmol/well vs. OD 450 nm) was generated using serial dilutions of lactate. Lactate concentrations were calculated with the formula provided by the kit manufacturer.

Cell cycle assay

Cells were cultured in 6-well plates and treated with 2 mg/ml CKI or 0.5 mg/ml oxymatrine. After culturing for 3, 6, 12, 24 and 48 hours, cells were harvested and subjected to cell cycle analysis by Propidium Iodide staining as previously reported [4]. Data were obtained by flow cytometry using Accrui (BD Biosciences, NJ, US) and analysed using FlowJo software (Tree Star Inc, Ashland, Oregon, USA).

Microscopy

After culturing for 48 hours on 8 well chamber slides, control and treated cells were fixed in 1% paraformaldehyde for 10 minutes at room temperature, washed with Phosphate Buffered Saline three times and permeabilized with 0.5% Triton X100 for 10 minutes. After fixation and permeabilization, cells were blocked with 5% Fetal Bovine Serum for 30 minutes. Permeabilized cells were stained with 5μg/ml of Alexa Fluor®594 conjugated anti-H2AX.X Phospho (red) (Biolegend, Ser139) in 5% Fetal Bovine Serum overnight followed with Alexa Fluor®488 conjugated Phalloidin (green) (Biolegend) staining for 20 minutes at 4℃.

Stained cells were mounted with 4',6-diamidino-2-phenylindole (DAPI) and visualized with an Olympus FV3000 (Olympus Corporation, Tokyo, Japan) confocal microscope using a 60 oil objective. Fluorescence intensity was quantified using Imaris software (Bitplane, Saint Paul, MN) and averaged using at least 10 cells in each experiment.

Flow-cytometry quantification of protein expression

Cells were cultured in 6-well plates and treated with CKI. After 24 and 48 hours, cells were harvested to detect intranuclear/intracellular levels of proteins involved in cell cycle and DNA DSBs pathways using the following antibodies; (cell cycle primary antibodies: (Cell Signaling Technologies, Danvers, MA, USA: P53 Rabbit mono-Ab, CCND1 Rabbit mono-Ab, CDK2 Rabbit mono-Ab) (Abcam, Cambridge, UK:CDK1 Rabbit mono-Ab), for these primaries, cell cycle isotype control: Cell Signaling Technologies: Rabbit igG, cell cycle secondary antibody Anti-rabbit (PE conjugated), additional primary antibody: CTNNB1 Rabbit mono-Ab (Alexa Fluor®647 conjugated) and isotype control: Rabbit IgG (Alexa Fluor®647 conjugated), both from Abcam)(DSBs antibody: Anti-H2AX (PE conjugated) primary antibody and isotype control: Mouse IgG1 (PE conjugated) both from BioLegend, San Diego, CA, USA) (DNA repair antibodies: primary antibodies - KU70 Rabbit mono-Ab (Alexa Fluor®647 conjugated) and KU80 Rabbit mono-Ab (Alexa Fluor®647 conjugated), Isotype control: Rabbit IgG (Alexa Fluor®647 conjugated), all from Abcam) Cells were sorted and the data acquired on a FACS Canto (BD Biosciences, NJ, US) or Accrui (BD Biosciences, NJ, US), and the data were analysed using FlowJo (Tree Star Inc.) software.

Cell cycle functional enrichment re-analysis

In order to identify the phases of the cell cycle affected by CKI, differentially expressed gene data from [4] was submitted to the Reactome database[11], and used to identify functionally enriched genes.

Statistical analysis

All measurements above were performed in triplicate and repeated at least three times. Statistical significance was determined by twoway ANOVA test; error bars represent standard deviation.

Results

Pathway validation

Based on our previous results indicating that CKI could suppress NAD(P)H synthesis [4] and (Supplementary Material, Figure S1), we examined the effect of CKI on energy metabolism by measuring glucose uptake, [ADP]/[ATP] ratio and lactate production. We measured glucose uptake in both CKI treated and untreated cells from 0 to 48 hrs after treatment and observed a reduction in glucose uptake (Fig. 1A). The growth curves for both cell lines were relatively flat after CKI treatment, in contrast to untreated cells. MDA-MB-231 cells, which are less sensitive to CKI in terms of apoptosis, had a higher level of glucose uptake than Hep G2 cells, which are more sensitive to CKI. Because the overall glucose uptake was consistent with the cell growth curves, the glucose consumption per million cells for each cell line under treatment was different. Untreated Hep G2 cells maintained a relatively flat rate of glucose consumption per million cells, while for CKI treated Hep G2 cells the rate of glucose consumption per million cells decreased with time, becoming significantly less towards 48 hrs. The glucose consumption variance for both untreated and treated MDA-MB-231 cells was high, but both overall glucose consumption and glucose consumption per million cells appeared to decrease over time.

Because changes in glucose consumption are mirrored by other aspects of energy metabolism, we assessed the energy charge of both CKI treated and untreated cells by measuring the [ADP]/[ATP] ratio at 24 and 48 hours after treatment (Fig. 1B). Hep G2 cells had a lower energy charge (higher [ADP]/[ATP] ratio) compared to MDA-MB-231 cells and after CKI treatment both cell lines showed a decrease in energy charge, consistent with our previous measurements using a 2,3-Bis(2-methoxy-4-nitro-5-sulfonyl)-2H-tetrazolium-5-carboxanilideinner salt (XTT) assay (Supplementary Material, Figure S1). However, the decrease in energy charge was earlier and much

more pronounced for Hep G2 cells compared to MDA-MB-231 cells.

The flip side of glucose consumption is the production of lactate via glycolysis, which is the initial pathway for glucose metabolism. We, therefore, measured lactate production in order to determine if the observed decreases in energy charge and glucose consumption were directly attributable to reduced glycolytic activity. We measured intracellular lactate concentration in both CKI treated and untreated cells at 24 and 48 hours after treatment (Fig. 1C) and found that lactate concentrations increased as a function of CKI treatment in both cell lines. This result is consistent with a build up of lactate due to an inhibition of the Tricarboxylic Acid (TCA) cycle leading to decreased oxidative phosphorylation and lower cellular energy charge. CKI must, therefore, inhibit cellular energy metabolism downstream of glycolysis, most likely at the level of the TCA cycle. Decreased energy charge can have widespread effects on a number of energy-hungry cellular processes involved in the cell cycle, such as DNA replication.

Having validated the effect of CKI on cellular energy metabolism, we proceeded to examine the perturbation of cell cycle and the expression of cell cycle proteins, as these are energy intensive processes. We had previously identified the cell cycle as a target for CKI based on transcriptome data from CKI treated cells [4, 8]. We carried out cell cycle profiling on CKI treated and untreated cells using Propidium Iodide staining and FACS (Fig. 2A) as described in Materials and Methods. The two cell lines displayed slightly different profiles to each other, but their response to CKI was similar in terms of an increase in the proportion of cells in G1-phase. For Hep G2 cells, CKI caused consistent reductions in the proportion of cells in S-phase accompanied by corresponding increases in the proportion of cells in G1-phase. This is indicative of a block in S-phase leading to accumulation of cells in G1-phase. For MDA-MB-231 cells, CKI did not promote a significant decrease in the proportion of cells in S-phase, but did cause an increase in the percentage of cells in G1 phase at 24hrs and a pronounced decrease in cells in G2/M phase at 12 hours.

We also examined the levels of key proteins involved in the cell cycle pathway (Cyclin D1:CCND1,Cyclin Dependent Kinase 1:CDK1, Cyclin Dependent Kinase 2:CDK2, Tumor Protein p53:TP53 and Catenin Beta 1:CTNNB1) at 24 and 48 hours after CKI treatment previously shown to have altered transcript expression by CKI (Fig. 2B). Both cell lines showed similar results for all five proteins, with decreased levels caused by CKI, and validated previous RNAseq data [4, 8]. CCND1 regulates the cell-cycle during G1/S transition. CDK-1 promotes G2-M transition, and

regulates G1 progress and G1-S transition. CDK-2 acts at the G1-S transition to promote the E2F transcriptional program and the initiation of DNA synthesis, and modulates G2 progression. TP53 acts to negatively regulate cell division. CTNNB1 acts as a negative regulator of centrosome cohesion. Down-regulation of these proteins is therefore consistent with cell cycle arrest/dysregulation and the cell cycle result in Fig. 2A. These results indicate that CKI alters cell cycle regulation consistent with cell cycle arrest. Cell cycle arrest is also an outcome that can result from DNA damage such as DSBs [12].

We had previously observed that DNA repair genes had lower transcript levels in CKI treated cells [4, 8], so hypothesised that this might result in increased numbers of DSBs. We measured the expression of γ-H2AX in both cell lines (Fig. 3A) and found that it was only over-expressed at 48 hours in CKI treated Hep G2 cells. We also carried out localization of γ-H2AX using quantitative immunofluorescence microscopy and determined that the level of γ-H2AX increased in nuclei of CKI treated cells in both cell lines (Fig. 3B). These results indicated an increase in DSBs as a result of CKI treatment. In order to confirm if reduced expression of DNA repair proteins was correlated with the increase in DSBs, we measured levels of Ku70/Ku80 proteins in CKI treated cells (Fig. 3C). In Hep G2 cells, Ku80, a critical component of the Non-Homologous End Joining (NHEJ) DNA repair pathway was significantly down regulated at both 24 and 48 hours after CKI treatment. In MDA-MB-231 cells, Ku70 expression was down-regulated at both 24 and 48 hours after CKI treatment, and Ku80 was down-regulated at 24 hours. Because Ku70/Ku80 are subunits of a required DNA repair complex, reduced expression of either subunit will result in decreased DNA repair. Our results, therefore, support a suppressive effect of CKI on DNA repair, likely resulting in an increased level of DSBs.

Effect of Oxymatrine, the principal alkaloid in CKI

Because CKI is a complex mixture of many plant secondary metabolites that may have many targets and there is little known about its molecular mode of action, we examined the effects of the most abundant single compound found in CKI, oxymatrine, on the most sensitive cell line, Hep G2. Oxymatrine is an alkaloid that has previously been reported to have effects similar to CKI, so we expected it might have an effect on one or more of our three validated pathways.

Oxymatrine, at 0.5 mg/ml which is equivalent to the concentration of oxymatrine in 2mg/ml CKI, did not have an equivalent effect on the cell cycle compared to CKI (Fig. 4A vs Fig. 2A). Oxymatrine caused only minor changes to the cell cycle with small but significant increases in the proportion of cells in G1-phase at 3 and 48 hours and a small but significant decrease in the proportion of cells in S1-phase at 48 hours. Oxymatrine also caused a significant increase in the proportion of cells undergoing apoptosis in Hep G2 cells, albeit at a lower level than CKI (Supplementary Material, Figure 2).

Oxymatrine had no effect on H2AX levels in Hep G2 cells (Fig. 4B). This was in stark contrast to the effect of CKI (Fig. 3A) at 48 hours and indicated that oxymatrine alone had no effect on the level of DSBs.

Surprisingly, oxymatrine had the opposite effect on energy metabolism compared to CKI, causing a decrease in [ADP]/[ATP] ratio indicating a large increase in the energy charge of the cells (Fig. 4C).

Integration of results

The effect of CKI on cancer cells was validated in all three of our candidate pathways: cell cycle, energy metabolism and DNA repair. Because these pathways are not isolated, but instead are integrated aspects of cell physiology CKI may act through targets in some or all of these three pathways or may act through other targets that either directly or indirectly suppress these pathways. CKI may also act through the synergistic effects of multiple compounds on multiple targets in our candidate pathways. This possibility is consistent with the partial and minor effects of oxymatrine on our candidate pathways.

Discussion

We have validated three pathways (cell cycle, energy metabolism and DNA repair) that are perturbed by CKI and that can be used as the focus for further investigations to identify specific molecular targets that mediate the perturbations.

Cell cycle perturbation by CKI

Our results show that CKI can perturb the cell cycle by altering the proportions of cells in G1-phase, S-phase and G2/M-phase. This result is similar to what we have observed before [4, 8], but has not been widely reported in the literature. The alkaloid oxymatrine, the most abundant compound present in CKI, has also been shown previously to perturb a number of signaling pathways [13] and alter/arrest the cell cycle in a variety of cancer cells [14, 15, 16, 17, 18] and we have confirmed this observation (Fig. 4A) in Hep G2 cells. Our results permit direct comparison with CKI because our experiments have been done using equivalent concentrations of oxymatrine alone or in CKI. While oxymatrine has an effect on the cell cycle, it is not as effective at perturbing the cell cycle as is CKI. This indicates that oxymatrine must interact with other compounds in CKI to have a stronger effect on the cell cycle.

Energy metabolism suppression by CKI

We have shown for the first time that CKI can inhibit energy metabolism as demonstrated by lower levels of NADH/NADPH and a higher [ADP]/[ATP] ratio. These results, combined with lower glucose utilisation and higher lactate levels indicate that this suppression was likely due to inhibition of the TCA cycle or oxidative phosphorylation. Previously, Gao *et al* [3] have reported that CKI significantly increased the concentration of pyruvate in the medium and this observation in combination with our results supports a decrease in metabolic flux through the TCA cycle as the likely cause of the reported suppression of energy metabolism. Interestingly, oxymatrine on its own had the opposite effect on [ADP]/[ATP] ratio compared to CKI, indicating that it can enhance energy metabolism and increase the energy charge of the cell.

DNA repair suppression by CKI

There is only one report in the literature of oxymatrine inducing DSBs [19] and no reports with respect to CKI. Our results show for the first time that not only does CKI induce DSBs, but that is also likely inhibits DNA repair by decreasing the expression of the Ku70/Ku80 complex required for NHEJ mediated DNA repair. It is worth noting, however, that the reported effect of oxymatrine on

DSBs [19] uses significantly higher (4-8 fold) concentrations of oxymatrine compared to our experiments. In our hands oxymatrine alone at 0.5mg/ml showed no effect on DSBs as judged by the level of γ-H2AX after 24 or 48 hours.

Conclusions

CKI causes suppression of energy metabolism and DNA repair along with altered cell cycle (summarized in Fig. 5). CKI has also previously been reported to induce apoptosis in cancer cells [4]. The overarching question is if CKI has independent effects on these three pathways or if the primary effect of CKI is through a single pathway that propagates effects to other, physiologically linked pathways. It may be that CKI suppresses energy metabolism thus disrupting downstream, energy-hungry processes such as DNA replication and DNA repair. Alternatively, there could be independent effects on DNA repair leading to checkpoint-induced cell cycle perturbation/arrest. Our results based on oxymatrine treatment of Hep G2 cells indicate that the cell-cycle is likely directly affected by oxymatrine and thus CKI. However, oxymatrine alone had no effect on DNA repair and boosted, rather than reduced the energy charge of the cell. Taken together, these results support a model of many compounds/many targets [20] for the mode of action of CKI, where multiple compounds affect multiple targets and the synergistic, observed effect is significantly different to that seen with individual components.

Acknowledgements

We would like to thank Prof. Frank Grutzner for providing DAPI, Adelaide Microscopy for training and equipment use and Jue Zhang, Bo Han and Dan Kortschak for helpful discussions.

Funding

This project is supported by The Special International Cooperation Project of Traditional Chinese Medicine (GZYYGJ2017035) and The University of Adelaide - Zhendong Australia - China Centre

for Molecular Chinese Medicine.

Availability of data and materials

All data analyzed in this study are available from the public source NCBI (https://www.ncbi.nlm.nih.gov/) and details can be found in the supplementary file.

Author's contributions

J.C, Z.Q., Y.H-L. and D.L.A. designed research; J.C., Y-H-L., Z.Q., T.N.A. and H.S. performed research; and J.C., Z.Q., Y.H-L. and D.L.A wrote the paper.

Ethics approval and consent to participate

Not applicable.

Consent for publication

Not applicable.

Competing interests

The authors declare that they have no competing interests.

References

1. Zhao Z, Fan H, Higgins T, Qi J, Haines D, Trivett A, et al. Fufang Kushen injection inhibits sarcoma growth and tumor-induced hyperalgesia via TRPV1 signaling pathways. Cancer Letters. 2014 Dec;355(2):232–241. Available from: http://dx.doi.org/10.1016/j.canlet.2014.08.037.

2. Wang W, You Rl, Qin Wj, Hai Ln, Fang Mj, Huang Gh, et al. Anti-tumor activities of active ingredients in Compound Kushen Injection. Acta Pharmacologica Sinica. 2015;36(6):676.

3. Gao L, Wang KX, Zhou YZ, Fang JS, Qin XM, Du GH. Uncovering the anticancer mechanism of Compound Kushen Injection against HCC by integrating quantitative analysis, network analysis and experimental validation. Sci Rep. 2018 Jan;8(1):624.

4. Qu Z, Cui J, Harata-Lee Y, Aung TN, Feng Q, Raison JM, et al. Identification of candidate anti-cancer molecular mechanisms of Compound Kushen Injection using functional genomics. Oncotarget. 2016 10;7(40):66003–66019.

5. Zhou SK, Zhang RL, Xu YF, Bi TN. Antioxidant and immunity activities of Fufang Kushen Injection Liquid. Molecules. 2012 May;17(6):6481–90.

6. Sun M, Cao H, Sun L, Dong S, Bian Y, Han J, et al. Antitumor activities of kushen: literature review. Evid Based Complement Alternat Med. 2012;2012:373219.

7. Xu W, Lin H, Zhang Y, Chen X, Hua B, Hou W, et al. Compound Kushen Injection suppresses human breast cancer stem-like cells by down-regulating the canonical Wnt/β-catenin pathway. J Exp Clin Cancer Res. 2011 Oct;30:103.

8. Cui J, Qu Z, Harata-Lee Y, Shen H, Aung TN, Wang W, et al. The Effect of Compound Kushen Injection on Cancer Cells: Integrated Identification of Candidate Molecular Mechanisms.;. (Manuscript submitted).

9. Ma X, Li RS, Wang J, Huang YQ, Li PY, Wang J, et al. The Therapeutic Efficacy and Safety of Compound Kushen Injection Combined with Transarterial Chemoembolization in Unresectable Hepatocellular Carcinoma: An Update Systematic Review and Meta-Analysis. Frontiers in Pharmacology. 2016 Mar;7. Available from: http://dx.doi.org/10.3389/fphar.2016.00070.

10. Zhongquan Z, Hehe L, Ying J. Effect of compound Kushen injection on T-cell subgroups and natural killer cells in patients with locally advanced non-small-cell lung cancer treated with concomitant radiochemotherapy. Journal of Traditional Chinese Medicine. 2016;36(1):14 – 18. Available from: http://www.sciencedirect.com/science/article/pii/S0254627216300024.

11. Fabregat A, Jupe S, Matthews L, Sidiropoulos K, Gillespie M, Garapati P, et al. The Reactome pathway knowledgebase. NUCLEIC ACIDS RESEARCH. 2018;46(D 1):D649–D655.

12. Shaltiel IA, Krenning L, Bruinsma W, Medema RH. The same, only different - DNA damage checkpoints and their reversal throughout the cell cycle. J Cell Sci. 2015 Feb;128(4):607–20.

13. Lu ML, Xiang XH, Xia SH. Potential Signaling Pathways Involved in the Clinical Application of Oxymatrine. Phytotherapy Research. 2016 May;30(7):1104–1112. Available from: http://dx.doi.org/10.1002/ptr.5632.

14. Li W, Yu X, Tan S, Liu W, Zhou L, Liu H. Oxymatrine inhibits non-small cell lung cancer via suppression of EGFR signaling pathway. Cancer Med. 2018 Jan;7(1):208–218.

15. He M, Jiang L, Li B, Wang G, Wang J, Fu Y. Oxymatrine suppresses the growth and invasion of MG63 cells by up-regulating PTEN and promoting its nuclear translocation. Oncotarget. 2017 Sep;8(39):65100–65110.

16. Li S, Zhang Y, Liu Q, Zhao Q, Xu L, Huang S, et al. Oxymatrine inhibits proliferation of human bladder cancer T24 cells by inducing apoptosis and cell cycle arrest. Oncol Lett. 2017 Jun;13(6):4453–4458.

17. Wu J, Cai Y, Li M, Zhang Y, Li H, Tan Z. Oxymatrine Promotes S-Phase Arrest and Inhibits Cell Proliferation of Human Breast Cancer Cells in Vitro through Mitochondria-Mediated Apoptosis. Biol Pharm Bull. 2017;40(8):1232–1239.

18. Ying XJ, Jin B, Chen XW, Xie J, Xu HM, Dong P. Oxymatrine downregulates HPV16E7 expression and inhibits cell proliferation in laryngeal squamous cell carcinoma Hep-2 cells in vitro. Biomed Res Int. 2015;2015:150390.

19. Wang Z, Xu W, Lin Z, Li C, Wang Y, Yang L, et al. Reduced apurinic/apyrimidinic endonuclease activity enhances the antitumor activity of oxymatrine in lung cancer cells. International journal of oncology. 2016;49(6):2331–2340.

20. Li FS, Weng JK. Demystifying traditional herbal medicine with modern approach. Nat Plants. 2017 Jul;3:17109.

Additional Files

Additional file 1 — Supplementary Information

Additional file contains supplementary figures and tables as referred to in the main body of the paper.

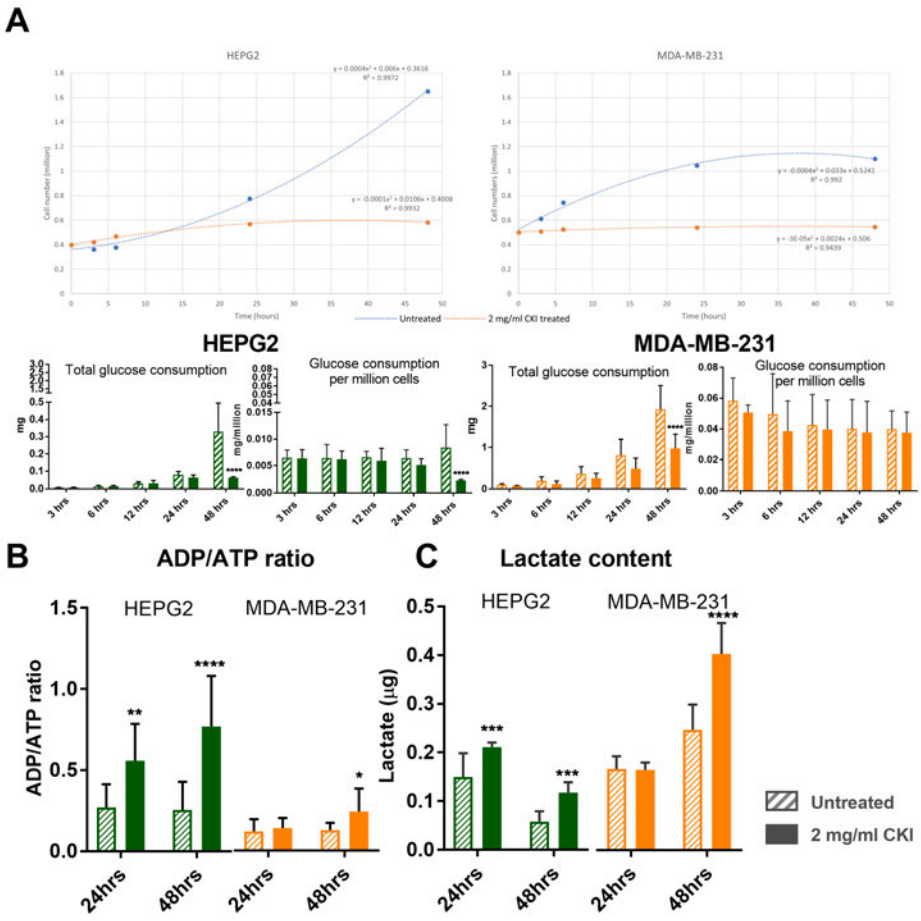

Figure 1. The energy metabolism determination assays in the two cell lines. A. Comparison of glucose consumption analysis between the two cell lines at 3, 6, 12, 24 and 48 hours. Overall glucose consumption is divided by cell number to calculate the consumption of glucose per million cells. B. [ATP]/[ADP] ratio assay result for the two cell lines at 24 and 48 hours. C. Lactate content detection for the two cell lines at 24 and 48 hours. Statistical analyses were performed using two-way ANOVA comparing treated with untreated (*p<0.05, **p<0.01, ***p<0.001, ****p<0.0001); bars show 1 standard deviation from the mean.

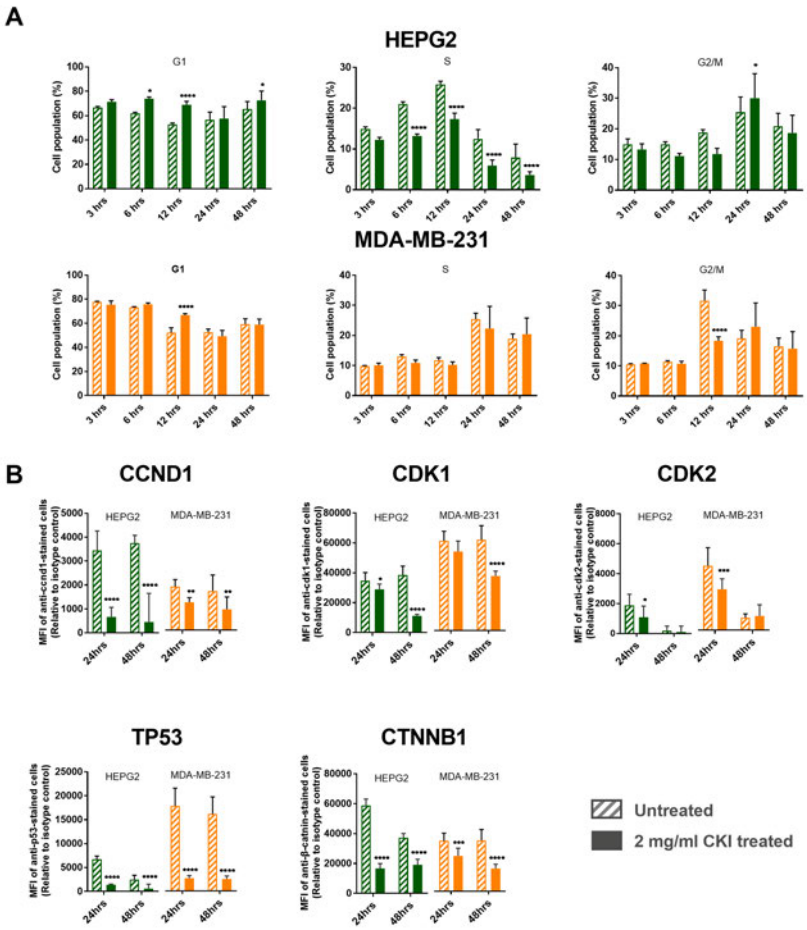

Figure 2. Cell cycle shift by CKI and undulating expression of the key proteins . A. Cell cycle shift regulated by CKI over 48 hours. In both cell lines, the earliest shifted cell cycle phase was S phase 6 hours after treatment. Compared to Hep G2, MDA-MB-231 showed delayed responses. B. Expression levels for 5 proteins (ccnd1, cdk1, cdk2, p53 and catenin β 1) as a result of CKI treatment at both 24 hours and 48 hours. Statistical analyses were performed using two-way ANOVA comparing with untreated (*p<0.05, **p<0.01, ***p<0.001, ****p<0.0001); bars show 1 standard deviation from the mean.

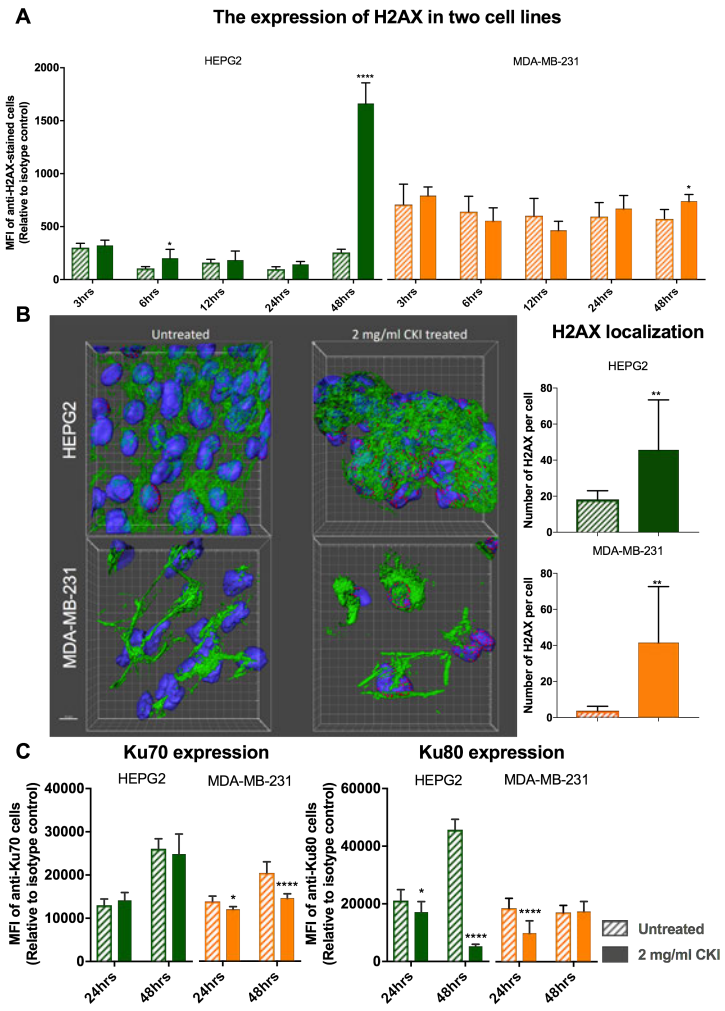

Figure 3. DSBs were increased by CKI treatment. A. γ-H2AX expression from 3 hours to 48 hours after treatment with 2 mg/ml CKI in two cell lines. B. Localization of γ-H2AX in two cell lines after CKI treatment for 48 hours. Green shows the cytoskeleton stained with an antibody to F-actin, blue is DAPI staining of nuclei, pink/red is staining of DSBs with antibody to γ-H2AX. The bar graph shows a quantification of the average number of γ-H2AX foci per cell detected in immunofluorescence images of 2 mg/ml CKI treated and untreated groups. At least 10 images of 3 independent replicate experiments were analyzed. C.Expression of DSBs repair proteins, Ku70 and Ku80, as a result of treatment with 2 mg/ml CKI in two cell lines. Statistical analyses were performed using two-way ANOVA comparing treated with untreated (*p<0.05, **p<0.01, ***p<0.001, ****p<0.0001); bars show 1 standard deviation from the mean.

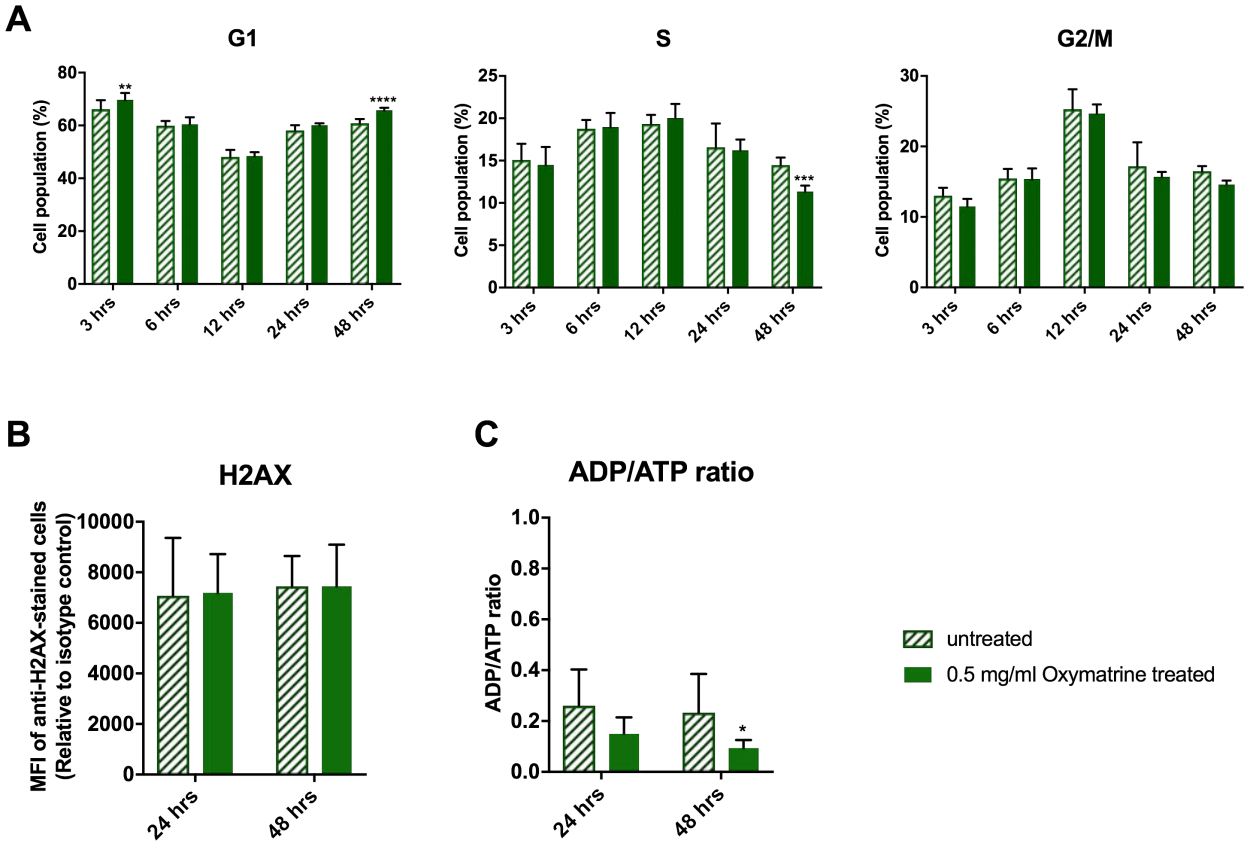

Figure 4. Effect of oxymatrine alone on validated pathways. Oxymatrine was tested at 0.5mg/mL which is equivalent to its concentration in CKI. A. Effect of oxymatrine on cell cycle in Hep G2 cells over 48 hours. B. Effect of oxymatrine on γ-H2AX (DSBs) levels after 24 and 48 hours. C. Effect of oxymatrine on [ADP]/[ATP] ratio after 24 and 48 hours. Statistical analyses were performed using two-way ANOVA comparing treated with untreated (*p<0.05, **p<0.01, ***p<0.001, ****p<0.0001); bars show 1 standard deviation from the mean.

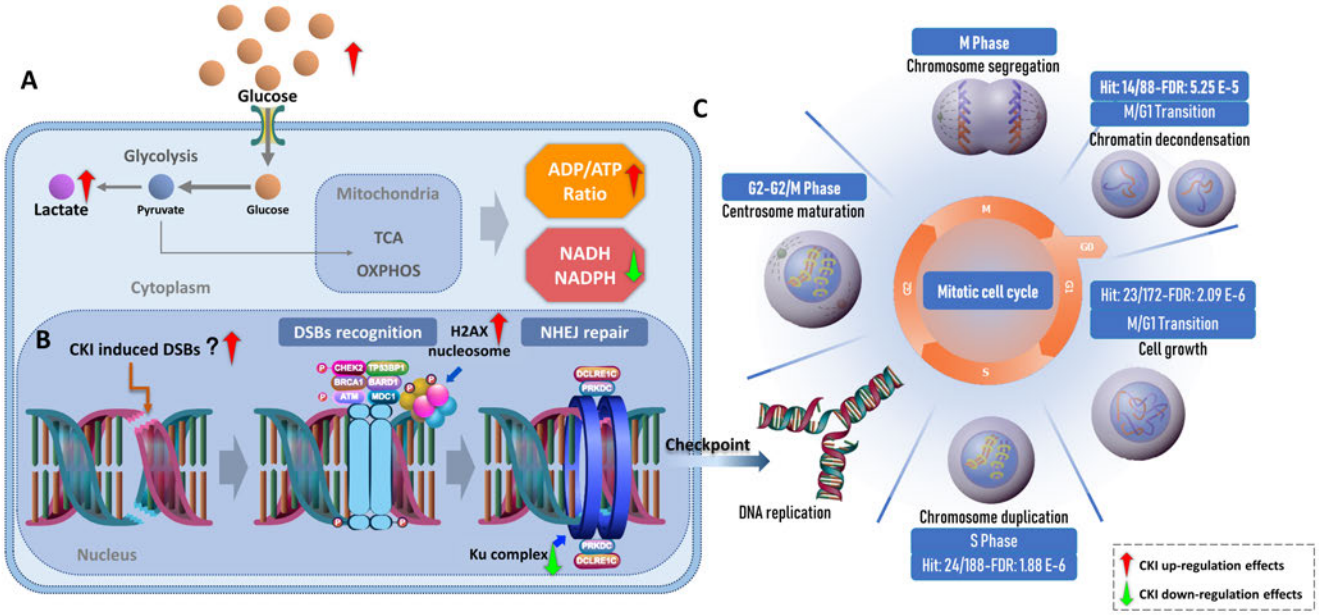

Figure 5. Integration of the three pathways altered by CKI. A. General presentation of energy metabolism affected by CKI. Glucose utilization is down-regulated by CKI. This is accompanied by increased lactate in the cytoplasm as CKI inhibits glucose metabolism downstream of glycolysis, leading to an increase in [ADP]/[ATP] and decrease in NADH/NADPH. B. Effects on DNA repair in cancer cells by CKI. CKI may be able to directly induce DSBs, but CKI may also indirectly induce DSBs by arresting checkpoint functions during the cell cycle. In addition, CKI may also inhibit NHEJ, the major repair mechanism for DSBs. C. Reactome functional enrichment of cell cycle genes based on shared differentially expressed (DE) genes from previous studies. From M/G1 to S phase, the shared DE genes from both cell lines were significantly enriched. Most of these DE genes, were down-regulated.

Chapter 5

Traditional Chinese Herbal Formula YQCT Reduces Gefitinib-induced Drug Resistance in Non-Small Cell Lung Cancer by Targeting Apoptosis and Autophagy Pathways

In previous chapters, we have applied transcriptome analysis and pathway validation to the analysis of CKI driven apoptosis. In this chapter, many of those methods were applied to the analysis of a different TCM formulation, Yiqi Chutan Tang (YQCT). In the absence of transcriptome data for response to YQCT, we have characterized candidate pathways associated with lung cancer cell drug resistance to Gefitinib and predict candidate targets relevant to the mechanism of action of YQCT.

Statement of Authorship

Title of Paper	Traditional Chinese Herbal Formula YQCT Reduces Gefitinib-induced Drug Resistance in Non-Small Cell Lung Cancer by Targeting Apoptosis and Autophagy Pathways
Publication Status	☐ Published ☐ Accepted for Publication ☑ Submitted for Publication ☐ Unpublished and Unsubmitted work written in manuscript style
Publication Details	

Co-Author

Name of Principal Author (Candidate)	Jian Cui
Contribution to the Paper	Assisted with analysed data, designed and prepared figures.
Overall percentage (%)	20%
Certification:	This paper reports on original research I conducted during the period of my Higher Degree by Research candidature and is not subject to any obligations or contractual agreements with a third party that would constrain its inclusion in this thesis. I am the third author of this paper.
Signature	Date 18/6/18

Co-Author Contributions

By signing the Statement of Authorship, each author certifies that:

i. the candidate's stated contribution to the publication is accurate (as detailed above);

ii. permission is granted for the candidate in include the publication in the thesis; and

iii. the sum of all co-author contributions is equal to 100% less the candidate's stated contribution.

Name of Principal Author	Jue Zhang
Contribution to the Paper	Experimental design, experiments design, data analysis, wrote paper
Signature	Date 16/06/2018

Name of Co-Author	Xiaomin Liu
Contribution to the Paper	Experimental design, assisted with experiments, assisted with data analysis, wrote paper
Signature	Date 16/06/2018

Name of Co-Author	David L. Adelson
Contribution to the Paper	Provided suggestions and proof-read the manuscript.
Signature	Date 18/6/2018

Name of Co-Author	Jing Wang
Contribution to the Paper	Experimental design, assisted with experiments, assisted with data analysis, wrote paper
Signature	Date 18/06/2018

Name of Co-Author	Thazin Nwe Aung
Contribution to the Paper	Provided suggestions and proof-read the manuscript.
Signature	Date 12/06/2018

Name of Co-Author	Zhipeng Qu
Contribution to the Paper	Provided suggestions and proof-read the manuscript.
Signature	Date 18/06/18

Name of Co-Author	Lingling Sun
Contribution to the Paper	Experimental design, assisted with experiments, assisted with data analysis, wrote paper
Signature	Date 18/06/2018

Name of Co-Author	Lizhu Lin		
Contribution to the Paper	Supervised the research, acquired funding for the experiments, experimental design, wrote paper		
Signature		Date	16/06/2018

Traditional Chinese Herbal Formula YQCT Reduces Gefitinib-induced Drug Resistance in Non-Small Cell Lung Cancer by Targeting Apoptosis and Autophagy Pathways

Jue Zhang [1], Xiaomin Liu [2], Jian Cui [3], David L. Adelson [4], Jing Wang [5], Thazin Nwe Aung [6], Zhipeng Qu [7], Lingling Sun [8] and Lizhu Lin [9,*]

[1] Guangzhou University of Chinese Medicine, Guangzhou 510000, Guangdong Province, China; jue.zhang01@adelaide.edu.au

[2] Guangzhou University of Chinese Medicine, Guangzhou 510000, Guangdong Province, China;
International Institute for Translational Chinese Medicine, Guangzhou University of Chinese Medicine, Guangzhou 510000, Guangdong Province, China; liuxiaomin5499@126.com

[3] Department of Genetics and Evolution, School of Biological Sciences, The University of Adelaide, Adelaide, South Australia 5005, Australia; jian.cui@adelaide.edu.au

[4] Department of Genetics and Evolution, School of Biological Sciences, The University of Adelaide, Adelaide 5005, South Australia, Australia; david.adelson@adelaide.edu.au

[5] Guangzhou University of Chinese Medicine, Guangzhou 510000, Guangdong Province, China; jingjingwxfx@163.com

[6] Department of Genetics and Evolution, School of Biological Sciences, The University of Adelaide, Adelaide 5005, South Australia, Australia; thazin.nweaung@adelaide.edu.au

[7] Department of Genetics and Evolution, School of Biological Sciences, The University of Adelaide, Adelaide 5005, South Australia, Australia; zhipeng.qu@adelaide.edu.au

[8] First Affiliated Hospital, Guangzhou University of Chinese Medicine, Guangzhou 510000, Guangdong Province, China; lingling.sun2017@gmail.com

[9] First Affiliated Hospital, Guangzhou University of Chinese Medicine, Guangzhou 510000, Guangdong Province, China; lizhulin26@yahoo.com

* Correspondence: lizhulin26@yahoo.com; Tel: +86 20 36588425

Abstract

Background: Epidermal growth factor receptor-tyrosine kinase inhibitors (EGFR-TKI) are first-line therapeutic agent for non-small cell lung cancer (NSCLC) patients with *EGFR* mutations. However, most patients with sensitizing *EGFR* mutations become resistant to EGFR-TKI after 9 to 13 months of EGFR-TKI treatment. Yiqi Chutan Tang (YQCT) has been prescribed for over 20 years to treat lung cancer in China. Over this period YQCT has been shown to reduce drug resistance of NSCLC patients. The objective of this study is to explore the underlying molecular mechanisms leading to drug resistance reduction of YQCT in NSCLC with *EGFR* mutations.

Methods: The major chemical compounds were characterized by High-performance liquid chromatography (HPLC), the cell viability and DNA synthesis were detected by A 3-(4, 5-dimethylthiazol-2-yl)-2, 5-diphenyltetrazolium bromide (MTT) and 5-ethynyl-2'-deoxyuridine (EdU), flow cytometry was used to distinguish cell cycle and apoptosis in different groups, the effect of autophagy activation is detected by western blot. In addition, Gene Ontology (GO) terms and Kyoto Encyclopedia of Genes and Genomes (KEGG) were also used for characterizing the potential molecular mechanisms of YQCT.

Results: In this report we show the application of YQCT decreases gefitinib-induced drug resistance via slightly arresting the cell cycle, inducing gefitinib-induced apoptosis and activating

the autophagy pathway.

Conclusions: At the molecular level, YQCT may reduce drug resistance and improve anti-cancer effects when associated with gefitinib. This could be a result of enhancement of apoptosis and autophagy in the EGFR-TKI resistant NSCLC cell line.

Keywords: EGFR-TKI; Gefitinib; Drug Resistance; Non-Small Cell Lung Cancer; Apoptosis; Autophagy; Yiqi Chutan Tang

Background

High incidence and mortality for lung cancer lead to low survival rates worldwide. Among all lung cancer cases, NSCLC is the most common subgroup (85%–90%) [1]. For NSCLC patients, platinum-based chemotherapy is the first line therapy of choice [2]. While treatments with EGFR-TKI, including gefitinib, erlotinib, afatinib, AZD9291, have been shown to be more effective in improving survival rate compared to standard platinum-based chemotherapy in patients with *EGFR*-mutated NSCLC [3, 4]. However, after 9 to 13 months of EGFR-TKI therapy, most patients with sensitizing *EGFR* mutations become resistant to EGFR-TKI, greatly reducing its effectiveness [5-8]. Therefore, there is an urgent need for new strategies to treat patients with EGFR-TKI resistance.

Traditional Chinese medicine (TCM) has been proposed to be an important source of effective antitumor therapies, as well as reduce drug resistance for NSCLC [9, 10]. YQCT is a formula used to treat NSCLC, which is consisted of American Ginseng (Xi Yang Shen), Bulbus Fritillariae Thunbergii (Zhe Bei Mu), Radix Ranunculi Ternati (Mao Zhua Cao), Bombyx Batryticatus (Jiang Can), Herba Sarcandrae (Zhong Jie Feng), Indian Iphigenia Bulb (Shan Ci Gu), Rhizoma Pinelliae (Ban Xia) and Lucid Ganoderma (Ling Zhi), has been shown to inhibit tumor growth [11], reduce

drug resistance in lung cancer cells [12, 13], prolong the median survival time [14] and reduce chemotherapy-related fatigue in NSCLC patients [15].

Our previous research suggests YQCT can inhibit EGFR-TKI-resistant tumor growth *in vivo*, and the mechanism may be related to the regulation of the endoplasmic reticulum stress (ER Stress) response by up-regulating CHOP / GADD153 and GADD34 protein expression [16]. CHOP is important in ER stress-induced apoptosis, with $CHOP^{-/-}$ mice shown to have a low apoptosis rate in response to ER stress [17]. Since the PERK/eIF2α/CHOP pathway is essential for inducing autophagy associated with ER stress [18, 19], CHOP also plays an important role in regulating autophagy, with CHOP able to regulate transcription of several autophagy-related genes (ATG), such as microtubule-associated protein 1 light chain 3β (MAP1LC3B) and autophagy-related gene 5 (ATG5) [20]. Furthermore, dysregulated autophagy may also trigger ER stress as a feedback mechanism [21, 22]. It appears the regulation of ER stress, apoptosis and autophagy are reflected in more than the aspect of YQCT's overall effect. Our previous research has discussed the anti-cancer mechanism of YQCT via ER stress and apoptosis [16, 23]. In this study, we focus on drug resistance reduction of YQCT in gefitinib-resistant human NSCLC cell line H1975 and explore the underlying molecular mechanisms.

Methods

Reagents

Dimethyl sulfoxide (DMSO) and MTT were provided by Sigma-Aldrich (St. Louis, MO, USA). BCA Kit, RIPA lysis buffer, Cell Cycle Analysis Kit and Apoptosis Analysis Kit were obtained from Beyotime Institute of Biotechnology (Haimen, Jiangsu, China). Cell-Light EdU Apollo 488 In Vitro Kit was obtained from Guangzhou Ribo Bio Co., Ltd. (Guangzhou, Guangdong, China).

Primary antibodies atg3, atg12, and secondary antibody were purchased from Cell Signaling Technology, Inc (Danvers, Massachusetts, USA). The β-actin primary antibody was purchased from Santa Cruz Biotechnologies Inc (Dallas, Texas, USA). Western blot detection reagents were provided by Bio-Rad Laboratories (Hercules, CA, USA). Gefitinib was purchased from Selleck Chemicals (Houston, Texas, USA).

YQCT Preparation

Herbs used were purchased from Guangdong Kang Mei Pharmaceutical Company Ltd (Jieyang, Guangdong, China). The herbs were soaked in double distilled water (1L) for 30 minutes, mixed and boiled in 8 volumes of water (v/w) by moderate heating for 2 hours, and finally re-boiled in 8 volumes of water for 1 hour [24]. The extracts were filtered and dried by lyophilization. The resulting supernatant was diluted in the cell culture media and filtered with a 0.22μM filter.
The plant materials were authenticated by one of the authors, Prof. Lizhu Lin, and the formula specimens were deposited at International Institute for Translational Chinese Medicine, Guangzhou University of Chinese Medicine (specimens ID: IITCM 58-65).

HPLC Analysis

Briefly, the samples solutions were put into the HPLC (Agilent 1200 HPLC system, Santa Clara, CA, USA) and separated on the chromatographic column C18 (4.6 mm×250mm, 2.7μm). The mobile phase consisted of acetonitrile (A) and 25mM acetic acid with ammonia (B). The gradient elution program was as follows: 0%-0% A at 0–10 minutes, 40%-90% A at 35–45 minutes, 90%-100% A at 45-50 minutes, 0%-0% A at 51-58 minutes. The flow rate was 1 ml/min and the detection

wavelength was at 254 nm. The injection volume was 10μL and the column temperature was maintained at 30℃.

Cell Culture

Human *EGFR* mutated lung cancer cell line H1975 was provided by the Chinese Academy of Science (Shanghai, China). All culture materials were purchased from Gibco Laboratories (Grand Island, NY, USA). Cells were maintained in RPMI-1640 medium supplemented with 10% FBS and 1% penicillin/streptomycin in a 5% CO_2 incubator at 37℃.

Cell Viability Assay

4×10^3 H1975 cells were seeded in 96-well plates and incubated for 24 hours. Following seeding and initial incubating the cells were incubated with YQCT and gefitinib. The effects of YQCT and gefitinib on cell viability were detected using the MTT assay. After 48 hours of incubation, 100μL of MTT stock solution (0.5mg/ml) was added into each well and the plates were incubated for another 4 hours. Finally, 150μL of DMSO was added to each well, the plates were shaken for 10 minutes for crystal dissolution. Absorbance and cell viability were then determined.

EdU Incorporation and Immunofluorescence Staining

100μL of 1:1,000 dilution of EdU-labeling reagent was added to culture medium after 48 hours of cell culture for EdU labelling. The culture medium was discarded after 2 hours followed by the addition of 50μL of cell fixative reagent to each well and incubation at room temperature for 30

minutes. The medium was discarded and 50ml (2 mg/ml) glycine was added to each well before further incubation in a shaker for 5 minutes. 100μL of 1 × Apollo reagent was added into the culture medium and incubated in a dark shaker for 30 minutes. The medium was again discarded and 100μL of 0.5% TritonX-100 was added. Finally, 100μL of 1 × Hoechst 33342 reagent was added and then incubated in a dark shaker for 30 minutes. Cells were detected by Leica spectral confocal fluorescent microscopy at 488 nm.

Cell Cycle Distribution Analysis

H1975 cells were seeded into 6-well plates overnight. Following adding 12.5μM of gefitinib combined with or without 0.5mg/ml YQCT for 48 hours incubation. Cells were then resuspended in 1 ml of PBS containing 1 mg/ml of RNase and 50μg/ml of PI and then were incubated in dark for 30 minutes at room temperature. A total of 1×10^4 cells were acquired by flow cytometer (BD Biosciences, San Diego, CA, USA) to determine cell cycle distribution under the drug treatments.

Quantification of Cellular Apoptosis Using Flow Cytometry

Apoptotic cells were quantitated using the annexin V: PI apoptosis detection kit. After cells were treated with gefitinib at 12.5 μM combined with or without 0.5mg/ml YQCT for 48 hours, cells were trypsinized, washed and re-suspended at a concentration of 1×10^6 cells/ml. Then cells were gently re-suspended in 1 × binding buffer with 2.5μl of annexin V: PI in a total volume of 100μl and incubated in dark for 15 minutes at room temperature. Apoptotic cells were quantified using flow cytometer (BD Biosciences, San Diego, CA, USA).

Western Blot Analysis

Cell lysates were prepared in RIPA lysis buffer containing 1% phenylmethanesulfonyl fluoride and 1% phosphatase inhibitor. The soluble protein fractions were collected after centrifugation at 1.35×10^4 g for 10 minutes. Protein concentrations were determined by BCA protein assay kit. 30mg of proteins were separated on 8–12% SDS-PAGE and were incubated with different antibodies overnight at 4℃. Membranes were incubated with the appropriate secondary antibody. Signals were measured by an ECL chemiluminescence detection agent.

Data Processing and Functional Annotation

PubChem IDs were submitted into BATMAN system [25] to identify genes that are regulated by nine major bioactive components in YQCT with a cut-off score of 20. After identifying highly relevant genes, functional enrichment analysis was performed based on KEGG and GO terms using cluster Profiler (v3.5) [26].

Statistical Analysis

Statistical analysis was performed using SPSS 24.0 software. Statistical comparisons were performed using the Independent-Samples T test. Data measurement was expressed as mean values ± standard deviation. $p < 0.01$ was considered significantly statistically significant.

Results

The chemical composition of YQCT

High-performance liquid chromatography (HPLC) was used to characterize YQCT, which reveal 9 major chemical compounds: Rosmarinic Acid, Resorcinol, Isofraxidin, Ganoderic Acid B, Ganoderic Acid C2, Ganoderic Acid A, Peimine, Peiminine and Beta-Sitosterol (Figure 1).

YQCT inhibits cell viability, DNA synthesis and reduces gefitinib-induced drug resistance in H1975 cells

A 3-(4, 5-dimethylthiazol-2-yl)-2, 5-diphenyltetrazolium bromide (MTT) cell viability assay showed that high concentration of YQCT inhibited H1975 cell viability at 48 hours (Figure 2a). In addition, 5-ethynyl-2'-deoxyuridine (EdU) was used to monitor DNA synthesis [27] and the results indicated that application of YQCT inhibited DNA synthesis *in vitro* in a dose-dependent fashion (Figure 2b). For this study, 0.5mg/ml of YQCT (0.5mg/ml of freeze-dried YQCT powder is extracted from 10mg/ml of YQCT formula) was selected as the routine concentration for the experiments, as the dose did not show obvious cytotoxicity, but could inhibit DNA synthesis.

The EGFR-TKI resistant lung cancer cell line, H1975, showed more obviously resistance to gefitinib (EGFR-TKI) challenge than EGFR-TKI sensitive lung cancer cell line A549 (Figure 2c). Compared to treatment with gefitinib alone, treatment with gefitinib combined with YQCT significantly decreased H1975 cell viability (Figure 2d).

These results indicate YQCT may inhibit cell viability and DNA synthesis, as well as improving the anti-cancer effect and reducing gefitinib-induced drug resistance in H1975 cells when combined with gefitinib.

YQCT induces slight cell cycle arrest, enhances gefitinib-induced apoptosis while activating the autophagy pathways

EdU is incorporated into replicated chromosomal DNA during the S phase of the cell cycle [27, 28]. As its incorporation is cell cycle-dependent, we used EdU to determine if YQCT can modulate the cell cycle in NSCLC. H1975 cells were treated with 12.5μM gefitinib either with or without the addition of 0.5mg/ml YQCT for 48 hours. The YQCT and gefitinib (combined group) and YQCT group showed a slight arrest at the G2/M phase in H1975 cells compared to the gefitinib group (Figure 3a, b).

Gefitinib-induced apoptosis in the presence and absence of YQCT was measured with a PI-FITC apoptosis assay in H1975 cells. Apoptotic cells were quantified by flow cytometric analysis. The percentage of late apoptotic cells in the combined group was 1.7 folds higher than gefitinib only for 48 hours (Figure 3c, d).

As apoptosis is relevant to autophagy [29], we examined whether apoptosis was also related to autophagy in this research. Autophagy-related 3 (atg3) and autophagy-related 12 (atg12), key transcription factors for microtubule-associated protein 1A/1B-light chain 3 (LC3) expression, were detected by western blot assay (Figure 3e). We observed up-regulated protein expression of atg3 and atg12 in H1975 cells in the combined group compared to gefitinib alone, indicating that autophagy was enhanced by YQCT.

Potential molecular mechanisms

To characterize the potential molecular mechanisms of YQCT anti-cancer activity, we submitted the PubChem IDs of the nine principal compounds (Additional file 1) to the Batman [25] database

to identify genes that were regulated by these bioactive components. 269 genes (gid.csv) were associated with these nine compounds (Additional file 2), 19 genes were relevant to cancer (figure 4a): tumor necrosis factor (*TNF*), apoptotic peptidase activating factor 1 (*APAF1*), death-associated protein kinase 2 (*DAPK2*), toll like receptor 3 (*TLR3*), receptor interacting serine/threonine kinase 1 (*RIPK1*), fibroblast growth factor 10 (*FGF10*), transforming growth factor beta 2 (*TGFB2*), AKT serine/threonine kinase 1 (*AKT1*), ALK receptor tyrosine kinase (*ALK*), annexin A1 (*ANXA1*), kinesin family member 14 (*KIF14*), ABL proto-oncogene 1, non-receptor tyrosine kinase (*ABL1*), androgen receptor (*AR*), A-Raf proto-oncogene, serine/threonine kinase (*ARAF*), aurora kinase A (*AURKA*), catenin beta 1 (*CTNNB1*), estrogen receptor 1 (*ESR1*), fibroblast growth factor receptor 2 (*FGFR2*), retinoic acid receptor alpha (*RARA*).

We carried out functional enrichment analysis for these genes based on Gene Ontology (GO) terms and Kyoto Encyclopedia of Genes and Genomes (KEGG) (Additional file 3, 4). Significantly over-represented GO and KEGG functional terms in protein-coding genes are shown in Tables 1 and 2. Apoptosis and cell cycle categories are shown in the GO terms (Figure 4b). Meanwhile, NSCLC related pathways identified as significantly affected by YQCT are shown in Figure 4c. From the analysis we focused on specific pathways related to cancer. Pathways in cancer and in NSCLC are shown in Figure 5a, b.

Table 1. Significantly over-represented GO terms in protein-coding genes

Title 1	Title 2	Title 3
GO:0008219	cell death	102
GO:0042493	response to drug	47
GO:0007049	cell cycle	47
GO:0097190	apoptotic signaling pathway	39

GO:1903047	mitotic cell cycle process	26
GO:0044770	cell cycle phase transition	19
GO:0007050	cell cycle arrest	11
GO:0097194	execution phase of apoptosis	6

Table 2. Significantly over-represented KEGG Pathway in protein-coding genes

Pathway	Description	Count
hsa05200	Pathways in cancer	40
hsa05202	Transcriptional misregulation in cancer	12
hsa04210	Apoptosis	10
hsa05222	Small cell lung cancer	8
hsa05223	Non-small cell lung cancer	8
hsa04151	PI3K-Akt signaling pathway	6
hsa04150	mTOR signaling pathway	4

Discussion

YQCT was formulated based on the TCM theories of enhancing immunity and removing phlegm. The nine bioactive compounds of YQCT were reported to have an anti-cancer effect [30] and reversal of drug resistance [31] by causing cell cycle arrest [32], inducing apoptosis [33] and activating autophagy [34, 35]. However, the effect of YQCT on drug resistance has not been studied.

EdU is an indicator of cell proliferation [27, 28]. According to the EdU and MTT assays, 0.5mg/ml of YQCT can inhibit cell proliferation, but shows no obvious cell cytotoxicity. Therefore, its effect of reducing drug resistance appears to be based solely on cell proliferation inhibition. Cell cycle

248 regulation is the basic mechanism underlying proliferation, differentiation and cell death [36]. As
249 shown in Figures 3a and 3b, our research provides further weight to the recent studies showing
250 gefitinib arrests TKI-resistant lung cancer cells in the G0/G1 phase [37, 38]. Cell cycle arrest leads
251 to DNA breaks, which ultimately leads to the inhibition of cell proliferation. YQCT group and
252 combined group showed a slight arrest in G2/M phase on H1975 cells, this result indicates that the
253 YQCT group and combined group could inhibit tumor cell proliferation via G2/M phase arrest
254 which is also consistent with the result of the EdU assay.
255 In the treatment of cancer, manipulating apoptosis by modulation of the key regulators of apoptosis
256 is a promising therapeutic strategy [39]. Gefitinib has an effect on apoptosis regulation by
257 competitively binding to the tyrosine kinase domain of EGFR, leading to the EGFR signaling
258 pathway being blocked [40]. The lack of gefitinib binding to the TKI domain in EGFR-TKI
259 resistant cell lines leads to a reduction in apoptosis, which reduces the effectiveness of NSCLC
260 treatment. Therefore, YQCT combined with gefitinib may be an effective therapy for NSCLC
261 because it induces apoptosis.
262 It is reported that autophagy occurs upstream of apoptosis and activates it, therefore inducing
263 apoptosis indirectly [29, 41]. Loss of autophagy or the inability to increase autophagic flux above
264 basal levels might contribute to the development of acquired EGFR-TKI resistance [42]. The
265 autophagy-related genes *ATG3* and *ATG12* are involved in tumorigenesis and cancer progression.
266 They also mediate essential steps in the early autophagy pathway which contributes to
267 autophagosome maturation and formation processes respectively [43]. Recent research shows that
268 cells lacking atg12 and atg3 proteins accumulate abnormal perinuclear late endosomes that are
269 unable to fuse with lysosomes, thereby abrogating autolysosome formation [44]. Our results
270 indicate YQCT induces autophagy by up-regulating atg3 and atg12 and in turn promoting the late

endosomes to fuse with lysosomes to form autolysosomes.

To find out potential reduce drug resistance mechanisms of YQCT, we found that 269 genes showed a significant relationship (score>20) with these 9 compounds in YQCT. Three of these genes, *APAF1*, *TNF* and *DAPK2*, were reported to mediate apoptosis and inhibit cell proliferation and metastasis [45-48]. GO terms also showed a significant relationship between YQCT and both apoptosis and cell cycle, as can be seen in Figure 4b.

In the pathways in cancer and, specifically NSCLC, the FGF-FGFR and EGF-EGFR pathways are of interest as they were relevant to YQCT. Both of them are upstream effectors of the PI3K-Akt pathway, which relevant to apoptosis. Our previous study indicated that YQCT down-regulates the expression of p-Akt in A549 lung cancer cells[49]. Moreover, our KEGG enrichment analysis suggested that the PI3K-Akt signaling pathway was affected by YQCT. From this, we speculate that YQCT down-regulates the PI3K-Akt pathway, up-regulates apoptosis by affecting both the FGF-FGFR and EGF-EGFR pathways. These results provide a potential research direction to screen the relevant pathways in more comprehensive studies.

Conclusions

We have demonstrated that YQCT can inhibit cell proliferation, slightly arrest cell cycle at G2/M phase, induce apoptosis and activate the autophagy pathway. Together these results indicate YQCT has the ability to reduce gefitinib-induced drug resistance. We speculate that this might be through up-regulation of apoptosis and autophagy in EGFR-TKI resistant NSCLC cells.

Although EGFR-TKI is very effective in patients with *EGFR* oncogenic mutations [50, 51], acquired drug resistance is still a problem. Our findings may help in the development of a new strategy for reducing gefitinib resistance during treatment of NSCLC patients with *EGFR* mutations.

List of abbreviations

EGFR-TKI: Epidermal growth factor receptor-tyrosine kinase inhibitors; NSCLC: Non-small cell lung cancer; YQCT: Yiqi Chutan Tang; TCM: Traditional Chinese medicine; ER Stress: Endoplasmic reticulum stress; ATG: Autophagy related genes; HPLC: High-performance liquid chromatography; MTT: 3-(4, 5-dimethylthiazol-2-yl)-2, 5-diphenyltetrazolium bromide; EdU 5-ethynyl-2'-deoxyuridine; Atg3: Autophagy related 3; Atg12: Autophagy related 12; LC3: Microtubule-associated protein 1A/1B-light chain 3; TNF: Tumor necrosis factor; APAF1: Apoptotic peptidase activating factor 1; DAPK2: Death associated protein kinase 2; TLR3: Toll like receptor 3; RIPK1: Receptor interacting serine/threonine kinase 1; FGF10: Fibroblast growth factor 10; TGFB2: Transforming growth factor beta 2; AKT1: AKT serine/threonine kinase 1; ALK: ALK receptor tyrosine kinase; ANXA1: Annexin A1; KIF14: Kinesin family member 14; ABL1: ABL proto-oncogene 1, non-receptor tyrosine kinase; AR: Androgen receptor; ARAF: A-Raf proto-oncogene, serine/threonine kinase; AURKA: Aurora kinase A; CTNNB1: Catenin beta 1; ESR1: Estrogen receptor 1; FGFR2: Fibroblast growth factor receptor 2; RARA: Retinoic acid receptor alpha; DMSO: Dimethyl sulfoxide.

Declarations

Ethics approval and consent to participate

Not applicable.

Consent for publication

Not applicable.

Availability of data and material

The datasets used and analyzed during the current study are available from the corresponding author on reasonable request.

Competing interests

The authors declare that they have no competing interests.

Funding

This research was funded by the National Nature Science Foundation of China (# 81573780).

Authors' contributions

LL drafted the work, revised it critically for important intellectual content; JZ, XL and JW performed the experiments; JZ, JC and LS interpret data for the work; LL, JZ, DLA, ZQ and TNA wrote or modify the manuscript, and final approval of the version to be published. All authors read and approved the final manuscript.

Acknowledgments

We are very grateful to James Galbraith from the University of Adelaide (Australia) for taking the time to read the manuscript in full and offer helpful comments.

Authors' information

LL is the director of Oncology Department of First Affiliated Hospital of Guangzhou University of Chinese Medicine. JZ, XL, JW and LS are the students of Guangzhou University of Chinese

Medicine. DLA is the chair of Bioinformatics of the department of Genetics and Evolution of the University of Adelaide, JC TNA and ZQ are fellows in this department.

Additional files

Additional files 1: Table 1. The principal components in the formula and the associated PubChem IDs (.doc 13.2kb)

Additional files 2: Table 2. Associated genes with the nine compounds (.csv 1.58kb)

Additional files 3: Table 3. GO terms enrichment (.xls 46.4kb)

Additional files 4: Table 4. KEGG pathways enrichment (.xls 18.3kb)

References

1. Baltayiannis, N., et al., *Lung cancer surgery: an up to date.* J Thorac Dis, 2013. **5 Suppl 4**: p. S425-39.
2. Al-Farsi, A. and P.M. Ellis, *Treatment paradigms for patients with metastatic non-small cell lung cancer, squamous lung cancer: first, second, and third-line.* Front Oncol, 2014. **4**: p. 157.
3. Yu, H.A. and W. Pao, *Targeted therapies: Afatinib--new therapy option for EGFR-mutant lung cancer.* Nat Rev Clin Oncol, 2013. **10**(10): p. 551-2.
4. Inoue, A., et al., *Updated overall survival results from a randomized phase III trial comparing gefitinib with carboplatin-paclitaxel for chemo-naive non-small cell lung cancer with sensitive EGFR gene mutations (NEJ002).* Ann Oncol, 2013. **24**(1): p. 54-9.
5. Yu, H.A., et al., *Analysis of tumor specimens at the time of acquired resistance to EGFR-TKI therapy in 155 patients with EGFR-mutant lung cancers.* Clin Cancer Res, 2013. **19**(8): p. 2240-7.
6. Rosell, R., et al., *Erlotinib versus standard chemotherapy as first-line treatment for European patients with advanced EGFR mutation-positive non-small-cell lung cancer (EURTAC): a multicentre, open-label, randomised phase 3 trial.* Lancet Oncol, 2012. **13**(3): p. 239-46.
7. Mok, T.S., et al., *Osimertinib or Platinum-Pemetrexed in EGFR T790M-Positive Lung Cancer.* N Engl J Med, 2017. **376**(7): p. 629-640.
8. Jia, Y., et al., *Overcoming EGFR(T790M) and EGFR(C797S) resistance with mutant-selective allosteric inhibitors.* Nature, 2016. **534**(7605): p. 129-32.
9. Jiao, L., et al., *Effects of Chinese Medicine as Adjunct Medication for Adjuvant Chemotherapy Treatments of Non-Small Cell Lung Cancer Patients.* Sci Rep, 2017. **7**: p. 46524.
10. Kang, X.H., et al., *Degradation of Mcl-1 through GSK-3beta Activation Regulates Apoptosis Induced by Bufalin in Non-Small Cell Lung Cancer H1975 Cells.* Cell Physiol Biochem, 2017. **41**(5): p. 2067-2076.
11. Wang, S., et al., *Effects of yiqi chutan tang on the proteome in Lewis lung cancer in mice.* Asian Pac J Cancer Prev, 2011. **12**(7): p. 1665-9.
12. 张恩欣, 周岱翰, and 侯超, *益气除痰方通过抑制 Akt 信号通路诱导顺铂耐药肺癌细胞凋亡的作用及*

分子机制研究. 中药新药与临床药理, 2016(03): p. 365-371.
13. 张恩欣, 周岱翰, and 侯超, *益气除痰方含药血清对顺铂耐药肺癌细胞增殖和细胞周期的影响.* 山东医药, 2016(06): p. 13-15.
14. 周岱翰, et al., *益气化痰法为主中医药治疗方案对老年非小细胞肺癌中位生存期的影响:一项多中心、前瞻性临床队列研究.* 世界中医药, 2014(07): p. 833-838+844.
15. 关洁珊, et al., *益气除痰方防治化疗相关性疲劳的疗效观察.* 辽宁中医杂志, 2016(06): p. 1211-1213.
16. 孙玲玲, et al., *益气除痰方调控内质网应激反应抑制 H1650 肺癌生长的研究.* 广州中医药大学学报, 2014(04): p. 573-577.
17. Oyadomari, S., et al., *Targeted disruption of the Chop gene delays endoplasmic reticulum stress-mediated diabetes.* J Clin Invest, 2002. **109**(4): p. 525-32.
18. Senft, D. and Z.A. Ronai, *UPR, autophagy, and mitochondria crosstalk underlies the ER stress response.* Trends Biochem Sci, 2015. **40**(3): p. 141-8.
19. B'Chir, W., et al., *The eIF2alpha/ATF4 pathway is essential for stress-induced autophagy gene expression.* Nucleic Acids Res, 2013. **41**(16): p. 7683-99.
20. Rouschop, K.M., et al., *The unfolded protein response protects human tumor cells during hypoxia through regulation of the autophagy genes MAP1LC3B and ATG5.* The Journal of clinical investigation, 2010. **120**(1): p. 127-141.
21. Deegan, S., et al., *Stress-induced self-cannibalism: on the regulation of autophagy by endoplasmic reticulum stress.* Cell Mol Life Sci, 2013. **70**(14): p. 2425-41.
22. Adolph, T.E., et al., *Paneth cells as a site of origin for intestinal inflammation.* Nature, 2013. **503**(7475): p. 272-6.
23. 李元滨, et al., *益气除痰方对耐顺铂肺癌移植瘤生长及下调 UPR 诱导细胞凋亡的研究.* 中华中医药杂志, 2014(12): p. 3906-3910.
24. Lou, J.S., et al., *Yu Ping Feng San reverses cisplatin-induced multi-drug resistance in lung cancer cells via regulating drug transporters and p62/TRAF6 signalling.* Sci Rep, 2016. **6**: p. 31926.
25. Liu, Z., et al., *BATMAN-TCM: a Bioinformatics Analysis Tool for Molecular mechANism of Traditional Chinese Medicine.* Sci Rep, 2016. **6**: p. 21146.
26. Yu, G., et al., *clusterProfiler: an R package for comparing biological themes among gene clusters.* Omics, 2012. **16**(5): p. 284-7.
27. Salic, A. and T.J. Mitchison, *A chemical method for fast and sensitive detection of DNA synthesis in vivo.* Proc Natl Acad Sci U S A, 2008. **105**(7): p. 2415-20.
28. Zeng, C., et al., *Evaluation of 5-ethynyl-2'-deoxyuridine staining as a sensitive and reliable method for studying cell proliferation in the adult nervous system.* Brain Res, 2010. **1319**: p. 21-32.
29. Lee, T.G., et al., *The combination of irreversible EGFR TKIs and SAHA induces apoptosis and autophagy-mediated cell death to overcome acquired resistance in EGFR T790M-mutated lung cancer.* Int J Cancer, 2015. **136**(11): p. 2717-29.
30. Sharmila, R. and S. Manoharan, *Anti-tumor activity of rosmarinic acid in 7,12-dimethylbenz(a)anthracene (DMBA) induced skin carcinogenesis in Swiss albino mice.* Indian J Exp Biol, 2012. **50**(3): p. 187-94.
31. Tang, X.Y., et al., *[Effect of Peimine on ERCC1 mRNA and LRP Expressions of A549/DDP Multidrug Resistance Cell Line].* Zhongguo Zhong Xi Yi Jie He Za Zhi, 2015. **35**(12): p. 1490-4.
32. Sook, S.H., et al., *Reactive oxygen species-mediated activation of AMP-activated protein kinase and c-Jun N-terminal kinase plays a critical role in beta-sitosterol-induced apoptosis in multiple myeloma U266 cells.* Phytother Res, 2014. **28**(3): p. 387-94.
33. Zhao, F., et al., *Ardisiphenol D, a resorcinol derivative identified from Ardisia brevicaulis, exerts antitumor effect through inducing apoptosis in human non-small-cell lung cancer A549 cells.* Pharm Biol, 2014. **52**(7): p. 797-803.
34. Lyu, Q., et al., *The natural product peiminine represses colorectal carcinoma tumor growth by inducing autophagic cell death.* Biochem Biophys Res Commun, 2015. **462**(1): p. 38-45.
35. Zheng, Z., et al., *Peiminine inhibits colorectal cancer cell proliferation by inducing apoptosis and autophagy and modulating key metabolic pathways.* Oncotarget, 2017. **8**(29): p. 47619-47631.
36. Kim, H. and H.Y. Lim, *Novel EGFR-TK inhibitor EKB-569 inhibits hepatocellular carcinoma cell proliferation by AKT and MAPK pathways.* J Korean Med Sci, 2011. **26**(12): p. 1563-8.

37. Wu, M., et al., *Antitumor activity of combination treatment with gefitinib and docetaxel in EGFR-TKI-sensitive, primary resistant and acquired resistant human non-small cell lung cancer cells.* Mol Med Rep, 2014. **9**(6): p. 2417-22.
38. Mu, X., et al., *Ubiquitin ligase Cbl-b is involved in icotinib (BPI-2009H)-induced apoptosis and G1 phase arrest of EGFR mutation-positive non-small-cell lung cancer.* Biomed Res Int, 2013. **2013**: p. 726375.
39. Ashkenazi, A., *Targeting the extrinsic apoptotic pathway in cancer: lessons learned and future directions.* J Clin Invest, 2015. **125**(2): p. 487-9.
40. Grunwald, V. and M. Hidalgo, *Developing inhibitors of the epidermal growth factor receptor for cancer treatment.* J Natl Cancer Inst, 2003. **95**(12): p. 851-67.
41. Wang, Z., et al., *Autophagy inhibition facilitates erlotinib cytotoxicity in lung cancer cells through modulation of endoplasmic reticulum stress.* Int J Oncol, 2016. **48**(6): p. 2558-66.
42. Fung, C., et al., *EGFR tyrosine kinase inhibition induces autophagy in cancer cells.* Cancer Biol Ther, 2012. **13**(14): p. 1417-24.
43. Cao, Q.H., et al., *Prognostic value of autophagy related proteins ULK1, Beclin 1, ATG3, ATG5, ATG7, ATG9, ATG10, ATG12, LC3B and p62/SQSTM1 in gastric cancer.* Am J Transl Res, 2016. **8**(9): p. 3831-3847.
44. Murrow, L. and J. Debnath, *ATG12-ATG3 connects basal autophagy and late endosome function.* Autophagy, 2015. **11**(6): p. 961-2.
45. Dyari, H.R.E., et al., *A novel synthetic analogue of omega-3 17,18-epoxyeicosatetraenoic acid activates TNF receptor-1/ASK1/JNK signaling to promote apoptosis in human breast cancer cells.* Faseb j, 2017. **31**(12): p. 5246-5257.
46. Schlegel, C.R., et al., *DAPK2 is a novel modulator of TRAIL-induced apoptosis.* Cell Death Differ, 2014. **21**(11): p. 1780-91.
47. Fook-Alves, V.L., et al., *TP53 Regulated Inhibitor of Apoptosis 1 (TRIAP1) stable silencing increases late apoptosis by upregulation of caspase 9 and APAF1 in RPMI8226 multiple myeloma cell line.* Biochim Biophys Acta, 2016. **1862**(6): p. 1105-10.
48. Kee, J.Y., et al., *CXCL16 suppresses liver metastasis of colorectal cancer by promoting TNF-alpha-induced apoptosis by tumor-associated macrophages.* BMC Cancer, 2014. **14**: p. 949.
49. 周京旭, et al., *益气除痰方抑制 p-AKT 活性诱导 A549 细胞失巢凋亡的研究.* 成都中医药大学学报, 2014(02): p. 38-41.
50. Forde, P.M. and D.S. Ettinger, *Targeted therapy for non-small-cell lung cancer: past, present and future.* Expert Rev Anticancer Ther, 2013. **13**(6): p. 745-58.
51. Cooper, W.A., et al., *What's new in non-small cell lung cancer for pathologists: the importance of accurate subtyping, EGFR mutations and ALK rearrangements.* Pathology, 2011. **43**(2): p. 103-15.

Figures and Legends

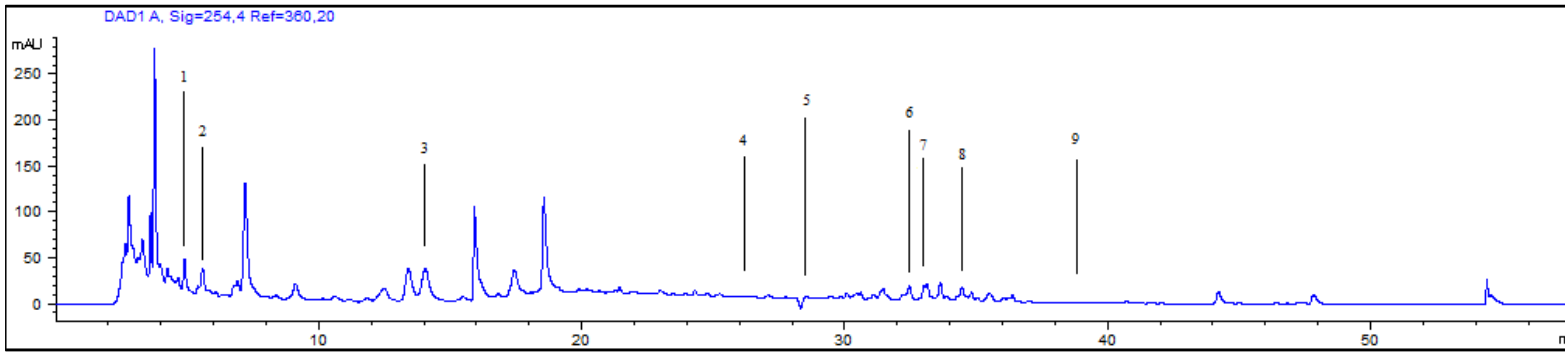

Figure 1. Alcohol extractions of YQCT were qualitatively analyzed with HPLC. The numbers in the chromatograms indicate the constituent peaks 1. Rosmarinic Acid, 2. Resorcinol, 3. Isofraxidin, 4. Ganoderic Acid B, 5. Ganoderic Acid C2, 6. Ganoderic Acid A, 7. Peimine, 8. Peiminine and 9. Beta-Sitosterol. A typical chromatogram is shown (*n =3*)

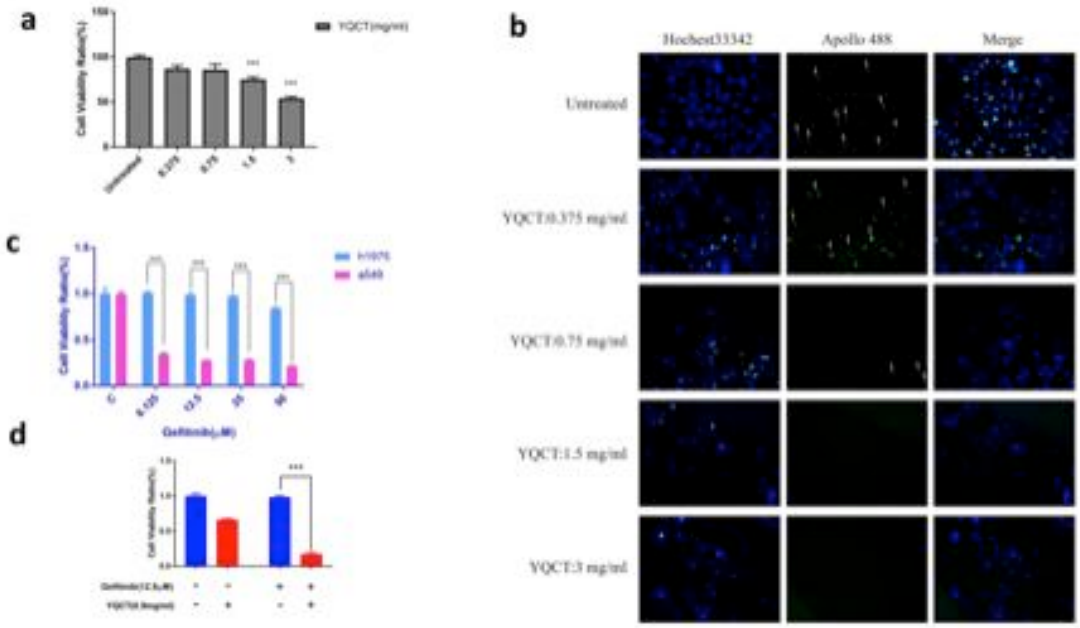

Figure 2. Effects of YQCT on H1975 cells. (a) MTT assay for cell viability. Cells were seeded in 96-well plates (4×10^3 cells/well) overnight and subsequently were treated with 6.25mg/ml, 12.5mg/ml, 25mg/ml and 50mg/ml YQCT for 48 hours. Values are cell viability ratios. (b) Cells were seeded in 96-well plates (4×10^3 cells/well) overnight and subsequently were treated with 6.25mg/ml, 12.5mg/ml, 25mg/ml and 50mg/ml YQCT for 48 hours, then were stained for EdU and visualized using a fluorescence microscope. (c) Cells were seeded in 96-well plates (4×10^3 cells/well) overnight and subsequently were treated with 6.25 μM, 12.5 μM, 25 μM and 50 μM gefitinib for 48 hours. Values are in percentage of cell viability. (d) Cells were seeded in 96-well plates (4×10^3 cells/well) overnight and treated with 12.5 μM gefitinib for 48 hours with or without 0.5mg/ml YQCT. Values are in percentage of cell viability. Independent-Samples T test were used for analysis, *** indicates $p < 0.01$ ($n \geqslant 3$).

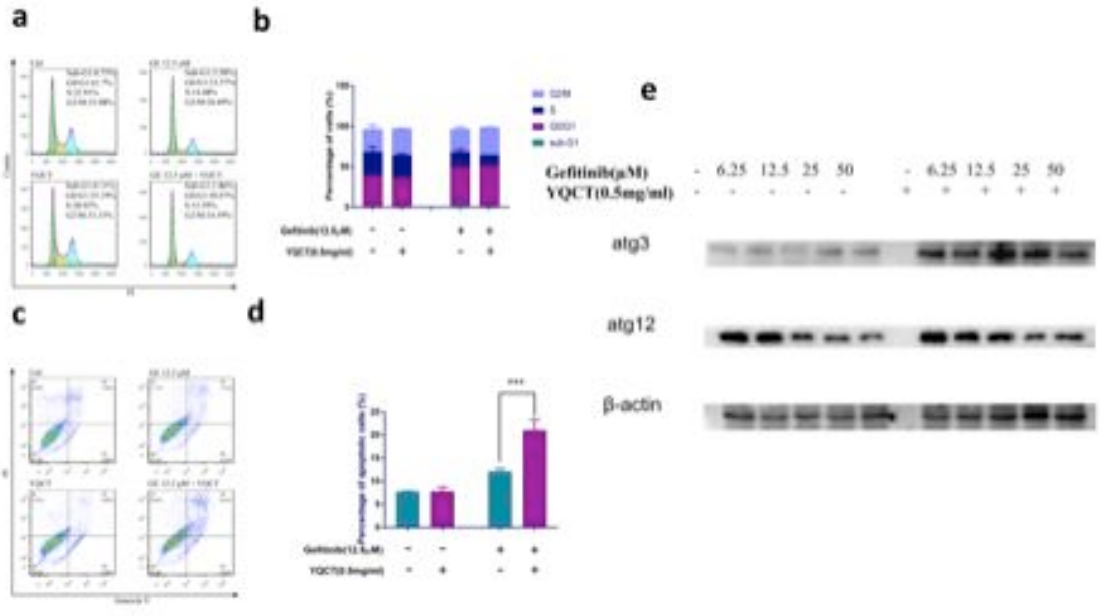

Figure 3. YQCT induces slight cell cycle arrest, enhances apoptosis and autophagy pathways. (a) Effect of YQCT on the cell cycle. FACS detection of propidium Iodide stained cells was used to measure the distribution of specific cell populations in Sub-G1, G0/G1, S, and G2/M phases in H1975 cells. Cells were treated with 12.5μM gefitinib with and without 0.5mg/mL YQCT for 48 hours and then analysed by flow cytometry. (b) Plots the data from (a) to better illustrate the quantitative changes in cell cycle phases. Data are the mean ± SD of independent experiments. (c) YQCT induced apoptotic cell death in H1975 cells. Cells were incubated with gefitinib at 12.5 μM in the presence and absence of 0.5mg/ml YQCT for 48 hours, then analysed by flow cytometry. Flow cytometric plots of specific cell population were calculated by FlowJo software. (d) Plots the data from (c) to better illustrate the quantitative changes in late apoptosis. Data represents the mean ± SD of independent experiments. Independent-Samples T test was used for analysis, *** indicates $p < 0.01$. (e) Western blot for autophagy proteins. H1975 cells were incubated with gefitinib at

494 6.25 μM, 12.5 μM, 25 μM and 50 μM in the presence or absence of 0.5mg/ml YQCT for 48 hours.

495 atg3, atg12 and β-actin were visualized via Western blot.

496

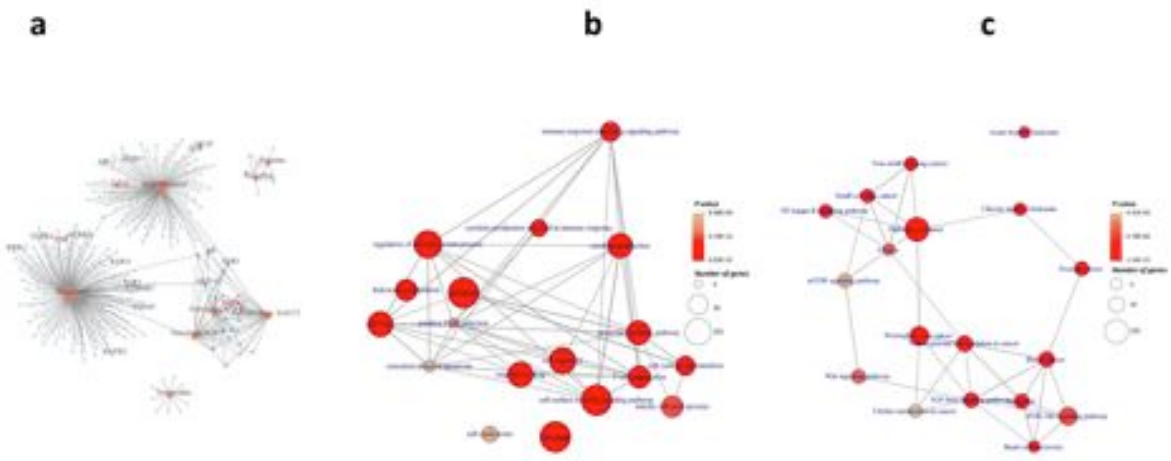

Figure 4. Potential molecular mechanisms of YQCT. (a) Genes regulated by YQCT. Orange nodes represent chemical components and blue nodes represent genes. (b) GO term enrichment results. The color of each node indicates the significance of the enriched term, the redder means the higher relevance. The size of each node represents the number of GO term associated genes, the bigger means the higher association. The name of most significant terms in each cluster were shown. (c) KEGG pathway enrichment results. The color of each node indicates the significance of the enriched term, the redder means the higher relevance. The size of each node represents the number of GO term associated genes, the bigger means the higher association. The name of most significant terms in each cluster were shown.

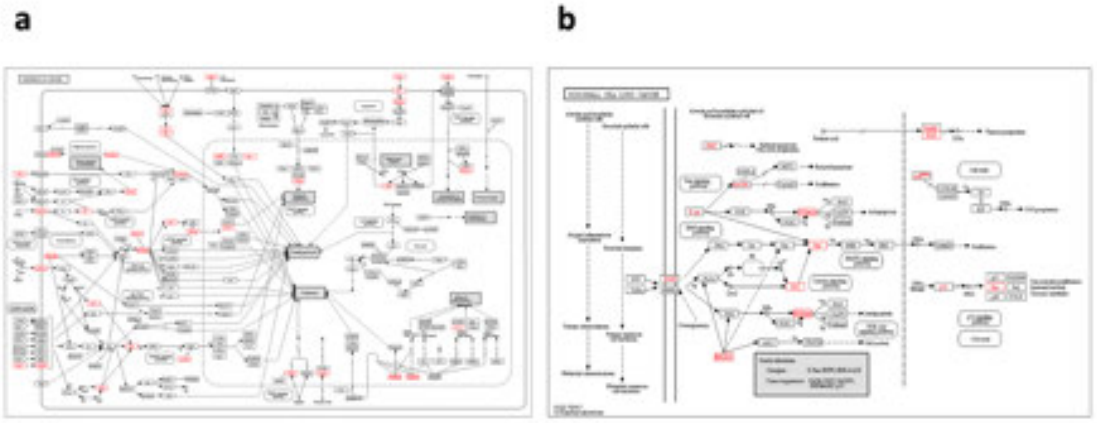

508

509 **Figure 5.** KEGG pathways relevant to YQCT. (a)Pathways in cancer. (b)Pathways in NSCLC.

510 Potential factors which relevant to YQCT were colored in red.

Chapter 6

Conclusions and Future Directions

TCM is a major source of alternative and complementary therapy, particularly in cancer therapy in China and surrounding countries. However, there is limited acceptance of TCM in western countries because of limited data with respect to molecular modes of action for TCM formulations. We have focussed on CKI as a TCM candidate for investigation in order to identify the molecular processes altered by CKI in cancer cells.

Throughout my thesis, I have used systems-biology and functional genomics methods to analyze the effects of CKI on cancer cells and extended these methods to another TCM formula. We have developed a novel approach to identify the gene networks and pathways that are perturbed or targeted by CKI based on transcriptome profiling.

Briefly, by comparing transcriptomes from different treatment groups, we can identify differentially expressed (DE) genes associated with responses to CKI. These genes were then mapped against existing computational annotations or pathway databases for biological systems to identify significant biological functions affected by CKI. We have replicated this analysis on several cancer cell lines and integrated these analyses to find core DE genes and biological functions. As a result of this approach, we have determined that CKI can modulate/perturb multiple complex pathways or biological processes. We have also validated the expression of key genes and proteins involved in these functions.

My study showed that CKI can regulate the expression of numerous genes in multiple cell lines, and most of these differentially expressed genes were positively regulated. Our results show that CKI primarily regulates the cell cycle, energy metabolism, and other pathways including DNA repair. While this systematic approach provided a comprehensive analysis of cancer cell responses to CKI in selected cell lines, there are still significant limitations to our results.

One of the primary limitations of this thesis is the limited number of cell lines and transcriptome datasets used for this analysis. Even though we integrated these analyses of three cell lines, we were still left with hundreds DE genes to investigate. This is a too large number of genes for detailed validation and required us to restrict the set of genes and pathways used for validation. The addition of additional cell lines and the inclusion of protein interaction networks to our analysis would have likely yielded a smaller, more manageable set of candidate genes for validation.

Another limitation was the method for selection of target proteins. Due to a lack of protein expression data, we selected the target proteins based on the expression level of DE genes from our transcriptome data. This limited the number of proteins we could test to those that we felt certain would be expressed at a high enough level to detect.

In addition, although our research subject was a TCM formulation, throughout the thesis, we rarely mentioned the relationship between our findings and TCM theories. This lack of connection between TCM theory and scientific verification is probably an impediment to the modernization of TCM.
Therefore, in this thesis, there are many aspects where further analysis would be fruitful. Specifically, it would be an improvement to expand our research to more cancer cell types, in order to identify a smaller, core set of mechanisms for CKI. The methods we used to identify core genes can be improved by better statistical analysis in order to include weightings for both statistical significance and expression fold change. In order to improve the selection of target proteins, the use of proteomics to complement transcriptome-based approaches would be superior.

Collectively, my findings have for the first time comprehensively identified specific, complex candidate mechanisms of action for CKI. These mainly serve to down-regulate biological processes thereby inducing cell death in cancer. Our results from this comparative analysis and identification of relevant biological networks have provided a basic set of concepts that can be applied to CKI/ TCM, and can be used as a starting point for the future scientific characterization of TCM theory.

Appendix A

Supplementary Tables

All the supplementary tables for chapters 2, 3 and 5 can be acquired from the shared Supplementary Tables online: `https://goo.gl/73LCzb`.

1. For chapter 2, there are five supplementary tables including:

    a) Table S1: Summary of RNA-seq datasets used in this study

    b) Table S2: Summary of significantly differentially expressed genes for different comparisons

    c) Table S3: Significantly perturbed KEGG pathways based on SPIA analysis

    d) Table S4: Numbers of transcripts in 53 co-expression modules

    e) Table S5: Significantly over-represented GO and KEGG terms in protein-coding genes from three CKI-5FU co-expression modules (count > 4 and P-value < 0.05)

    f) Table S6: Primers used for qPCR

2. For chapter 3, there are four supplementary tables including:

    a) Table S1. RT-qPCR target genes and their primer sequences.

    b) Table S2. Mapping rate of each cell line.

    c) Table S3. List of DE genes in each cell line at each time point.

    d) Table S4. The summary of the functional analysis of both separate datasets and shared datasets.

        i. Sheet 1-4: GO enrichment of each cell line at two time points. Selection standard: cut off p value<0.01, cut off q value<0.01.

        ii. Sheet 5-8: KEGG enrichment of each cell line at two time points. Selection standard: cut off p value<0.01, cut off q value<0.01.

        iii. Sheet 10-12: DO enrichment of each cell line at two time points. Selection standard: cut off p value<0.01, cut off q value<0.01.

        iv. Sheet 13: GO enrichment of shared genes by both cell lines. Selection standard: cut off p value<0.01.

        v. Sheet 14: KEGG enrichment of shared genes by both cell lines. Selection standard: cut off p value<0.01.

3. For chapter 5, there are four supplementary tables including:

    a) Table S1. The principal components in the formula and the associated

    b) Table S2. The gene enriched from BATMAN

    c) Table S3. GO terms. Selection standard: cut off p value<0.01, cut off q value<0.01.

    d) Table S4. KEGG pathways. Selection standard: cut off p value<0.01, cut off q value<0.01.

Appendix B

Supplementary for Chapter 2

Identification of candidate anti-cancer molecular mechanisms of Compound Kushen Injection using functional genomics

SUPPLEMENTARY FIGURES AND TABLES

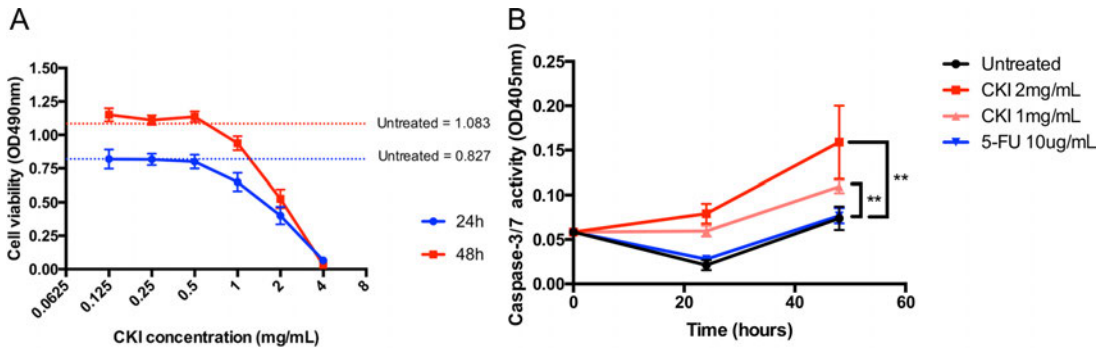

Supplementary Figure 1: CKI inhibited MCF-7 cell growth in a dose-dependent fashion and increased caspase-3/7 activity. A. The level of viability of cells after different treatments were measured using XTT:PMS. Data are represented as mean ±SEM (n=9). X-axis is log2 scaled. **B.** The level of caspase-3/7 activity in cells was measured with Caspase-3/7 Colorimetric Assay Kit. Data are represented as mean ±SEM (n=3). Statistical analyses were performed using two-way ANOVA (**p<0.01, ***p<0.001).

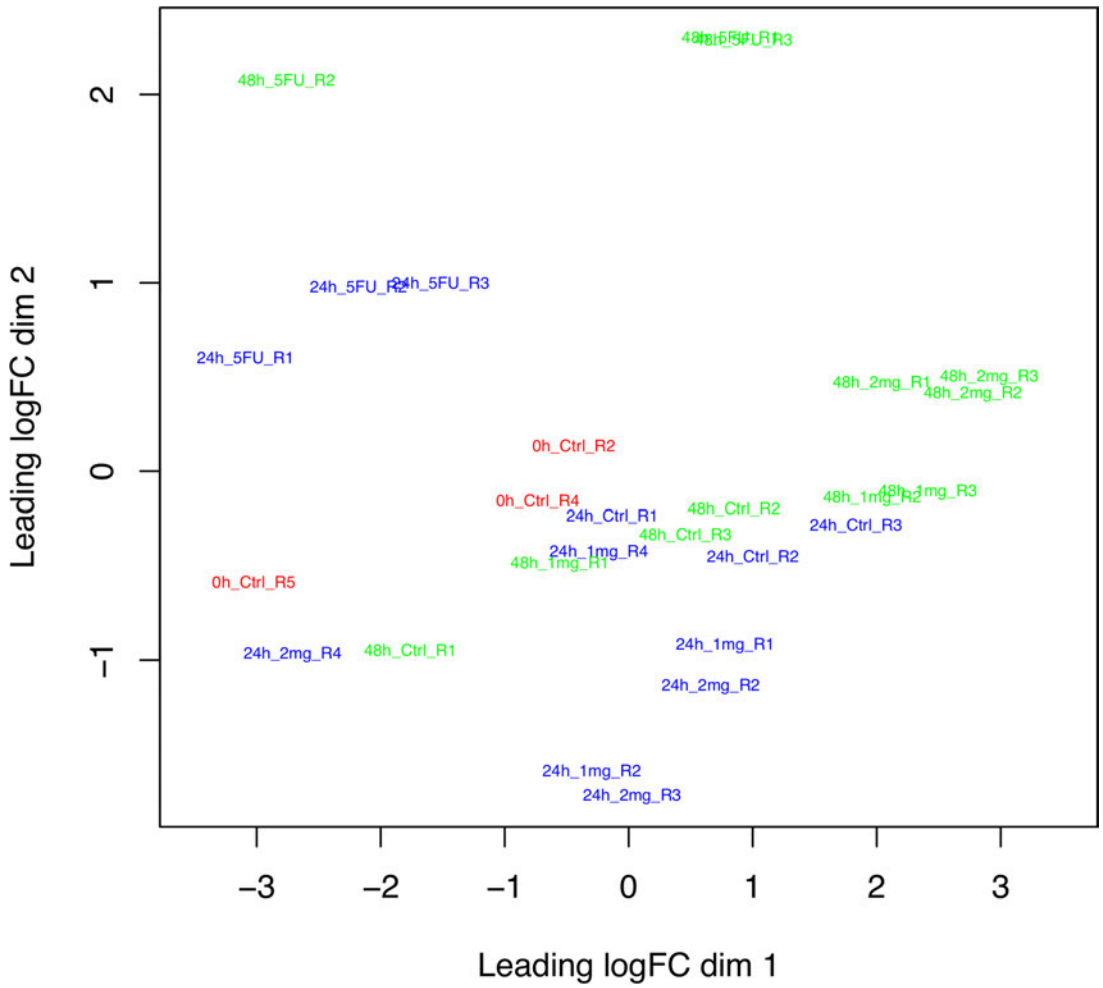

Supplementary Figure 2: Multiple dimensional scaling (MDS) plot for samples based on expression profiles of all genes.

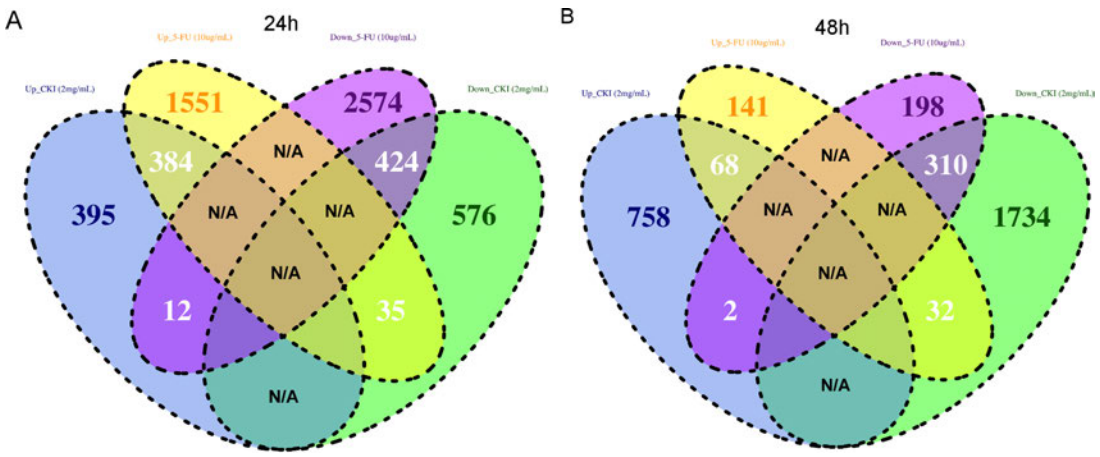

Supplementary Figure 3: Venn diagrams showing the overlap of DE genes in cells treated with CKI (2 mg/mL) or 5-FU for A. 24 hours or **B.** 48 hours.

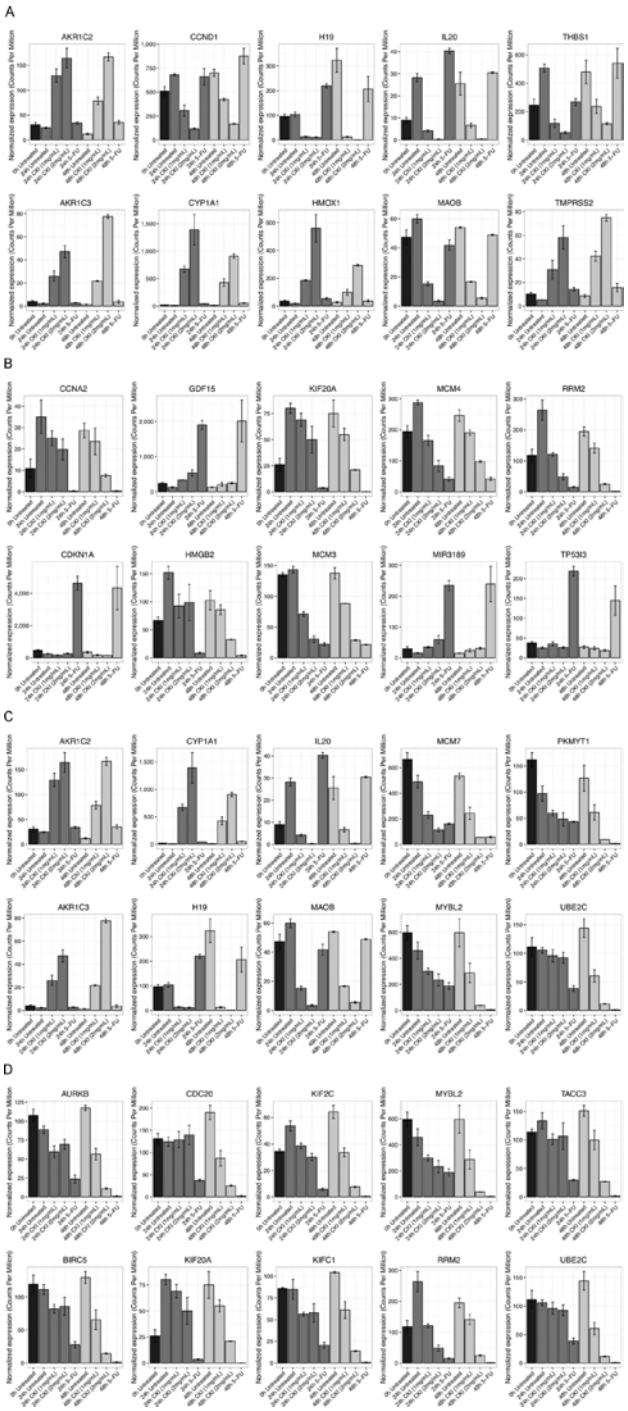

Supplementary Figure 4: Normalised expression values of the top10 significantly differentially expressed genes in cells treated with CKI (2 mg/mL) or 5-FU for 24 hours A. and **B.** or 48 hours **C.** and **D.**

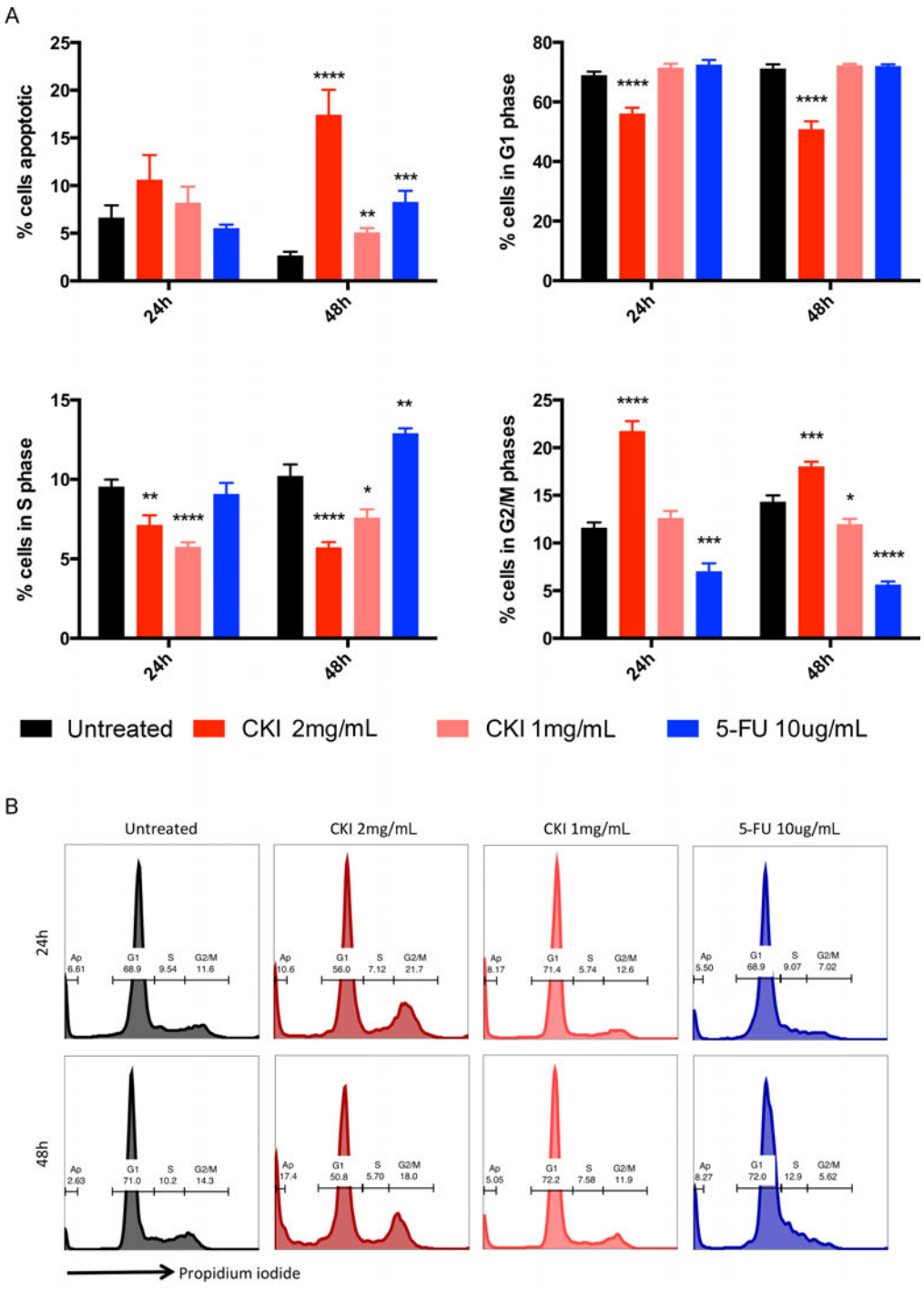

Supplementary Figure 5: Effect of CKI on cell cycle and apoptosis in MCF-7 cells. Proportions of cells in either apoptosis, G1, S or G2/M phase were determined by measuring the DNA contents of permeabilised cells stained with Propidium Iodide. **A.** Percentages of cells in each cell cycle phase. **B.** Representative histograms of PI staining with gating designation. Data are represented as mean ±SEM (n=9). Statistical analyses were performed using t-test comparing with "Untreated" (*p<0.05, **p<0.01, ***p<0.001, ****p<0.0001).

Supplementary Figure 6: Flowchart of *de novo* identification of lncRNAs from RNA-seq dataset. Digits in red colour represent the numbers of transcripts after corresponding data processing.

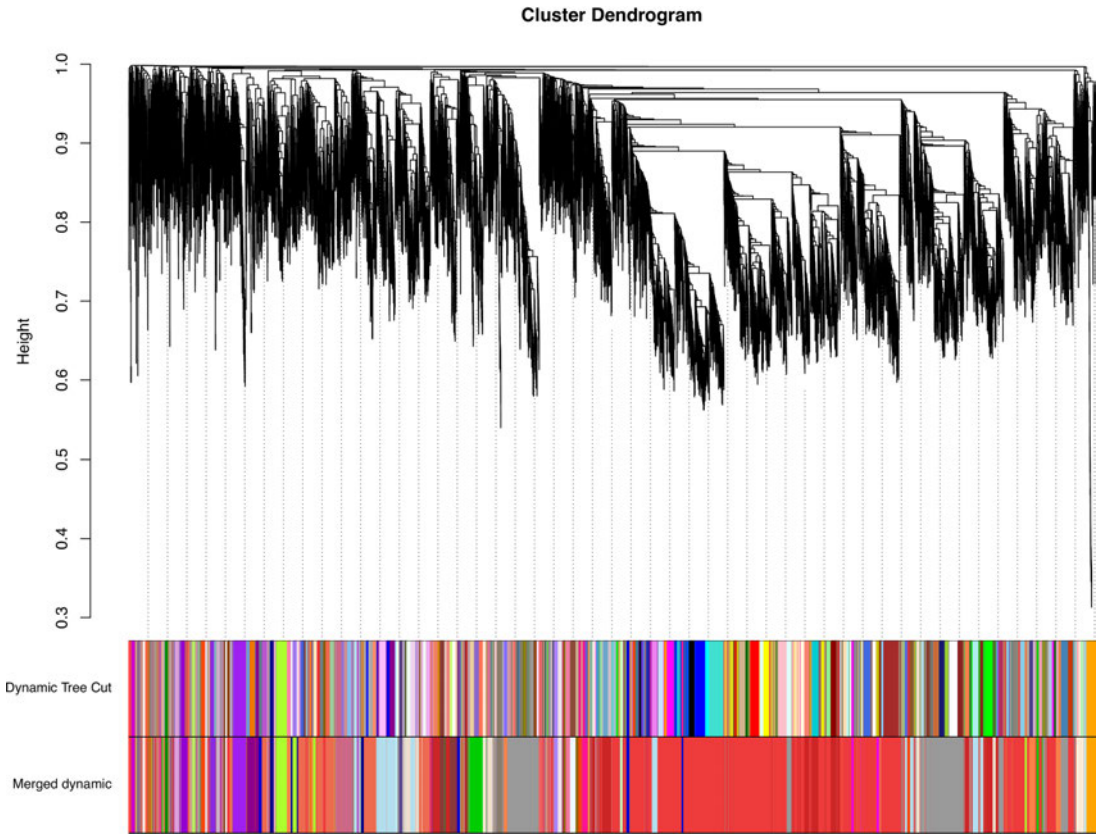

Supplementary Figure 7: Clustering dendrogram of genes, with dissimilarity based on topological overlap, together with co-expression module colors. Merged dynamic modules (lower color band) mean highly co-expressed modules are merged based on eigengene correlations in original clustered modules (upper color band).

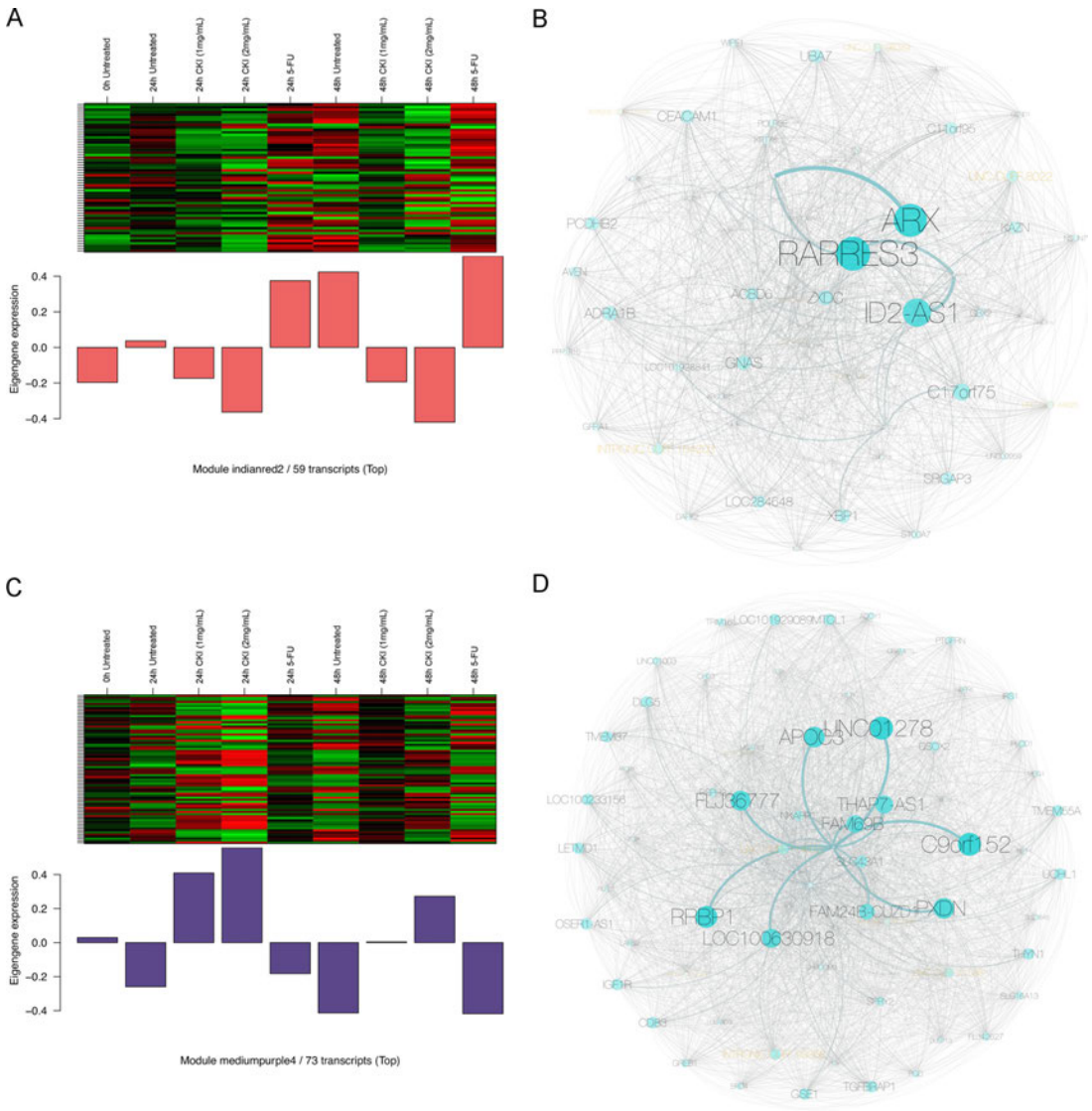

Supplementary Figure 8: Expression patterns of transcripts in CKI-specific modules "indianred2" and "mediumpurple2" are shown in the top panels A. and **C.** and the barplot in the bottom panels (A and C) shows the eigengene values for different samples. Green represents "under-expressed" and red represents "over-expressed" in the heatmap. The "eigengene value" is defined as the first principal component of this module, so it can be considered as representative of the gene expression profiles in this module. Visualization of CKI-specific modules "indianred2" and "mediumpurple2" **B.** and **D.** The black labels represent refGenes and gold labels represent lncRNAs. The size of the node/label and edge weight is proportional to betweenness centrality.

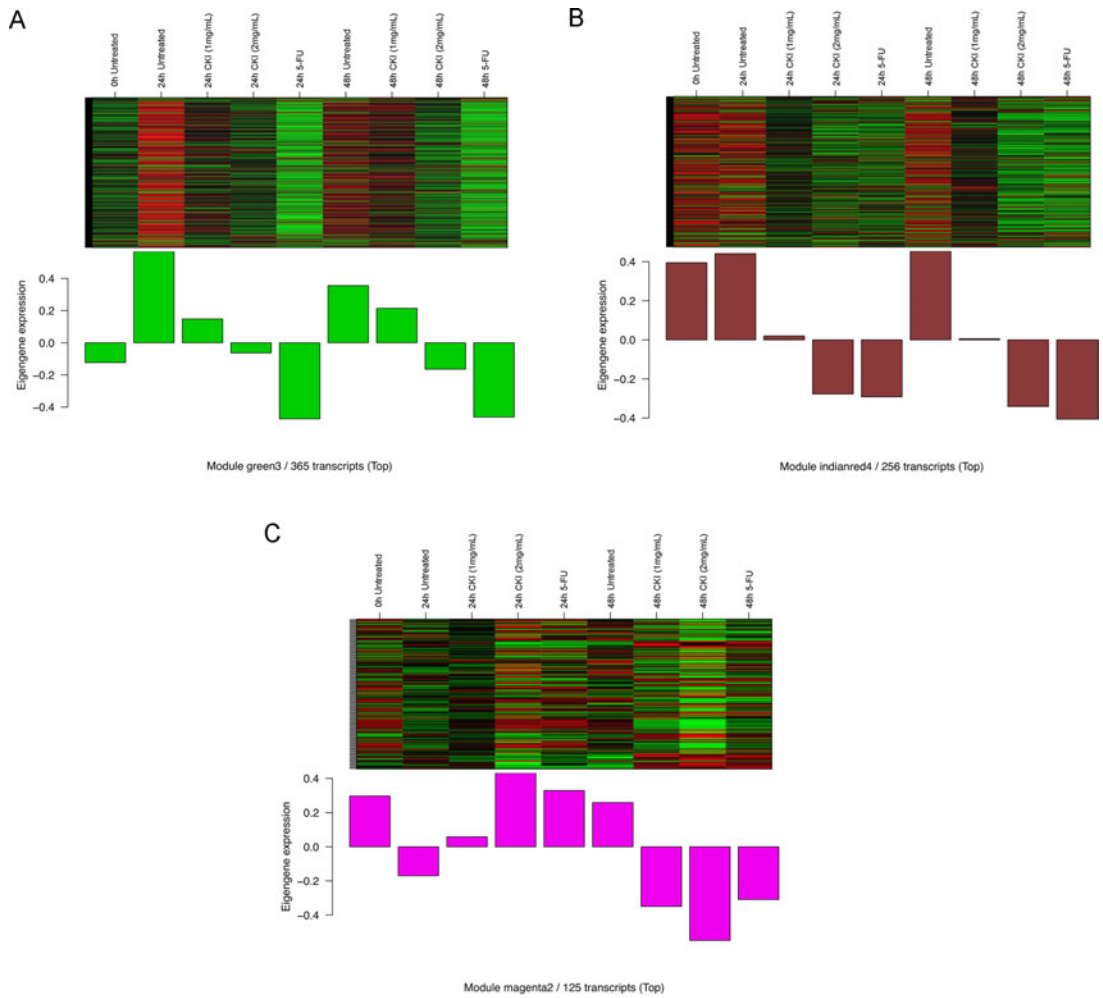

Supplementary Figure 9, Representative CKI-5FU co-expression modules. Expression patterns of transcripts in CKI-5FU modules **A.** "green3", **B.** "indianred4" and **C.** "magenta2" are shown in the top panels, and the barplot in the bottom panels show the eigengene values in different samples. Green represents "under-expressed" and red represents "over-expressed" in the heatmap. The "eigengene value" is defined as the first principal component of this module, so it can be considered as representative of the gene expression profiles in this module.

Appendix C

Supplementary for Chapter 3

Figure S1. MDS plot of the DE gene distribution of two cell lines under different conditions.

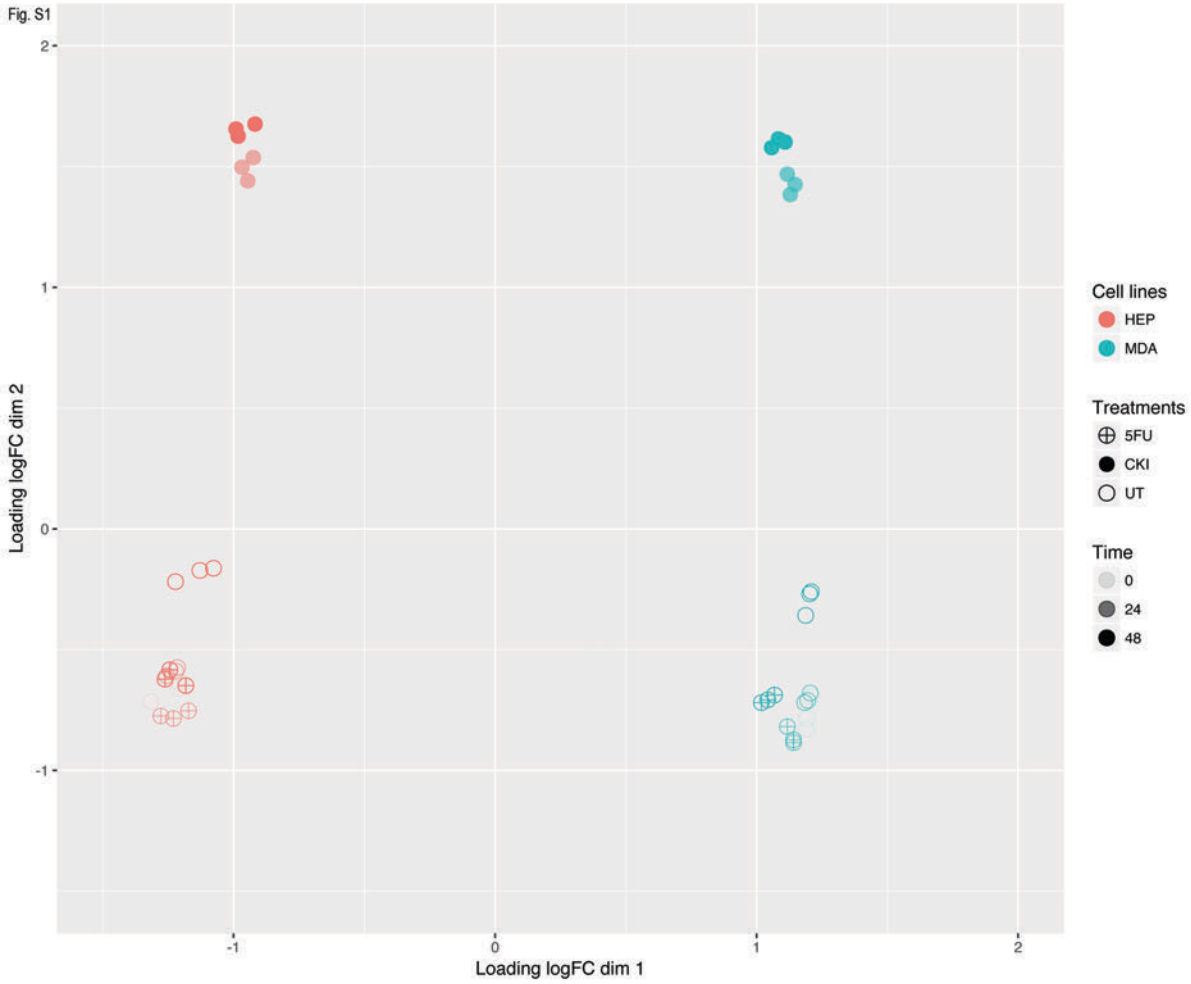

Figure S2. The GO semantic similarity analysis of each data set.

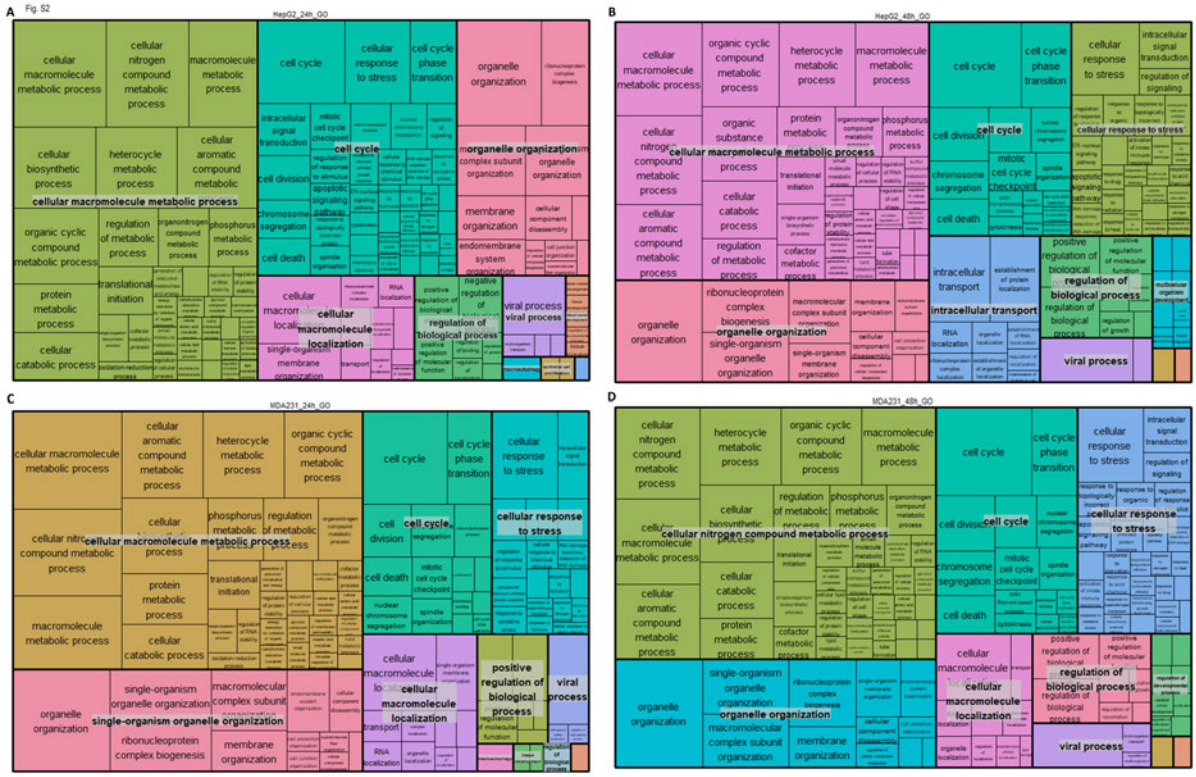

(A-D) Each small square represents a GO biological process functions in level 3. Size of the squares positively correlates with the statistical significance of related biological process. Different colour is to distinguish biological process clusters that are descripted by the top shaded functional representatives.

Figure S3. DE genes distribution of two cell lines in the pathways in cancer.

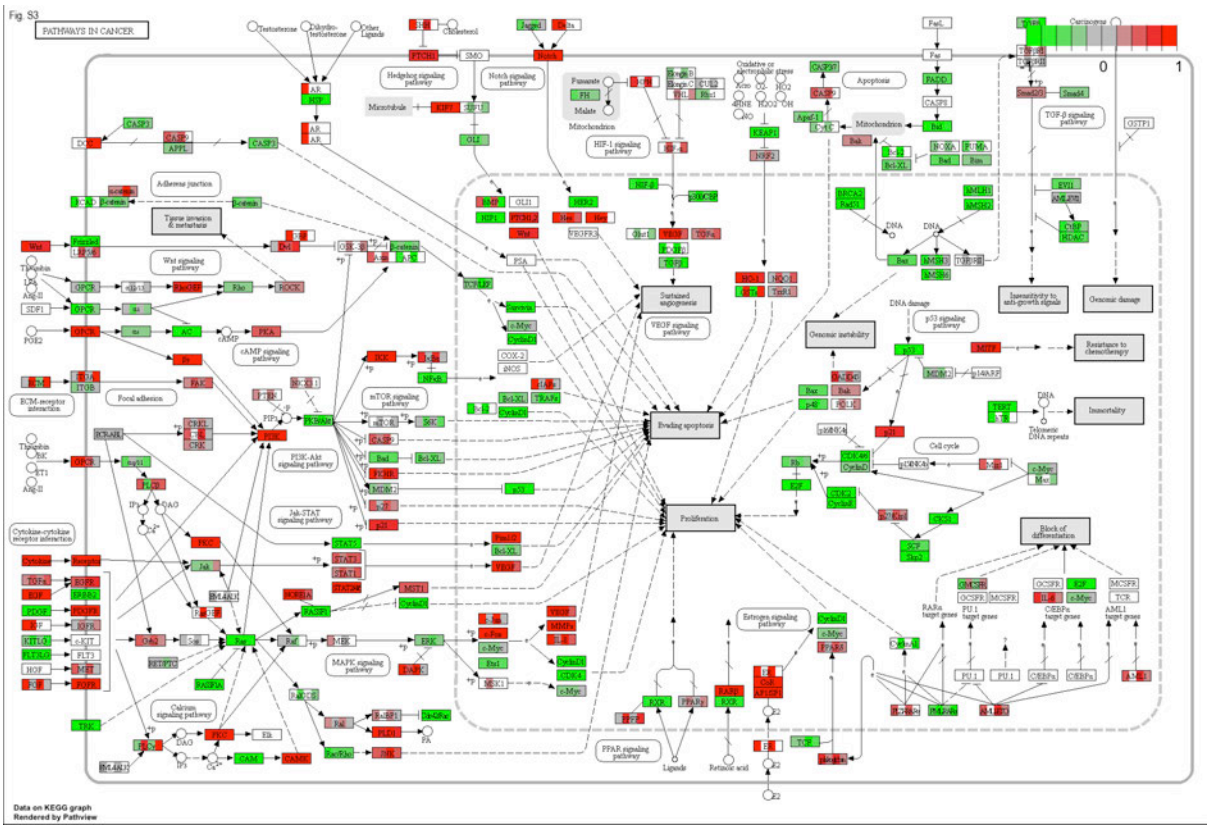

In the cell cycle pathway, each coloured box is separated into 4 parts, from left to right representing 24h CKI treated HepG2, 48h CKI treated HepG2, 24h CKI treated MDA-MB-231 and 48h CKI treated MDA-MB-231.

Figure S4. The heatmap of core genes of three cell lines.

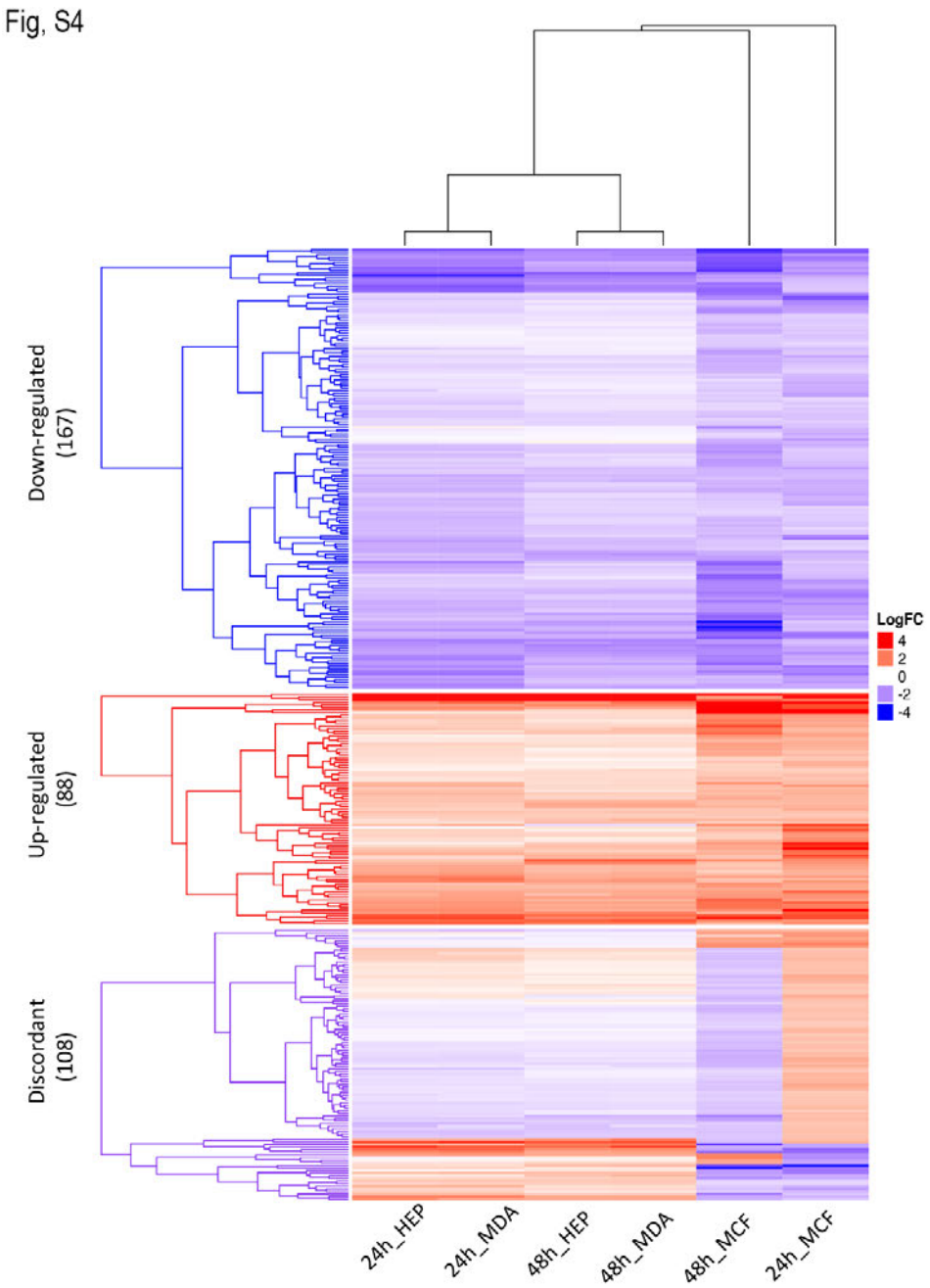

Heatmap revealing the expression fold changes of core genes in three cell lines at two time points. All the core genes can be separated into 3 clusters, namely consistently up/down regulated genes and uneven genes.

Appendix D

Supplementary for Chapter 4

Supplementary Material: Cell Cycle, Energy Metabolism and DNA Repair Pathways in Cancer Cells are Suppressed by Compound Kushen Injection

Jian Cui, Zhipeng Qu, Yuka Harata-Lee, Thazin Nwe Aung, Hanyuan Shen and David L Adelson

The University of Adelaide, School of Biological Sciences, Dept of Molecular and Biomedical Sciences

1 SUPPLEMENTARY DATA

1.1 Methods

XTT assay: The wells of 96-well tray were seeded with 4×10^3 cells per well for HEPG2 cells and 8×10^4 cells per well for MDA-MB-231 cells in 50 μL of medium and cultured overnight. On the following day, 50 μL of either medium, CKI or 5-FU were added to the cells. Viability of the cells was measured at 0, 24 and 48 hours after the treatment by adding XTT:PMS (50:1; Sigma-Aldrich). After 4-hour incubation at 37C optical density (OD) of each well was read at 490nm. The background OD was also measured and the average was subtracted from the OD readings of appropriate wells.

1.2 Figures

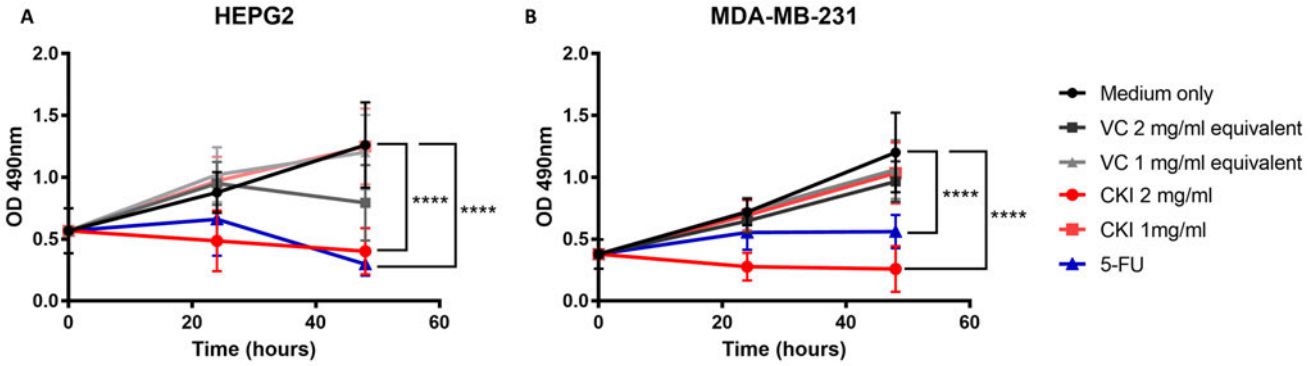

Figure S1. XTT assay result of HEPG2 and MDA-MB-231 cell lines. The XTT assay measures levels of NADH and NADPH by producing a formazan dye product that can be detected at 490nm. **A**. XTT assay result for HEPG2 cells. The assay was carried out at three time points: 0, 24, and 48 hours. 5 treatment groups were used and compared, 150 μg/ml 5-FU as a positive control for a cytotoxic agent, 1 mg/ml and 2 mg/ml CKI as well as the corresponding concentration of vehicle control (VC). CKI has a clear effect on the amount of formazan dye produced indicating a significant and marked suppression in the production of NADH and NADPH. **B**. XTT result of MDA-MB-231 cells. This test is with a low concentration of 5-FU (20 μg/ml). CKI has a clear and marked effect on the level of formazan dye produced indicating a significant and marked suppression in the production of NADH and NADPH. Statistical analyses were performed using two-way ANOVA comparing with untreated (****$p<0.0001$); bars show 1 standard deviation from the mean.

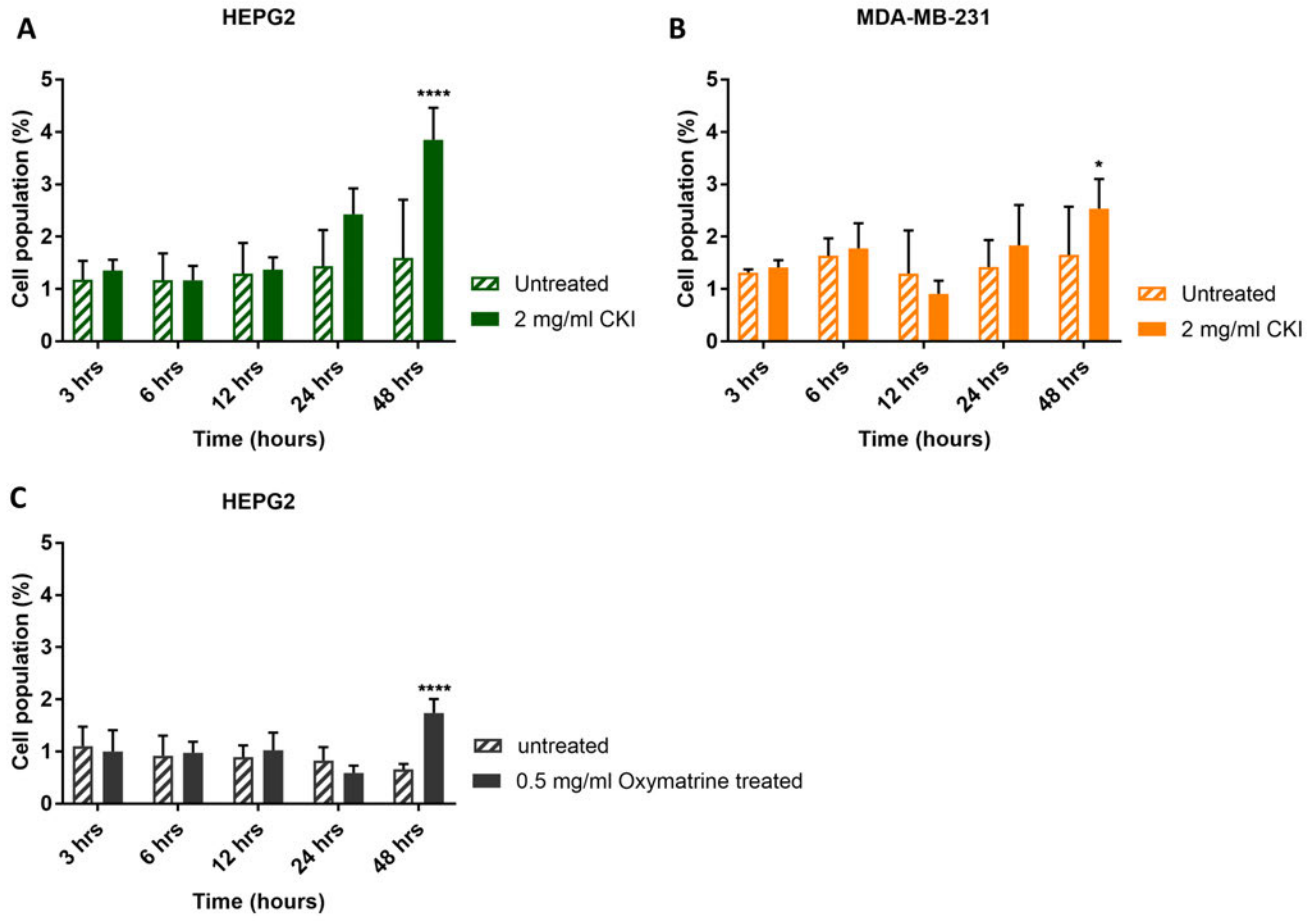

Figure S2. Cell apoptosis assay. A. Cell apoptosis in HEPG2 cells treated with CKI. The assay was carried out at 5 time points to detect apoptosis levels between untreated and 2 mg/ml CKI treated groups. From 3 to 12 hours, both groups maintained a baseline level of apoptosis. After 24 hour, apoptosis of CKI treated cells increased, with the difference attaining statistical significance at 48 hours. **B**. Cell apoptosis in MDA-MB-231 cells treated with CKI. From 3 to 24 hours, both groups show similar, if noisy results. By 48 hours apoptosis has increased and was statistically significantly different to the control. **C**. Cell apoptosis in HEPG2 cells treated with oxymatrine. We compare apoptosis levels between an untreated group and a group treated with 0.5 mg/ml oxymatrine. From 3 to 24 hours we observed a baseline level of apoptosis. By 48 hours apoptosis in the oxymatrine treated group is significantly greater than in the control group. Statistical analyses were performed using two-way ANOVA comparing with untreated (****$p<0.0001$); bars show 1 standard deviation from the mean.

Appendix E

Abbreviations

Abbreviations

AKR1C2	Aldo-keto reductase family 1 member C2
AKT	AKT 224 serine/threonine kinase 1
ALK	ALK receptor tyrosine kinase
ALK	ALK receptor tyrosine kinase
AMPK	5′ AMP-activated protein kinase
ANOVA	Analysis of variance
APAF1	Apoptotic peptidase activating factor 1
ARAF	A-Raf proto-oncogene, serine/threonine kinase
ATG	Autophagy related gene
AURKA	Aurora kinase A
BAD	BCL2 associated agonist of cell death
BATMAN	A Bioinformatics Analysis Tool for Molecular mechanism of Traditional Chinese Medicine
BAX	Bcl2 associated x, apoptosis regulator
BCL2	BCL2, apoptosis regulator
BNIP3	BCL2 interacting protein 3
BRCA	Breast and ovarian cancer susceptibility protein
CCND1	Cyclin D1
CCND3	Cyclin D3
CDK1	Cyclin dependent kinase 1
CDK2	Cyclin dependent kinase 2
CKI	Compound Kushen injection
CPM	Copy number per million
CTNNB1	Catenin beta 1
CXCL16	C-X-C motif chemokine ligand 16
CYP1A1	Cytochrome P450 family 1 subfamily A member 1
DAPI	4’,6-diamidino-2-phenylindole
DAPK2	Death associated protein kinase 2
DMF	Dimethoxyflavone
DMSO	Dimethyl sulfoxide
E2F2	E2F transcription factor 2
EBC-6	Bioactive in blushwood
ECL	Chemiluminescence detection agent
EGFR	Epidermal growth factor receptor
EMT	Epithelial-mesenchymal transition
ERCC1	ERCC excision repair 1, endonuclease non-catalytic subunit
ERINLG-4	Flavonoid from Streptomyces spp.
ETV4	ETS variant 4
H19	H19, imprinted maternally expressed transcript (non-protein coding)
HCC	Family with sequence similarity 126 member A
HCC	Thyroid carcinoma, Hurthle cell
IDH1	Isocitrate dehydrogenase (NADP(+)) 1, cytosolic
MAP1LC3B	Microtubule associated protein 1 light chain 3 beta

MTT	3-(4, 5-38 dimethylthiazol-2-yl)-2, 5-diphenyltetrazolium bromide
MXT	Methotrexate
MYC	MYC proto-oncogene, bhlh transcription factor
MYD88	Myeloid differentiation primary response 88
NADH	Nicotinamide adenine dinucleotide phosphate
NHEJ	Non-homologous end joining
NSCLC	Non-small cell lung cancer
ORF	Open reading frame
PCNA	Proliferating cell nuclear antigen
PTEN	Phosphatase and tensin homolog
RARA	Retinoic acid receptor alpha
SDF	The stromal cell-derived factor
SFDA	The State Food and Drug Administration
SLIT2	Slit guidance ligand 2
SMAD7	SMAD family member 7
SPIA	Signalling pathway impact analysis
STAT	Signal transducer and activator of transcription 3
TCA	The Tricarboxylic Acid
TCM	Traditional chiese medicine
TGFB2	Transforming growth factor beta 2
TKI	Tyrosine kinase inhibitors
TMM	Trimmed mean of M-values method in edger (R package)
TMPRSS2	Transmembrane serine protease 2
TNF	Tumor necrosis factor
TP53	Tumor protein p53
TRPV1	Transient receptor potential cation channel subfamily V member 1
VEGF	Vascular endothelial growth factor
WGCNA	An R package for weighted correlation network analysis
WIF1	WNT inhibitory factor 1
XTT	2,3-Bis(2-methoxy-4-nitro-5-sulfonyl)-2H-tetrazolium-5-carboxanilideinner salt
YQCT	Yiqichutan fomula